AD A064128

DDC FILE COPY.

LEVEL II

(10)

TR 2217

(11) 1 SEPTEMBER 1978

(14) NAC-TR-2217

NAC publication

(12) 73p.

(6)

IMPROVED STANDARD ELECTRONIC MODULES, THERMAL AND MECHANICAL ANALYSES AND DESIGN.

NAVAL WEAPONS SUPPORT CENTER, CRANE AND NAVAL AVIONICS CENTER, INDIANAPOLIS

Fiscal Year

FY 1977 SUMMARY REPORT. for FY77

(9)

410 501

APPROVED FOR PUBLIC RELEASE.
DISTRIBUTION UNLIMITED.

(10) William G. Tew

NAVAL AVIONICS CENTER

INDIANAPOLIS, INDIANA 46218

79 01 31 064

DISCLAIMER NOTICE

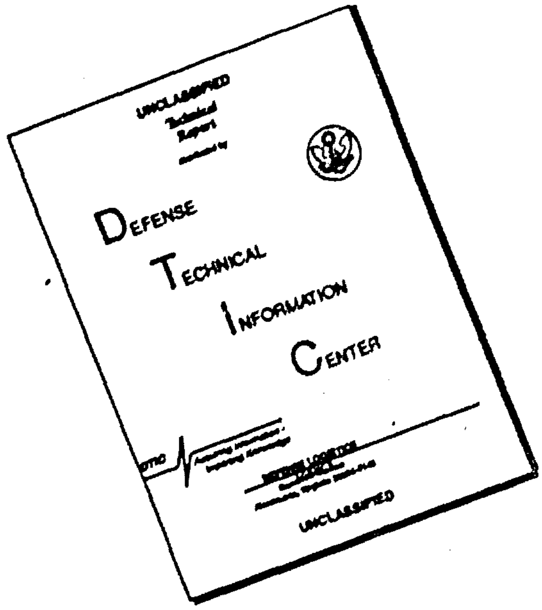

THIS DOCUMENT IS BEST QUALITY AVAILABLE. THE COPY FURNISHED TO DTIC CONTAINED A SIGNIFICANT NUMBER OF PAGES WHICH DO NOT REPRODUCE LEGIBLY.

NOTICE

The discussions or opinions concerning commercial products herein do not constitute an endorsement or condemnation by the Government or agencies thereof, nor do they convey or imply the right to a license for the fabrication or use of such products.

NAC TR-2217

10

PREFACE

The Naval Avionics Center, Indianapolis (NAC), in conjunction with the Naval Weapons Support Center, Crane (NWSC), designed and tested a new module family which is compatible with and which has thermal and component density capability greater than Standard Electronic Modules (SEM) under the following Naval Ocean Systems Center (NOSC) authorization:

> Standard Electronic Modules (SEM) Exploratory Development tasking from the NOSC in accordance with the task statement attached to Work Request N0095377WR09153, entitled, "Improved SEM Packaging Development".

This writer wishes to acknowledge the contribution of Ron B. Lannan and Larry E. Nash of NWSC, Crane, in the development of Section IV, Thermal Analyses, and their contribution in the development of the module design; James Parmerlee, in the development of the Water Cooled Card Cage Analyses; Ron Huss, in the writing of the Introduction and Conclusions; Dave Hershberger, in the development of the Stress Deflection Analysis on a 100-Pin Wrapost Plate; Mel Swager, in contributions on producibility; and many others in the Navy and industry who have made useful contributions.

Prepared by: William D. Taw
WILLIAM TAW

Reviewed by: James Parmerlee
JAMES PARMERLEE

Approved by: John J. McAllen
JOHN McALLEN
Manager of Engineering
Division 930

R. H. Huss
R. H. HUSS
SEM Program Manager, NAC

D. M. REECE
SEM Program Manager, NWSC

LEVEL II

ABSTRACT

This report covers the design, development, and thermal modeling and testing of a new module family, the Improved Standard Electronic Modules (ISEM), which is compatible with the existing SEM Program modules.

Naval Ocean Systems Center (NOSC) directed Naval Avionics Center (NAC), in conjunction with Naval Weapons Support Center (NWSC), to develop, test, and fabricate the Improved SEM.

TABLE OF CONTENTS

TABLE OF CONTENTS (continued)

APPENDIX

LIST OF FIGURES

TABLE OF CONTENTS (continued)

LIST OF FIGURES (continued)

TABLE OF CONTENTS (continued)

LIST OF FIGURES (continued)

LIST OF TABLES

I. CONCLUSIONS

1. The improved SEM configuration provides increased component mounting area, thermal capacity, and input/output pin capability (2A configuration) as compared to the existing SEM configuration. Increased capabilities are as follows:

PARAMETERS	EXISTING SEM	IMPROVED SEM	PERCENT INCREASE
a. Component Mounting Area (IN^2)			
(1) 1A	2.33	3.10	33 %
(2) 2A	5.33	7.09	33 %
b. Thermal Capacity (Watts/Module)			
(1) 1A DIP Frame			
(a) Direct Air Impingement (15 Ft./Sec) and .3 Pitch	4.5	8.1	80 %
(b) Conduction to Side Guides (Water Cooled)			
Vertical Cutouts	3.6	4.8	33.3 %
Horizontal Cutouts	-	8.1	
(c) Conduction to Top (Water Cooled)			
Vertical Cutouts	4.5	6.4	42.2 %
Horizontal Cutouts	-	4.5	
(2) 1A Center Frame			
(a) Direct Air Impingement (15 Ft./Sec) and .3 Pitch	7.4	11.2	51.4 %
(b) Conduction to Side Guides (Water Cooled)	7.6	12.9	69.7 %
(c) Conduction to Top (Water Cooled)	7.2	14.9	106.9 %

PARAMETERS	EXISTING SEM	IMPROVED SEM	PERCENT INCREASE
(3) 2A DIP Frame			
(a) Direct Air Impingement (15 Ft./Sec) and .3 Pitch	10.8	14.3	32.4 %
(b) Conduction to Side Guides (Water Cooled)			
Vertical Cutouts	4.0	6.0	50 %
Horizontal Cutouts	-	8.2	
(c) Conduction to Top (Water Cooled)			
Vertical Cutouts	9.3	13.8	48.4 %
Horizontal Cutouts	-	8.4	
(4) 2A Center Frame			
(a) Direct Air Impingement (15 Ft./Sec) and .3 Pitch	18.6	27.9	50 %
(b) Conduction to Side Guides (Water Cooled)	7.3	12.0	64.4 %
(c) Conduction to Top (Water Cooled)	15.6	30.0	92.3 %
c. Input/Output Connector (Pins)			
(1) 1A DIP and Center Frame	40	40	0
(2) 2A DIP and Center Frame	80	100	25 %

2. Producibility of the improved SEM T-Top frame configuration at a reasonable production cost using volume production techniques has yet to be demonstrated. Potential production techniques and industry sources have been defined, but require verification through hardware fabrication.

3. Optimal compatibility between existing and improved SEM hardware will be achieved in the ISEM card cage development. From a mechanical viewpoint, one-way compatibility will exist, i.e., existing and improved SEM can be mixed in the future ISEM card cage.

4. Use of the 100-pin input/output connector can result in a significant deformation of the wrap plate, approximately .050 inch, at the maximum specified insertion force. A card cage structural design technique to reduce the bowing effect has been determined.

5. A simple, inexpensive module extractor design has been developed. Because of dimensional differences between the 1A and 2A configurations and card cage guide rail heights (for existing and new equipment designs), four extractor configurations are possible as follows:

   a. 1A Module (existing card cage designs)
   b. 2A Module (existing card cage designs)
   c. 1A Module (new card cage designs)
   d. 2A Module (new card cage designs)

II. RECOMMENDATIONS

1. Producibility of the improved SEM T-Top frame should be demonstrated as part of the FY78 SEM R & D program to verify that the frames can be produced at reasonable cost using volume production techniques.

2. Design and development of card cage structures should be pursued as part of the continuing SEM R & D program to realize full advantage of the potential thermal capabilities of the improved SEM configurations.

3. SEM program documentation should be updated to reflect the improved SEM configurations.

4. The proposed module extractor design should be more fully evaluated to verify the effectiveness of the approach and to examine whether the four configurations could be reduced to two configurations.

5. The need for a hybrid "deep dish" 2A frame design should be examined. It is believed that this configuration will be required, based on increasing usage of hybrid circuitry. If the use is verified, funding should be made available for its development.

III. INTRODUCTION

This report summarizes the data from the various engineering studies, analyses, and testing; identifies the resulting improved SEM configurations; and provides conclusions and recommendations related to this effort and proposed future SEM packaging tasks.

During FY 1976 a series of developmental module studies was conducted under the auspices of the Standard Electronic Modules (SEM) Exploratory Development (6.2) Program. The objective of these studies, conducted by the Naval Avionics Center, Indianapolis (NAC) and the Naval Weapons Support Center (NWSC), Crane, was to identify a family of conceptual standard module configurations with controlled electrical, mechanical, and thermal interfaces which would be compatible with large electronic functions having multisystem commonality. As documented by page 1-1, these studies concluded that the improved SEM family is considered to be the optimum selection for a new module family. The improved SEM family is defined as a module family retaining the existing SEM (1A, 2A, and 2B) overall module dimensions with the circuit board area extended within .050 inch of the top surface of the module, the side guides (ribs) extended within .050 inch of the full height of the module and increased from .090 inch to .150 inch per side in span, and the 2A 80-pin connector expanded to 100 pins.

During FY 1977 NAC and NWSC, Crane were assigned the task of developing the improved SEM 1A and 2A concepts into hardware configurations. Specifically, the objective of the FY 1977 SEM exploratory development assignment was to implement and evaluate thermal and mechanical design concepts for the improved SEM 1A and 2A center frame and DIP configurations. The module tasks included under this effort were the following:

. Thermal design
. Mechanical design
. Producibility analysis

- SEM/ISEM compatibility analysis
- Module extraction design
- Card cage interface considerations

The approach to the accomplishment of these module tasks was as defined by the following task descriptions.

1. Thermal design - Using a preliminary improved SEM mechanical configuration, a thermal scheme was defined for the module from the device case to the ultimate heat sink allowing for both conduction and convection cooling. A thermal model was developed, and the thermal characteristics/profile of each of the module configurations predicted. Thermal load modules were fabricated and subjected to extensive laboratory testing in both conduction and convection cooling modes. Thermal results were used to determine/modify the module guide rib configuration and the module top surface configuration.

2. Mechanical design - Mechanical studies and analyses were performed to establish the mechanical and physical aspects of the module configuration. Design considerations included frame material, frame thickness, connector attachment, board/substrate attachment, module pitch, and structural rigidity for mechanical environments.

3. Producibility analysis - Studies were performed to ensure a producible design at a reasonable cost. Design considerations included mechanical tolerances; adaptability to stamping, forming, and/or extruding operations; and tooling costs.

4. SEM/ISEM compatibility analysis - The compatibility of existing SEM with the proposed improved SEM configurations was analyzed to ensure maximal compatibility between the two module families. Considerations included mechanical and thermal compatibility at the card cage level, and the effect of the 2A module 100-pin connector on the back panel and card cage structure design.

5. Module extraction design - A module extractor design was developed for improved SEM. Design considerations included mechanical advantage, compatibility with card cage "end" modules, design simplicity, and low production cost.

6. Card cage interface considerations - Mechanical and thermal interface design characteristics were analyzed to ensure compatibility and minimal thermal resistance between the improved SEM and the card cage. Design considerations included tolerance build-up, module top surface flatness, guide rib configuration, etc.

Deliverables included as part of the FY 1977 SEM R&D module effort were as follows:

1. Engineering drawings for

   . module frames

   . printed circuit board outline

   . 100 pin connectors

   . module extractors

2. Prototype hardware

   . improved 1A DIP frame (5 each)
   . improved 1A center frame (5 each)
   . improved 2A DIP frame (5 each)
   . improved 2A center frame (5 each)
   . 2A module extractor (2 each)

IV. THERMAL DESIGN

A. COMPUTER-AIDED THERMAL MODELING

1. Computer-aided thermal modeling was utilized to characterize the thermal resistance patterns of several Improved SEM (ISEM) and existing SEM module frames. The purpose of the modeling was to provide specific frame thermal resistance data so that power sizing could be made for each module frame design under consideration. In addition, the modeling results allowed direct comparison of existing SEM and Improved SEM frame thermal performance at both the intra-module (qualification) and system level. The computer modeling results combined with the empirically derived system-level thermal interface data (both convection and conduction) provided the thermal parameters necessary to predict maximum module power dissipations for modules utilizing the various frames considered.

This computer analysis involves the thermal characterization of both existing SEM and ISEM frame designs. The following frame designs, with their respective component populations, were analyzed:

FRAME DESIGN	COMPONENT POPULATION
SEM 1A DIP FRAME	FIVE 16-PIN DIPS
SEM 2A DIP FRAME	TWELVE 20-PIN DIPS
ISEM 1A DIP FRAME	NINE 16-PIN DIPS
ISEM 1A DIP FRAME	THREE 16-PIN DIPS + ONE 24-PIN DIP
ISEM 1A CENTER FRAME	TWENTY-FOUR 16-PIN FLATPACKS
ISEM 1A CENTER FRAME	TWELVE 24-PIN FLATPACKS
ISEM 2A DIP FRAME	SIXTEEN 16-PIN DIPS
ISEM 2A DIP FRAME	SIX 16-PIN DIPS + FOUR 24-PIN DIPS
ISEM 2A CENTER FRAME	FORTY-EIGHT 16-PIN FLATPACKS
ISEM 2A CENTER FRAME	TWENTY-EIGHT 24-PIN FLATPACKS

The heat conducting ribs in the existing SEM DIP frames were oriented vertically for this analysis, whereas the ribs on the ISEM DIP frames were oriented horizontally. If one is interested in the frame hotspot to fin thermal resistance for an ISEM DIP frame with a vertical rib orientation, the resistance values for an existing SEM DIP frame can be used with negligible error.

Thermal resistance solutions were obtained for all frame designs and component layout configurations using three metal alloys having different thermal conductivities: aluminum alloy 5052, aluminum alloy 6101, and copper alloy 113. The existing SEM frames are currently being manufactured with aluminum alloy 5052, although this analysis renders resistance values for all three metal alloys. The heatsink frame thicknesses used in this analysis were .050 inch for the DIP frames and .032 inch for the center frames.

The DICAP version of the Cybernet Services' Syscap II circuit analysis program was used to solve for the frame node to heatsink thermal resistance values. All frame designs were modeled using thermal resistance networks with the node temperatures being solved by the computer. The Syscap II program has the capacity for a 255 node model. The heatsink for the model was assumed to be 0°C at either the fin or the guide rib or at both the fin and the guide simultaneously. Therefore, thermal resistance values were solved for three conditions: (1) heatsink at the fin, (2) heatsink at the guide rib, and (3) heatsink at both the fin and the guide rib. Thermal resistance values for condition (1) would be useful in calculating module power capacities whenever forced-air fin cooling or fin conduction into a top-mounted coldplate was used as a system cooling mode. Values from condition (2) would be useful in calculating module power capacities whenever guide rib conduction cooling into a card guide cold plate was used in the system. Condition (3) represents a system cooling mode whereby heat is conducted through both the fin and the guide rib simultaneously, while maintaining the same fin and guide rib interface temperature. It should be noted that the thermal resistance values obtained from this analysis must be combined with other resistances (junction-case, case-frame, fin/guide rib-system heatsink) in order to compute the module power dissipation capacity.

2. For the purpose of this report, the method for the development of the ISEM 2A DIP frame thermal model will be used as an example. All other frame design models were developed in a similar manner. The ISEM 2A DIP frame used in this example is populated with sixteen 16-pin DIPS.

The first step in developing the ISEM 2A DIP frame model was to select node locations based on the mechanical dimensions of the frame and the location of the frame cut-outs for DIP lead clearances. Figure IV-1 shows the node layout pattern with associated node locating dimensions for half of the ISEM 2A DIP frame. Only half of the frame was modeled because it is symmetrical about the frame centerline, as shown. Referring to Figure IV-1, nodes were placed at the center of each DIP to permit heat source loading over the frame. All nodes were numbered (row, column) as in a cartesian coordinate system. Nodes were vertically and horizontally aligned wherever possible. In this example, node 42 was not vertically aligned with any other node because more resolution was needed to model the frame transition section between the fin and the guide rib. The guide rib nodes were placed 0.150 inch from the outside edge of the guide rib and the fin nodes were placed 0.070 inch from the top of the fin. The width of the top of the fin was not considered as a heat conducting element, although the impact of this assumption is addressed later in this report.

The next step in developing the ISEM 2A DIP frame model was to specify, code, and calculate the branch resistances shown in Figure IV-2. As shown in Figure IV-2, each resistor in the network was coded in accordance with Syscap II program instructions. RH resistors represent horizontal resistances, whereas RV resistors represent vertical resistances in the network. Current sources (113, 123, 133, etc.) were placed at each DIP component node location to simulate heat source loading at that point.

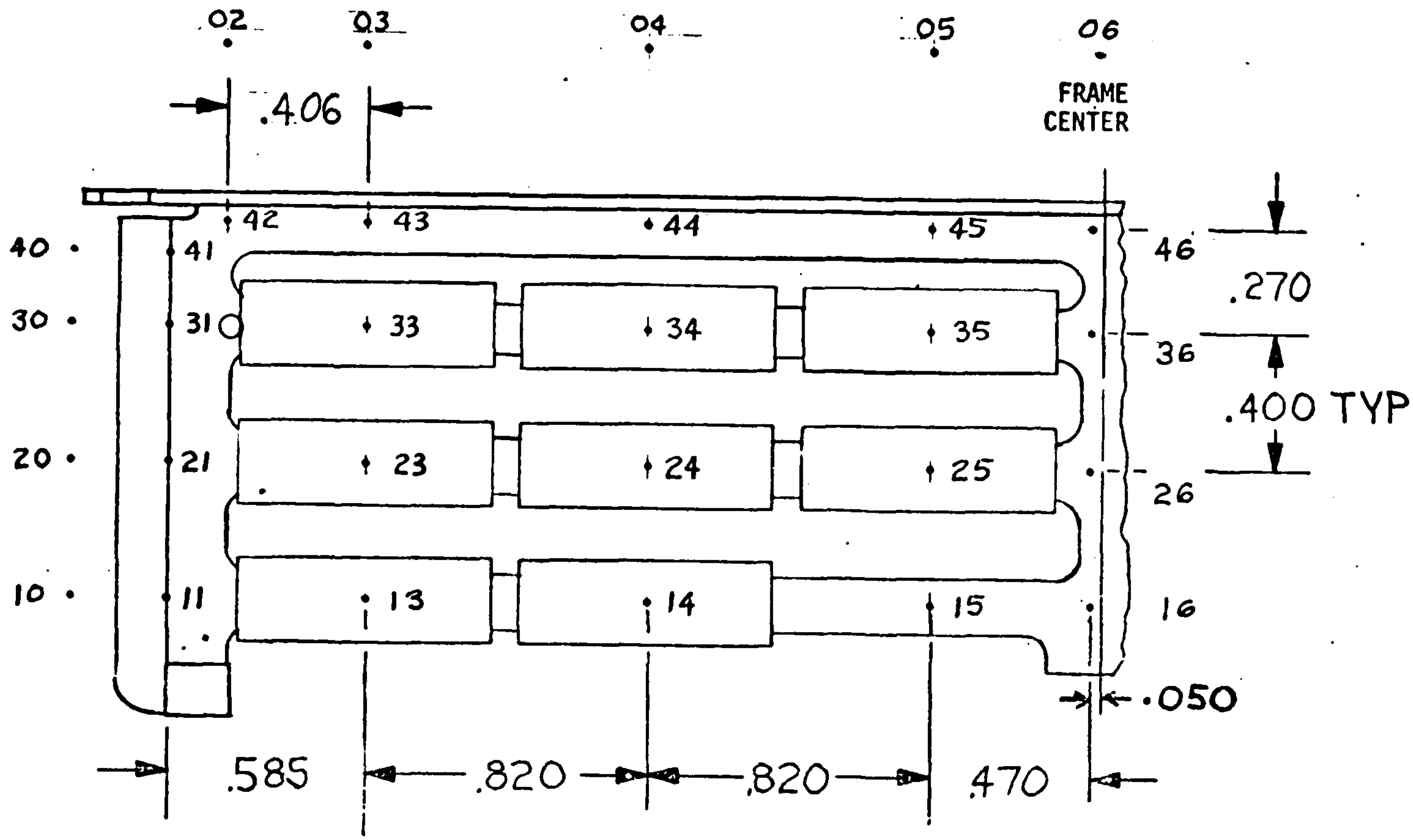

THERMAL MODEL NODE LAYOUT

ISEM 2A DIP FRAME WITH 16 - 16 PIN DIPS

FIGURE IV-1

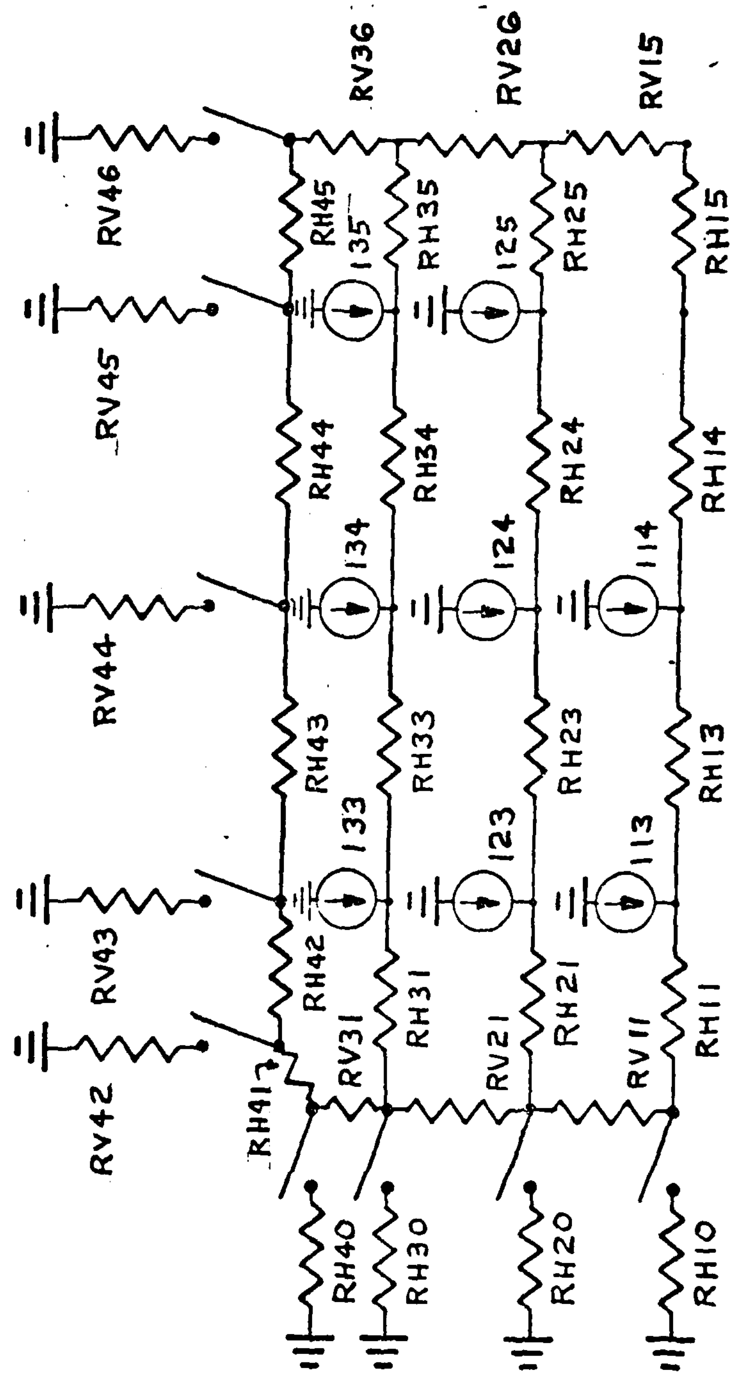

THERMAL MODEL RESISTANCE NETWORK

ISEM 2A DIP FRAME WITH 16 - 16 PIN DIPS

FIGURE IV-2

The heat input into each current source node was 0.5 watts/#DIPS, resulting in a total module power of one watt, since only one-half of the frame was modeled. Because the fin and/or guide rib interface acts as the sink at 0°C (ground potential), the resultant computer output node temperature can be read directly as thermal resistance, in °C/module watt. Figure IV-2 also shows perimeter resistors (RH10, RH20, RH30, RH40 and RV42 through RV46, inclusive) which allow either the fin or the guide rib or both the fin and the guide rib to be switched to ground potential. These resistors have values of 0.01°C/watt to effect a short circuit to ground (infinite heatsink).

Table IV-1 shows the resistance value calculations which were made for each branch resistor using aluminum alloy 5052. Most of these resistances are calculated from the one-dimensional Fourier steady-state heat conduction equation:

$$R = L/KA$$

Where: L = length of heat transfer path (inches)
K = thermal conductivity of alloy (watts/in-°C)
A = cross-sectional area of heat transfer path (in^2)

For the metal alloys used in this analysis, the thermal conductivities are as follows:

K (aluminum alloy 5052) = 3.51 watts/in-°C
K (aluminum alloy 6101) = 5.48 watts/in-°C
K (copper alloy 113) = 9.90 watts/in-°C

The resistances RH11, RH21, RH31, RH15, RH25, RH35, and RV36 are actually a combination of a one-dimensional resistance and a two-dimensional spreading resistance. RH41 is solely a two-dimensional spreading resistance. The methodology for calculating the spreading resistance portion for RH21 is shown in Figure IV-3. The other spreading resistances were calculated in the same manner. Figure IV-4 shows the method for

TABLE IV-1

CALCULATION OF RESISTANCE VALUES
ISEM 2A WITH SIXTEEN 16-PIN DIPS, ALLOY 5052

RESISTOR NAME	L,IN	A,IN^2	$\frac{L}{A},\frac{1}{IN}$	$\frac{L}{A\ sp},\frac{1}{IN}$	$\frac{L}{Atot},\frac{1}{IN}$	R,°C/W
RH43(43,44)	.820	.05(.14)	117.14	--------	117.14	33.37
RH44(44,45)	.820	.05(.14)	117.14	--------	117.14	33.37
RH45(45,46)	.470	.05(.26)	67.14	--------	67.14	19.13
RH33(33,34)	.820	.05(.16)	102.50	--------	102.50	29.20
RH34(34,35)	.820	.05(.16)	102.50	--------	102.50	29.20
RH23(23,24)	.820	.05(.16)	102.50	--------	102.50	29.20
RH24(24,25)	.820	.05(.16)	102.50	--------	102.50	29.20
RH13(13,14)	.820	.05(.16)	102.50	--------	102.50	29.20
RH14(14,15)	.820	.05(.16)	102.50	--------	102.50	29.20
RV11(11,21)	.400	.05(.290)	27.59	--------	27.59	7.86
RV21(21,31)	.400	.05(.290)	27.59	--------	27.59	7.86
RV31(31,41)	.200	.05(.290)	13.79	--------	13.79	3.93
RV16(16,26)	.400	.05(.05)	160.00	--------	160.00	45.58
RV26(26,36)	.400	.05(.05)	160.00	--------	160.00	45.58
RH42(42,43)	.406	.05(.14)	58.04	--------	58.04	16.54
RH41(41,42)	----	--------	------	10.93	------	3.13
RH31(31,33)	.445	.05(.16)	55.64	10.00	65.65	18.70
RH21(21,23)	.445	.05(.16)	55.64	10.00	65.64	18.70
RH11(11,13)	.445	.05(.16)	55.64	10.00	65.64	18.70
RH35(35,36)	.445	.05(.16)	55.64	2.80	58.44	16.65
RH25(25,26)	.445	.05(.16)	55.64	2.30	58.44	16.65
RH15(15,16)	.445	.05(.16)	55.64	2.80	58.44	16.65
RV36(36,46)	.200	.05(.05)	79.99	4.43	84.42	24.05

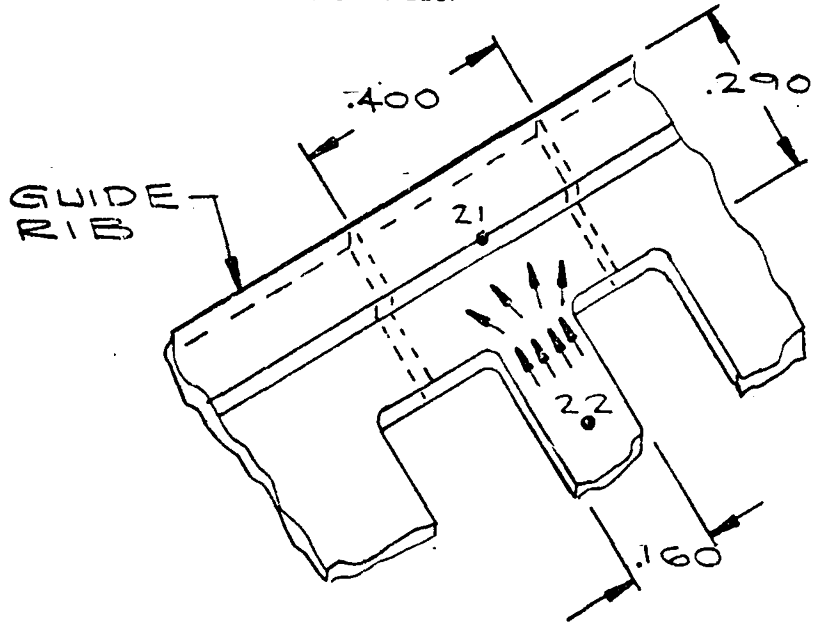

From GE's Heat Transfer Design Data Book Section G502.4, page 15, using the chart by E.H. Gale:

$a = \frac{.400}{2} = .200"$ $\qquad a/b = \frac{.200}{.145} = 1.379$

$b = \frac{.290}{2} = .145"$ $\qquad w/b = \frac{.080}{.145} = .552$

$w = \frac{.160}{2} = .080"$ $\qquad h$ = material thickness = 0.050"

From the chart, $\frac{T_w - T_s}{q'/k} = -0.50$

$$R_{sp} = -\frac{T_w - T_s}{q'/k} \quad \frac{1}{hk}$$

k (5052 aluminum) = 3.51 watts/in-^{o}C

$$R_{sp} = -(-0.50)\left(\frac{1}{(.05)(3.51)}\right) = \underline{\underline{2.85^{o}\ C/WATT}}$$

SPREADING RESISTANCE CALCULATION FOR RH 21

FIGURE IV-3

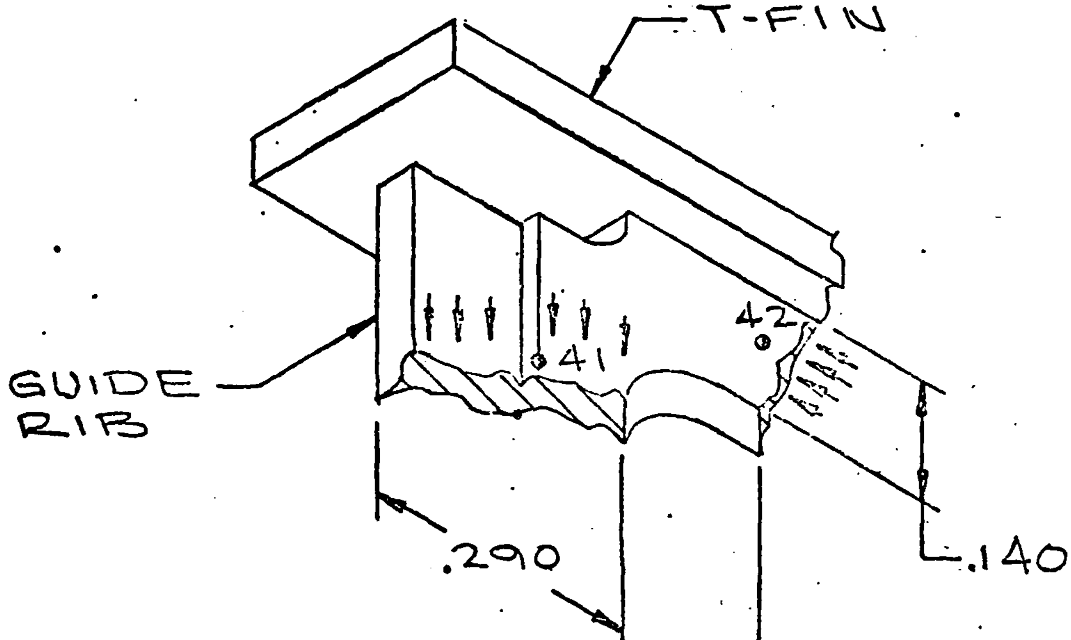

The equation for cylindrical spreading is:

$$R_{sp} = \frac{1}{k\theta t} \ln \frac{r_2}{r_1}$$

k = 3.51 Watts/in-^{o}C for aluminum alloy 5052

t = material thickness = 0.05"

$r_2\theta$ = length of arc of heat influx = 0.14"

$r_1\theta$ = length of arc of heat flux = 0.29"

r_2-r_1 = average length of travel

$$r_2-r_1 = \left[(0.29 + 0.039)^2 + (0.14/2)^2\right]^{1/2} = 0.113"$$

$$\theta = (r_2\theta - r_1\theta) / (r_2-r_1) = (.14 - .29) / 0.113 = -1.327$$

$$R_{sp} = \frac{\ln(.14/.29)}{(3.51)(-1.327)(.05)} = \underline{\underline{3.13^{o}C/WATT}}$$

CYLINDRICAL SPREADING RESISTANCE CALCULATION FOR RH 41

FIGURE IV-4

calculating RH41. The heat flow through this section was approximated by cylindrical spreading.

Resistance calculations similar to the ones in the foregoing example were performed for all frame designs. Calculations were intially performed for aluminum alloy 5052 and then scaled by the ratio of the thermal conductivities to obtain values for aluminum alloy 6101 and cooper alloy 113. These resistance data subsequently were used as an input to the DICAP circuit analysis program.

3. Table IV-2 shows a summary of the hotspot frame node to fin or guide rib resistances for all frame designs and metal alloys. Thermal resistance values for aluminum alloy 6101 and copper alloy 113 are listed for existing SEM, although these frames are not currently manufactured using these alloys. In all subsequent comparisons, aluminum alloy 5052 will be used for existing SEM frames. The existing SEM 1A and SEM 2A center frames were not included in the modeling analysis because they were judged to be essentially a thermal equivalent of the ISEM center frames, assuming the same metal alloy is used.

Current SEM program thermal requirements specify a maximum allowable temperature rise of 45°C from the junction of the component to the fin (with no heat losses through the guide ribs) and to the guide ribs (with no heat losses through the fin). These requirements have to be met, regardless of system cooling method, and are verified during module qualification by actual thermal testing. As a result, when predicting the maximum "qualification power" for a specific frame design and component layout, one must use the maximum thermal resistance value, regardless of whether it's to the fin or to the guide ribs. Using this rationale, maximum "qualification powers" were calculated for ISEM and existing SEM based on a maximum temperature rise of 45°C from junction to heatsink interface (fin or guide rib). These maximum power values are shown in Table IV-3 for selected frame designs. These values were based on junction to frame thermal resistances of 35°C/component watt

TABLE IV-2

WORST CASE THERMAL RESISTANCE TO FIN OR GUIDE RIB

(ALL VALUES IN °C/MODULE WATT)

FRAME DESIGN	COMPONENT LAYOUT	HEAT SINK LOCATION	AL 5052	CA 113	AL 6101
SEM 1A DIP Frame	Five 16-Pin DIPS	Guide Rib	8.52	3.04	5.46
		Fin	4.23	1.50	2.71
SEM 2A DIP Frame	Twelve 20-Pin DIPS	Guide Rib	10.63	3.78	6.81
		Fin	1.85	0.66	1.19
ISEM 1A DIP Frame	Nine 16-Pin DIPS	Guide Rib	4.28	1.52	2.74
		Fin	16.53	5.88	10.59
ISEM 1A DIP Frame (see Note 1)	Three 16-Pin DIPS plus One 24-Pin DIP	Guide Rib	9.10	3.24	5.83
		Fin	14.01	4.98	8.97
ISEM 1A Center Frame	Twenty-Four 16-Pin Flatpacks	Guide Rib	2.09	0.74	1.33
		Fin	2.21	0.79	1.41
ISEM 1A Center Frame	Twelve 24-Pin Flatpacks	Guide Rib	2.10	0.75	1.35
		Fin	2.26	0.80	1.45
ISEM 2A DIP Frame	Sixteen 16-Pin DIPS	Guide Rib	6.85	2.44	4.39
		Fin	8.62	3.07	5.52
ISEM 2A DIP Frame (see Note 2)	Six 16-Pin DIPS plus Four 24-Pin DIPS	Guide Rib	6.77	2.41	4.34
		Fin	7.62	2.71	4.88

TABLE IV-2 (Continued)

FRAME DESIGN	COMPONENT LAYOUT	HEAT SINK LOCATION	AL 5052	AL 6101	CA 113
ISEM 2A Center Frame	Forty-Eight 16-Pin Flatpacks	Guide Rib	4.32	2.77	1.54
		Fin	1.07	0.69	0.38
ISEM 2A Center Frame	Twenty-Eight 24-Pin Flatpacks	Guide Rib	4.28	2.74	1.54
		Fin	1.08	0.69	0.39

NOTES: (1) For modeling purposes, the power dissipation of the 24-pin dip was assumed to be 33% of the total module power with the remaining power distributed uniformly among the 16-pin DIPS.

(2) For modeling purposes, the power dissipation of each 24-pin DIP was assumed to be 12.5% of the total module power. The remaining power (50% of total) was distributed uniformly among the 16-pin DIPS.

TABLE IV-3

MAXIMUM QUALIFICATION POWER

FRAME DESIGN	COMPONENT POP.	DIP RIB ORIENTATION	MAX. QUALIFICATION POWER (WATTS)		
			AL 5052	AL 6101	CA 113
SEM 1A DIP Frame	Five 16-Pin DIPS	Vertical	2.90	-	-
ISEM 1A DIP Frame	Five 16-Pin DIPS	Vertical	-	3.60	4.50
ISEM 1A DIP Frame	Nine 16-Pin DIPS	Horizontal	-	3.10	4.60
SEM 2A DIP Frame	Twelve 16-Pin DIPS	Vertical	3.32	-	-
ISEM 2A DIP Frame	Twelve 16-Pin DIPS	Vertical	-	4.63	6.72
ISEM 2A DIP Frame	Sixteen 16-Pin DIPS	Horizontal	-	5.84	8.55
SEM 1A Center Frame	Sixteen 16-Pin Flatpacks	N/A	7.55	-	-
ISEM 1A Center Frame	Twenty-Four 16-Pin Flatpacks	N/A	-	11.50	13.67
SEM 2A Center Frame	Thirty-Two 16-Pin Flatpacks	N/A	7.26	-	-
ISEM 2A Center Frame	Forty-Eight 16-Pin Flatpacks	N/A		11.20	16.13

for DIPS, 60°C/component watt for flatpacks, and reflect the use of two .035" thick alumina substrates for the center frame designs.

Perusal of Table IV-3 shows that maximum qualification power values for AL 6101 and CA 113 were not presented for the existing SEM frame designs. This was done because existing SEM frame tooling exists only for AL 5052 and re-tooling these frames for different metal alloys may require significant tooling investments for both extrusion and stamping operations. Because of the poor thermal conductivity of AL 5052 (3.51 watts/in-°C) compared to AL 6101 (5.48 watts/in-°C), the momentum of the FY-77 SEM packaging effort has been carried toward the manufacture of ISEM frames with AL 6101 and CA 113. For this reason, power values for ISEM frames using AL 5052 were not presented.

Because of improvements in the frame thermal conductivities and the increased component populations for ISEM, significant benefits are realized over existing SEM for maximum qualification power. For the 1A DIP frame, ISEM offers power improvements ranging from 7%-24% for AL 6101 and from 55%-58% for CA 113. For the 2A DIP frame, ISEM offers power improvements ranging from 39%-76% for AL 6101 and from 102%-157% for CA 113. Likewise, for the 1A center frame, ISEM power improvements range from 52% for AL 6101 to 81% for CA 113. For the 2A center frame, ISEM power improvements range from 54% for AL 6101 to 122% for CA 113.

A review of Appendix A of this report reveals that, in most system cooling mode conditions, ISEM modules can dissipate more power than the amount which is able to be qualified (per SEM program thermal requirements). As a result of this disparity between system power and qualification power, the module thermal design may require use of a copper alloy DIP heatsink frame for module powers in excess of 6 watts for the ISEM 2A and in excess of 3.6 watts for the ISEM 1A. The ISEM 1A and ISEM 2A center frame modules, as seen from Table IV-3, are capable of qualification for powers up to 11.5 watts and 11.2 watts, respectively.

Some adjustment or additions to current SEM qualification specifications may be desirable to better take advantage of water cooled card cages, direct air impingement, and other parameter changes since the specifications were originally written.

The width of the top of the fin in the computer model, as a heat conducting element, was neglected. Concerning this, a separate computer solution was made considering the ISEM fin top as being .270 inch wide and .050 inch thick along its length. This solution was for the ISEM 2A DIP frame with sixteen 16-pin DIPS, and revealed a 6% reduction in the hotspot to guide rib thermal resistance with no change in the hot-spot to fin thermal resistance. Even less error will result for the center frame designs, because there is a much lower thermal resistance to the guide ribs inherent in the design.

In summary, this analysis has revealed that the ISEM frame designs offer significant thermal advantages over existing SEM. Maximum qualification powers for AL 6101 ISEM 1A module frames range form 3.60 watts for the ISEM 1A DIP frame to 11.50 watts for the ISEM 1A center frame. In comparison, existing SEM 1A frames are capable of qualification powers ranging from 2.90 watts for the 1A DIP frame to 7.55 watts for the 1A center frame. Likewise, comparable ISEM thermal advantages were revealed for the 2A frame designs. For AL 6101 ISEM 2 A frames, qualification powers range from 5.84 watts for the ISEM 2A DIP frame to 11.20 watts for the ISEM 2A center frame. On the other hand, existing SEM 2A qualification powers range from 3.20 watts for the SEM 2A DIP frame to 7.26 watts for the SEM 2A center frame.

For greater detail on the computer solution to the Computer-Aided Thermal Modeling, refer to Standard Electronic Modules Exploratory Development Program Improved SEM Thermal Analysis, FY-77 Final Report of 30 November 1977, by Ron B. Lannan and Larry E. Nash of NWSC, Crane.

B. THERMAL TESTING

1. Thermal testing was performed in several areas to determine the heat dissipating capabilities of the ISEM module frame. Load module frames, printed wiring boards, and systems hardware were designed and fabricated to provide realistic data.

Testing was conducted for forced air convection over the fin, direct air impingement upon the components, conduction cooling through the "T" fin "ear", and conduction cooling through the fin. The .280" wide "T" and the standard .180" wide "L" fin configurations were both evaluated for the fin conduction and convection testing. Conduction cooling through the guide rib was investigated using recent test data collected under Government contract.

All tests were conducted with 2A size DIP load modules. Power capacities appearing in this report for 1A size modules are extrapolated from data collected on 2A modules.

2. Based on thermal testing results, the ISEM module frame exhibits improved thermal performance over the existing SEM frame in every cooling mode.

For forced convection over the fin, the improvement is slight at moderate velocities with no improvement at the higher velocities. It can reasonably be stated that in most instances there would be no penalty associated with using the ISEM "T" fin for this common mode of cooling.

Direct air impingement offers one of the brightest prospects for increased cooling capacity. In this mode, the ISEM's superiority over existing SEM IS chiefly attributed to the increased component mounting area which allows more components per module. System pressure drop may become critical in some instances, but generally would not pose an insurmountable problem. The benefits of a .4" system mounting pitch versus a .3" pitch would generally have to be weighed for each specific situation. For the majority of instances, a moderate velocity of 15'/sec and .3" mounting pitch would be more than adequate, thermally.

The ISEM module frame interface surfaces with the card cage are vastly improved over those of existing SEM. The improved side guide and fins offer increased areas to substantially reduce thermal resistances across the interfaces. The improved side guide, together with its corresponding improved clip, exhibit thermal interface resistances of approximately one-half that associated with the existing configuration. Likewise, the improved fin exhibits one-fourth the interface resistance of the conventional .180" wide "L" fin. This is attributed to the increased area of the "T" and the typical underforming of the "L". This underforming reduces the interface area ratios more than the ratio of the two fin areas and, in some severe instances, creates a line contact with the cold plate. The "ear over" configuration, figure A-10, was envisioned as a supplemental interface for conduction into the card guide. From test data, it can be seen that if the "ears" are not clamped down, an adverse effect can result. If one considers the "ear" interface resistance in parallel with an IERC clip interface resistance, there will be approximately a 4.5 percent increase in module power capacity. This is for an AL 6101 alloy ISEM 2A populated with sixteen 16-pin DIPS.

All projected module power capacities assume aluminum alloy 6101. Power capacities may be increased by using copper alloy CA 110 or CA 113. For certain frame configurations, power capacities may be increased by as much as 50% with copper.

Power capacities are also influenced by device populations. In this study, certain device populations were arbitrarily assumed to arrive at a power capacity. These assumptions may not be valid for all module designs. For instance, the 1A ISEM DIP frame capacities are for a device population of nine 16-pin DIPS, however, from a producibility aspect, it may be unfeasible and one would maybe only populate the module with six

16-pin DIPS. In the latter case, the power capacity (assuming uniform loading) would be less than for the former case.

For detail on the testing, see Appendix A.

C. CONCLUSION

1. As a result of the improvements in frame material thermal conductivities and the 30% increase in available component mounting area, ISEM modules offer power capability increases at the module level over existing SEM modules from 24% to 157%.

2. For ISEM 2A DIP frame modules with power dissipations in excess of approximately 6 watts, copper alloy heatsink frames may be necessary to meet SEM program thermal requirements. Use of a copper alloy frame increases module capability to approximately 9 watts.

3. ISEM 1A and ISEM 2A center frame modules with AL 6101 heatsink frames can meet SEM program thermal requirements for power dissipations up to approximately 12 watts. Use of copper alloy heatsink frames for these modules can increase power dissipation capability to 14 watts and 16 watts, respectively, for the ISEM 1A and ISEM 2A center frame modules.

4. Direct air impingement upon the components offers the highest power capacity of the investigated system cooling methods. The investigated cooling methods are listed below, in order of descending power capacities.

   a. Direct Air Impingement
   b. Conduction to the Fin Interface
   c. Conduction to guide rib interface
   d. Force convection across the fin.

5. Direct air impingement power capacity for a ISEM 2A center frame module ranges from a high of 40 watts at .4 inch spacing and 25 ft/sec

air velocity to a low of 17 watts at .3 inch spacing and a 5 ft/sec air velocity. These capacities are based on 45°C air and 105°C maximum junction temperature.

6. Pressure drop is significantly higher for direct air impingement than for convection over the fin.

7. The ISEM "T" fin is slightly superior to the SEM "L" fin for fin forced convection cooling. The fin-air thermal resistance and the system pressure drop are both lower for ISEM than for SEM.

8. Based on system thermal performance, the following card cage configurations were determined to be optimum for the noted cooling conditions and for both segregated and integrated SEM/ISEM packaging.

Cooling Mode	Card Cage
1. Fin force-air convection	Standard height
2. Guide rib conduction	Extended height
3. Combination of 1 and 2 above	Standard height

V. MECHANICAL DESIGN

A. BACKGROUND

1. The objective of this task was to perform mechanical and structural analyses and to establish the mechanical and physical aspects of a new module family. Main emphasis was on greater thermal capability and on higher circuit density while maintaining compatibility with the Standard Electronic Modules (SEM) program. The two configurations of interest were the center frame module and the offset module (DIP frame module).

Table V-1 is a summary of existing SEM and the new module family, Improved SEM (ISEM), overall physical characteristics.

B. MECHANICAL ANALYSIS

1. Since the primary mode of heat dissipation considered for existing SEM has been conduction, this was also the primary mode investigated for the new module. Other modes of heat dissipation, such as direct air impingement, were studied, but the mechanical design was centered around conduction cooling.

The equation given for heat conduction through a solid, with a uniform temperature distribution along the path of flow with a constant cross-sectional area, is given as:

$$q = - K A \frac{\Delta T}{\Delta X}$$

Where: q = the heat flow

K = the thermal conductivity of the material

A = the cross-sectional area normal to the direction of heat flow

ΔT = the thermal potential

ΔX = the length of the heat flow path

TABLE V-1

MODULE SUMMARY

MODULE	TOTAL MODULE SIZE				ACTIVE CIRCUIT SIZE			NUMBER OF CONNECTOR PINS	CIRCUIT MOUNTING AREA
	THICK	SPAN	HT	PITCH	THICK	SPAN	HT		
SEM 1A (DIP)	.290	2.620	1.890	.30	.290	2.330	1.00	40	2.33
SEM 2A (DIP)	.290	5.620	1.890	.30	.290	5.330	1.00	80	5.33
SEM 1A (CENTER)	.290	2.620	1.890	.30	.290	2.330	1.00	40	2.33
SEM 2A (CENTER)	.290	5.620	1.890	.30	.290	5.330	1.00	80	5.33
ISEM 1A (DIP)	.290	2.740	1.890	.30	.290	2.330	1.33	40	3.099
ISEM 2A (DIP)	.290	5.740	1.890	.30	.290	5.330	1.33	100	7.089
ISEM 1A (CENTER)	.290	2.740	1.890	.30	.290	2.330	1.33	40	3.099
ISEM 2A (CENTER)	.290	5.740	1.890	.30	.290	5.330	1.33	100	7.089

NOTES: 1. The dimension of 1.890 for the height of the module is measured from the card cage back panel.

As can be seen from the equation, the heat flow increases as the length of the heat flow path decreases and the cross-sectional area, thermal conductivity of the material, and the thermal potential increases. Since this section deals with the mechanical analysis of the module, the variables K, A, and ΔX were considered as follows:

a. The thermal conductivity of the frame, K, directly affects the conduction cooling of the module; therefore, the material should be selected with a high thermal conductivity. But, the material also determines possible fabrication techniques, as well as strength and weight of the frame. Therefore, the selection of a material is the result of optimization between all factors that were considered. Further discussion into the material selection is given at the end of the mechanical analysis.

b. The cross-sectional area plays an equally important role in the amount of heat dissipation by conduction cooling. For interfaces between the component and the frame and between the frame and the card cage and/or cold plate on top of the module, the cross-sectional area normal to the direction of heat flow is the thermal contact surface between the interfacing parts. Because of this fact, the side guides on the new module were increased to .150 inch wide, instead of .090 inch wide as on existing SEM. The height of the guides was increased from 1.086 to 1.450 inches. The result of doing this was to increase the amount possible of surface contact area of the frame to the card cage by 221.9%.

The other interface consideration was conduction cooling to a cold plate on top of the module. This method of cooling presents a problem of obtaining a low thermal interface resistance between the cold plate and the modules.

Thermal interface resistance between a module and the cold plate is due primarily to four factors:

(1) Flatness and surface finish of the top of the module;

(2) Flatness and surface finish of the cold plate;

(3) Amount of contact pressure between the module and the cold plate.

(4) Size of the interface area.

The flatter the mating surfaces between the module and the cold plate, the more contact surface area would result. But the flatness of either module or cold plate cannot be closely controlled without machining. From a production standpoint, the less machining required, the cheaper the part. Therefore, machining should be kept at a minimum. If machining was completely eliminated, most fabrication processes can hold a flatness within .010 to .020, depending upon the size of the part. If both module and cold plate were held to this flatness, there could be locations along the mating area between the module and the cold plate with a .030 gap at nominal conditions. The thermal resistance of the thermal joint can be lowered by pressing the two mating parts together to force the two parts to conform to each other's irregularities. The ISEM utilizes Belleville washers to apply an upward force to produce this contact pressure. Figure V-1 shows a card cage setup in which conduction is via a cold plate contacting the module top surface.

Another problem of getting surface contact between all the modules in a system and a cold plate arises because of the total tolerances involved in the height of the modules, the height of the wrap plate bushings and the thickness of the wrap plate. A module can be as much as .025 inch taller than another module. To compensate for this potential difference, the Belleville washers again are used to push each module the distance required for good contact. The insert depth of the connector into the bushing is .150 inch. The possible loss of .025 inch in connector contacts due to the Belleville washers should

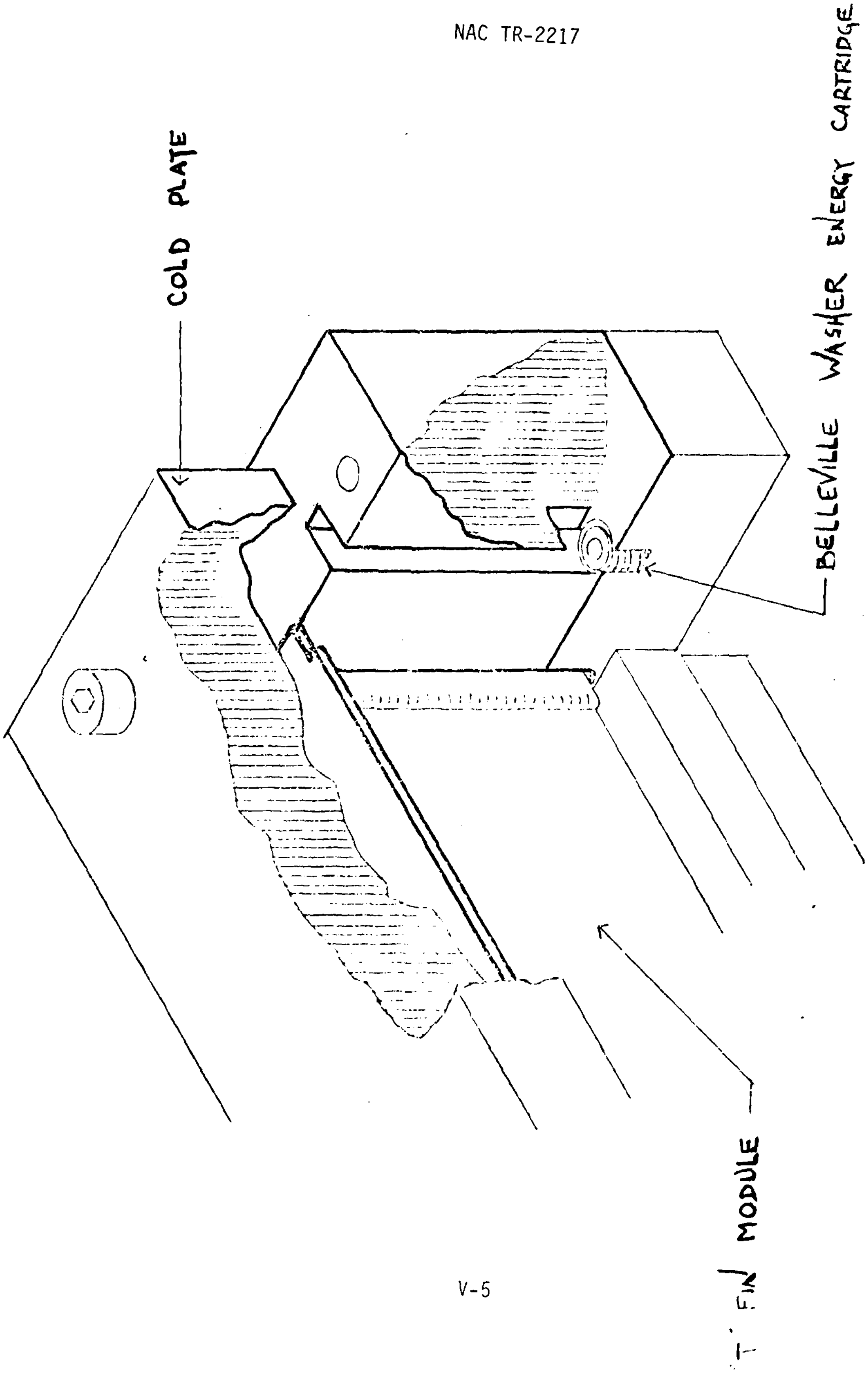

TOP COOLING

FIGURE V-1

not degrade the electrical connection between the module and the wrap plate.

The Belleville washers must apply a force greater than the extraction force of the module; and, the travel distance in which the force is continuously applied must be greater than .025 inch.

The maximum extraction force per pin for the connector is ten ounces. Therefore, the extraction force required for a forty-pin connector used on a 1A module could be 25 lb_f or 12.5 lb_f per row. For the 2A module with one hundred pins, the extraction force could be 62.50 lb_f or 31.25 lb_f per row.

Another means of reducing the thermal interface resistance would be to increase the possible contact surface area between the module and the cold plate. This is accomplished by fabricating a top which is in the shape of a "T", rather than an "L", as on the SEM. Figures V-2 and V-3 show the differences between the SEM and ISEM for a 2A module. The "T" is .270 inch wide and 5.280 inches long, while the SEM's "L" is .180 inch wide, 5.320 inches long, for the 2A dip frame, Figure V-3.

Because of the bend radius on the "L" top, the maximum possible contact area is:

$$5.320 \times (.180 - .070) = .585 \text{ in}^2$$

The maximum contact area for the "T" top is:

$$5.280 \times .270 = 1.426 \text{ in}^2$$

Therefore, the "T" top provides 2.43 times as much contact area.

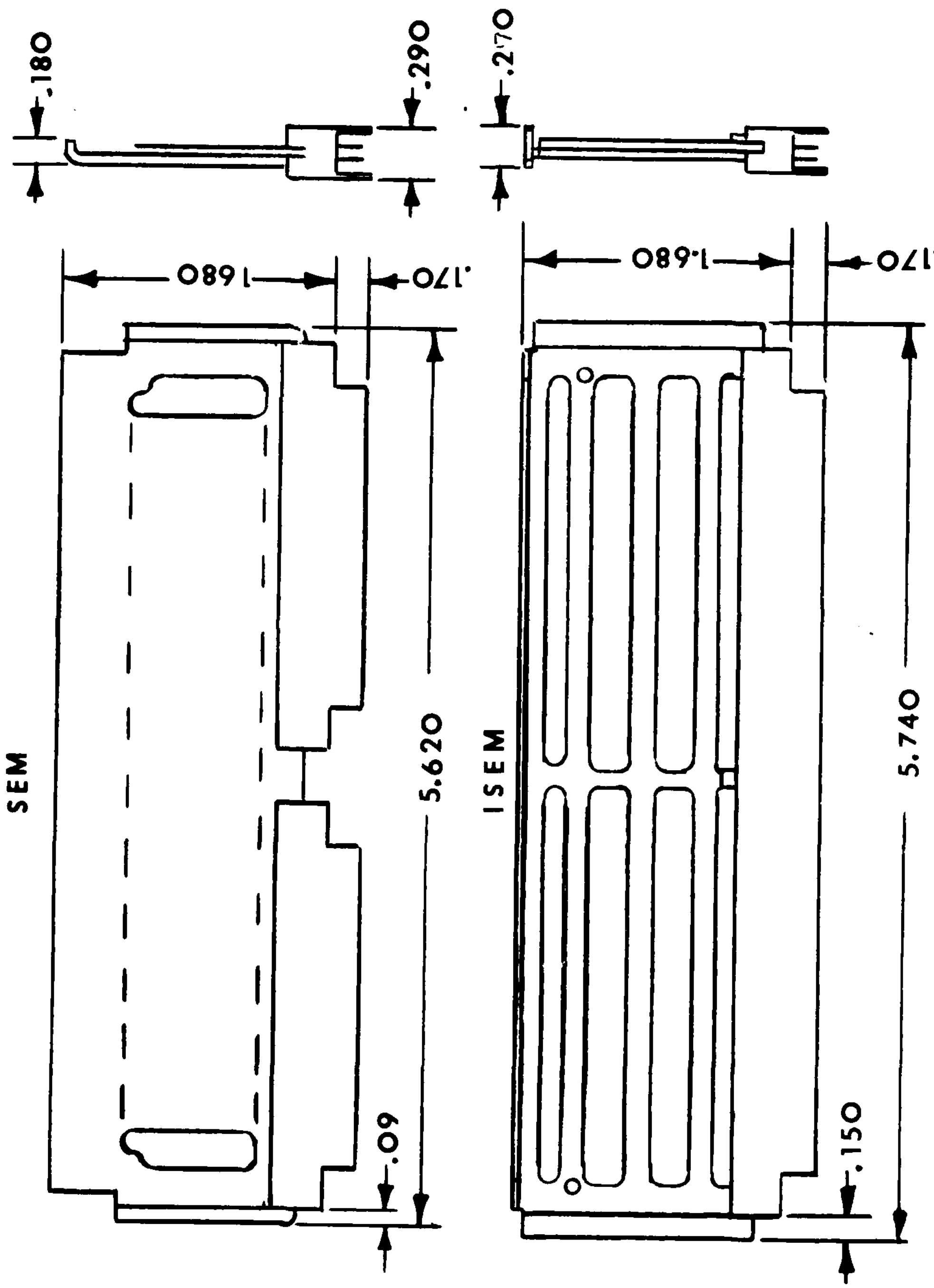

DIP FRAME MODULES

FIGURE V-2

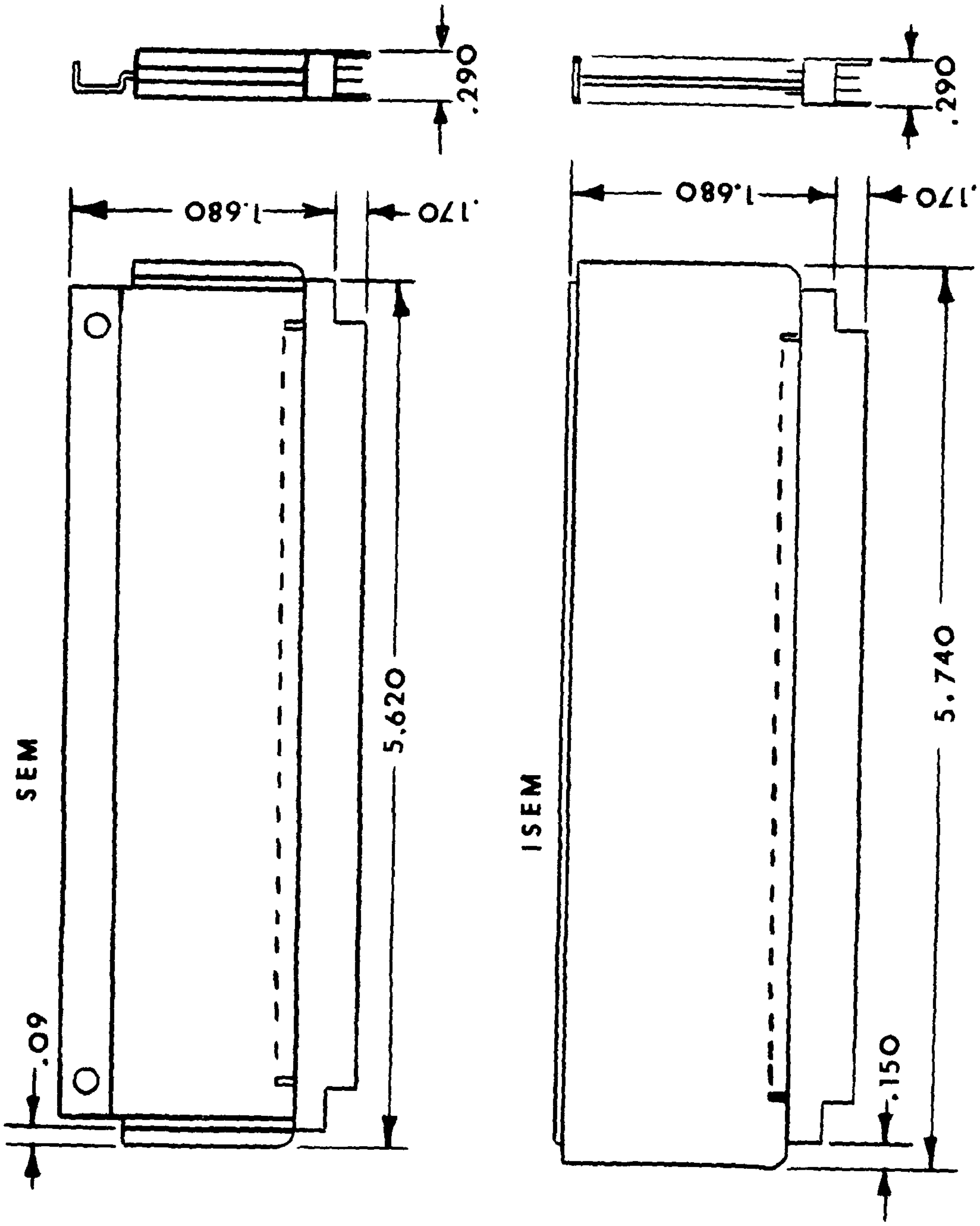

CENTER FRAME MODULES

FIGURE V-3

The final thermal interface consideration is between the component and the frame. Since the total contact area depends mostly on the component which is defined in MIL-M-38510C, it is beyond the scope of this task to analyze this area.

For heat flow through the frame, the greater the cross-sectional area, the greater the heat flow. In the case of the DIP frame in which cutouts are present, increasing the rib width and the frame thickness would increase the thermal conduction to the side guide or the "T" top. In increasing the width of the ribs, Figure V-4 shows the maximum width of the ribs. As for the thickness, Figure V-5 shows the maximum allowable thickness.

SEM allows a .150 inch rib width and a .050 rib thickness. ISEM uses a .160 rib width, but keeps a .050 inch rib thickness, even though Figure V-5 shows it can only be .040 inch maximum. Continuing with .050 inch is justifiable, because the DIPS available do not reach the maximum height allowed by MIL-M-38510C. In addition, the advantage of being able to use the SEM connectors, offsets the very small chance that the DIP height would cause the module to exceed the boundaries for .300 pitch.

For the center frame module, the same holds true. If the cross-sectional area increases, so does the thermal conductivity. In this case, only the frame thickness can be changed. Figure V-6 shows the calculation for the maximum thickness for a .300 pitch module. Figure V-6 indicates that a .034 inch thick frame is possible, but a .030 inch frame was chosen for compatibility with SEM connectors.

c. The final variable in increasing the thermal conductance is the length of the heat flow path from the component to the card cage or cold plate.

CALCULATION OF MAXIMUM RIB WIDTH

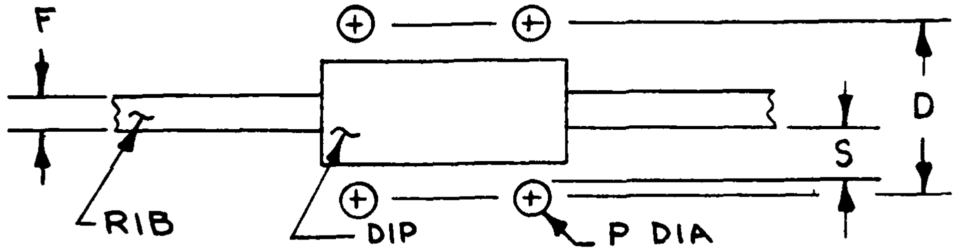

WITHOUT LOCATIONAL TOLERANCES OF THE FRAME RELATIVE TO THE DIP:

$F_{max} = D - P - 2\ (S)$

D = .290 MIN. IAW MIL-M-38510C

P = .065 PAD DIA.

S = .020 MIN.

THEREFORE:

$F_{max} = .290 - .065 - 2\ (.020) = .185$

TAKING INTO CONSIDERATION LOCATIONAL TOLERANCES OF THE FRAME RELATIVE TO THE DIP:

RIB WIDTH TOLERANCE -------------------------------- .010
TOLERANCE FROM THE RIB TO THE RIVET HOLES --------- .007
TOLERANCE FROM LOCATIONAL RIVET HOLE TO DIP HOLES - .008

TOTAL TOLERANCE ------------------------------------ .025

$F_{max} = .185 - .025 = .160$

FIGURE V-4

CALCULATION FOR THE MAXIMUM FRAME THICKNESS FOR A DIP FRAME ON .30 PITCH

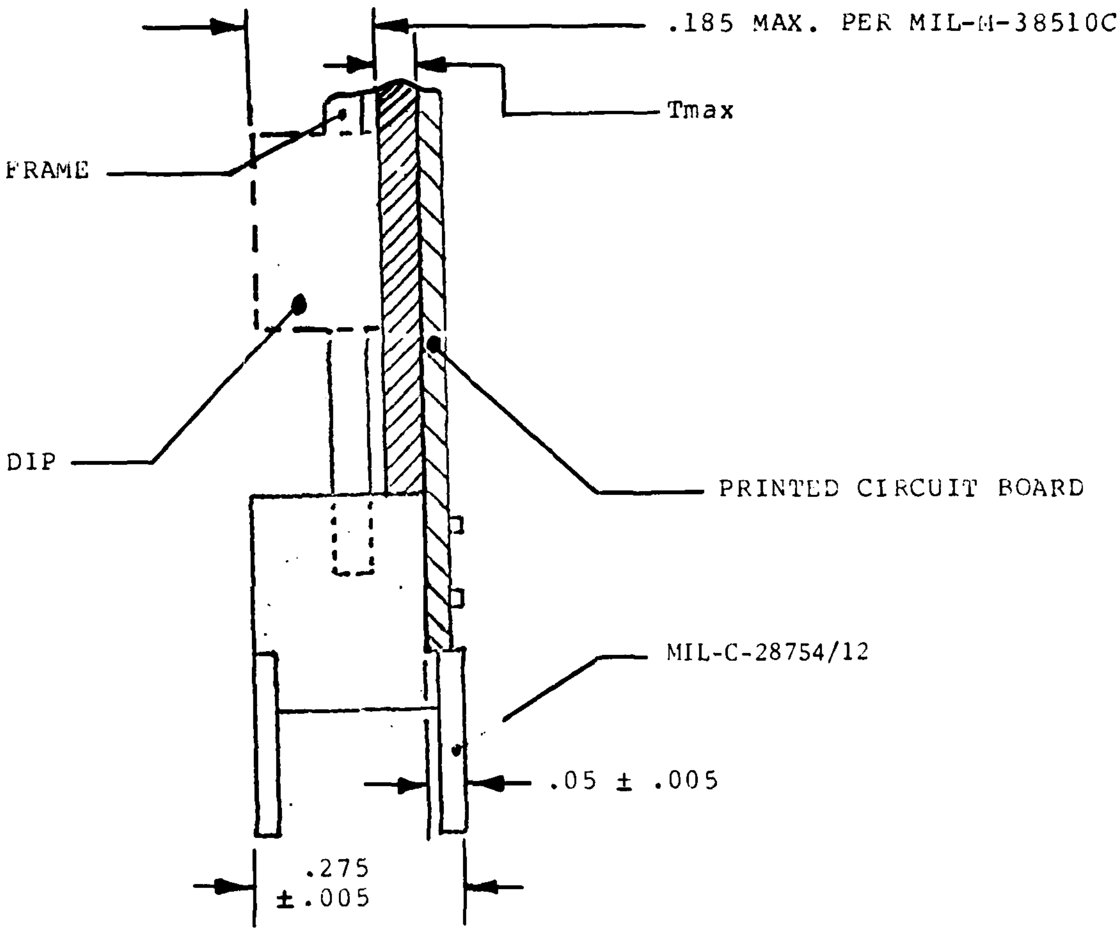

Tmax = .290 - [(.055 + (.290 - .270) / 2) + .185]
Tmax = .040 (this assumes that the dip will reach the maximum allowable height)

FIGURE V-5

CALCULATION FOR THE MAXIMUM FRAME THICKNESS FOR THE CENTER FRAME ON .30 PITCH

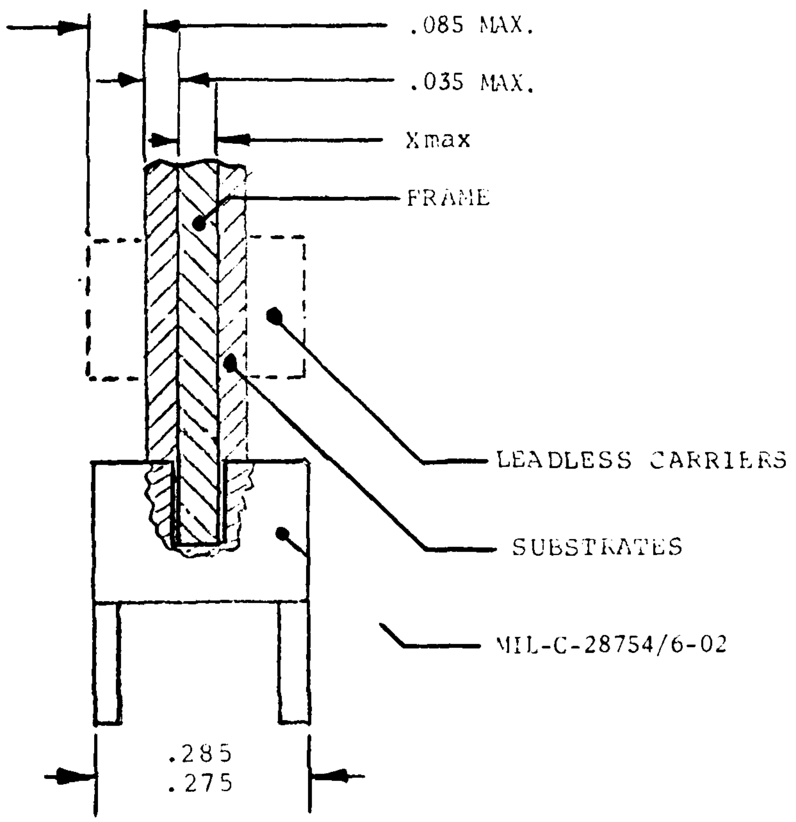

$$X_{max} = .290 - (.085 + .035 + .008 \text{ [solder + adhesive]}) \times 2$$
$$X_{max} = .034$$

FIGURE V-6

For the dip frame, the length of the heat flow path depends upon the rib configuration. The shortest thermal distance for conduction to a top cold plate would be a frame with a vertical rib configuration. For conduction to the card cage, the shortest thermal path would be a frame with a horizontal rib configuration. Both of these configurations may be used with the ISEM, since the ISEM can accommodate both card cage and top cold plate conduction cooling. To standardize a particular rib configuration, the criteria of component density was used. From Table VI-1, the maximum component density occurs on the horizontal rib configuration. Since the width of the component area on the ISEM is the same as on the SEM and the height of the ISEM cannot accommodate two rows of DIPS vertically, using a vertical rib configuration on the ISEM gives nearly the same DIP population as on the SEM. With a horizontal rib configuration, three rows of DIPS can be fitted into the added height of the ISEM, while the SEM could only fit one. This results in the higher DIP density of the horizontal rib configuration. Figure V-7 shows an ISEM module with components.

d. The center frame module has no problems concerning direction of heat flow, since there are no frame cutouts.

e. Some of the more exotic printed wiring boards which are designed for greater heat transfer by conduction are the aluminum core boards and the ceramic on metal boards.

The advantages of using these printed wiring boards are:

(1) Frames for DIP and center fin module could be eliminated, reducing the module cost due to tooling and frame fabrication.

(2) Module assembly would be cheaper and simpler due to the elimination of the frames.

IMPROVED SEM 2A OUTLINE

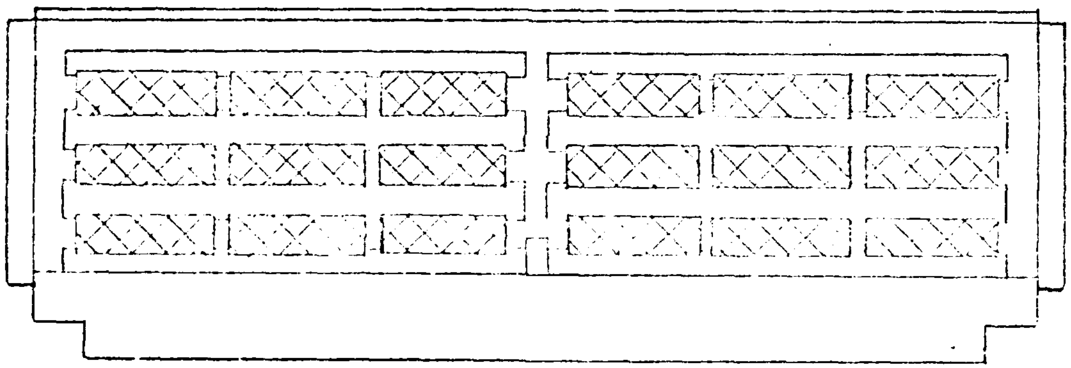

SHOWN: EIGHTEEN 16-PIN DUAL IN-LINES (.750" LONG)

FIGURE V-7

(3) The thermal conductivity for the DIP frame would be higher, since there would be more material available.

(4) Different frame configurations required for different conditions for the DIP module would be eliminated.

2. The material for the frame requires the following properties, as a result of the mechanical analysis:

a. It should have a high thermal conductivity.

b. It should be ductile and forgeable, since the fabrication process is by impact extrusion. The reason for using impact extrusion is discussed in Section VI.

c. It should be corrosion resistant.

d. It should have a high yield strength to be able to withstand extraction forces, insertion forces, and contact pressure forces exerted by the Belleville washers.

e. It should be inexpensive.

f. It should be readily available.

Table V-2 gives a list of possible material to use for the frame. The SEM uses aluminum 5052, the common aluminum used for forming. Its properties are all very good, except for the thermal conductivity and forgeability. When compared with aluminum 1100 or 6101, the thermal conductivity of aluminum 5052 is only 63.6% of the other two. Both aluminum 1100 and 6101 are forgeable. Aluminum 1100 has a slightly higher thermal conductivity than 6101, but shows a lower yield strength. It is desirable to have a high yield strength, since the thickness of

TABLE V-2
MATERIAL SELECTION

MATERIAL	THERMAL COND. BTU-IN/ HR FT.^{2} °F	FORMABILITY (COLD)	MACHINABILITY	CORROSION	YIELD STR (KSI)	FORGEABILITY	* STK FORMS
AL 5052 H32	960	FAIR	MED	GOOD	28	--	STBWPO
AL 6061 T6	1160	MED	MED	GOOD	40	--	STEBPWF
AL 1100 H16 H14	1530 1530	FAIR GOOD	MED MED	GOOD GOOD	20 17	GOOD GOOD	STEBWFO STEBWFO
AL 3003 H14 H16 H18	1100 1100 1070	FAIR MED MED	MED MED MED	GOOD GOOD GOOD	21 25 27	GOOD GOOD GOOD	ALL ALL ALL
AL 6101 T6	1510	FAIR	FAIR	GOOD	28	FAIR	TPEB
CU 110	2712	GOOD	POOR	GOOD	10-45	GOOD	ALL

DENSITY OF CU = .323 lb/CU IN.

DENSITY OF AL = .099 lb/CU IN.

*STK FORMS: B - BAR OR ROD, E - EXTRUSION, F - FORGING OR FORGING STK,
O - FOIL, P PIPE, S - SHEET OR PLATE T TUBE, W WIRE

the DIP frame is only .050 inch, while the center frame is only .032 inch. With regard to availability, aluminum 1100 is very common, while the 6101 can be obtained only in large production quantities, in excess of 1000 lb per purchase.

The thermal conductivity for copper is even better. It is 1.796 times more thermally conductive than aluminum 6101, and possesses good ductility, availability and strength. But copper does have a few drawbacks. It is 3.263 times heavier than aluminum and 3.892 times more expensive by volume. If copper is considered from a system standpoint, with regard to power density, a module with a copper frame gives the same watts per ounce as a module with an aluminum frame, but consumes less system volume. In other words, more high powered components may be placed on a copper frame than an aluminum frame for the same watts per module. This would mean less copper frame modules would be required than aluminum frame modules for the same number of components required in a system based on power only. Table V-3 shows the calculation involved. The cost of using a copper frame, based on the total module cost, comes to an increase of .05% over that of an aluminum module.

In conclusion, copper may be used for high wattage, small packaging volume applications, where weight is not a critical factor. If weight is critical and the total wattage of the module is low, it is more cost-effective to use aluminum 6101.

C. STRUCTURAL ANALYSIS

1. Because of the requirement for compatibility between the SEM and the ISEM, and because of component interchangeability between them, the SEM and ISEM share many of the same structural features. As a result of this, the method of attaching the ISEM frame to the connector is the same as the SEM. Figure V-5 and V-6 show how the frame is bonded to the connector. The cross-sectional area of the tab on the 1A and 2A

TABLE V-3

COPPER / ALUMINUM FRAME TRADEOFF

1. COST AND WEIGHT TRADEOFF

PARAMETER	ALUMINUM	COPPER
DENSITY (POUNDS PER CUBIC INCH)	.098	.323
COST PER POUND (DOLLARS PER POUND)	.51	.60
WEIGHT OF A 2A MODULE (POUNDS)	.094	.169
MATERIAL COST OF A 2A MODULE (DOLLARS)	.048	.10

ASSUMING THAT THE COST OF A 2A MODULE IS 100 DOLLARS PER MODULE, THE COST OF MATERIAL FOR EITHER ALUMINUM OR COPPER BECOMES INSIGNIFICANT.

2. ANALYSIS OF POWER DENSITY FOR 30 ISEM MODULES IN A 1/4 ATR BOX

PARAMETER	ALUMINUM	COPPER (K=1.5)	COPPER (K=2.0)
MODULE WEIGHT (OUNCES)	1.5	2.7	2.7
BOX WITH OUT MODULES (OUNCES)	56.2	56.2	56.2
WEIGHT OF BOX DIVIDED BY THE NUMBER OF MODULES (OUNCES)	1.87	1.87	1.87
WEIGHT OF MODULE PLUS WEIGHT OF BOX PER MODULE (OUNCES)	3.37	4.55	4.55
THERMAL RESISTANCE FROM FRAME RIB TO AIR (C/W)	4.1	4.1	4.1
THERMAL RESISTANCE FROM HEAT SINK TO RIB (C/W)	3.4	2.27	1.7
THERMAL RESISTANCE FROM HEAT SINK TO AIR (C/W)	7.5	6.37	5.8
WATTS PER MODULE	10.0	11.8	12.9
[illegible] (W/OZ)	[illegible]	[illegible]	[illegible]

DIP frame and the amount of bonding surface area determines the strength of the assembly. This calculation is shown in Figure V-8. The 2A DIP frame also has the problem of a long span between attachment to the connector. This allows a deflection between the attachment point and a consequent weakness, because of the cutouts in the frame. The calculations for the deflection are in Figure V-9. As a result of this, a center support has been added to attach the frame to the connector, which helps in two respects:

a. It helps the frame during handling before the printed circuit board is added, by rigidizing the frame.

b. It helps dissipate the heat from the center of the module to the top.

The center frame module does not have the problems of the DIP frame, because there are no cutouts to weaken the frame structure. The "T" top helps stiffen the frame, regardless of the .030 frame thickness.

The attachment of the printed circuit board to the frame is similar for both SEM and ISEM. It is attached by using an epoxy. An added feature required on the DIP frame is the use of locational rivet holes. These holes serve the following purposes:

a. help attach the printed circuit board to the frame.

b. can be used as a locating feature for automatic insertion tools.

c. help locate components on the printed circuit board, relative to the frame cutouts.

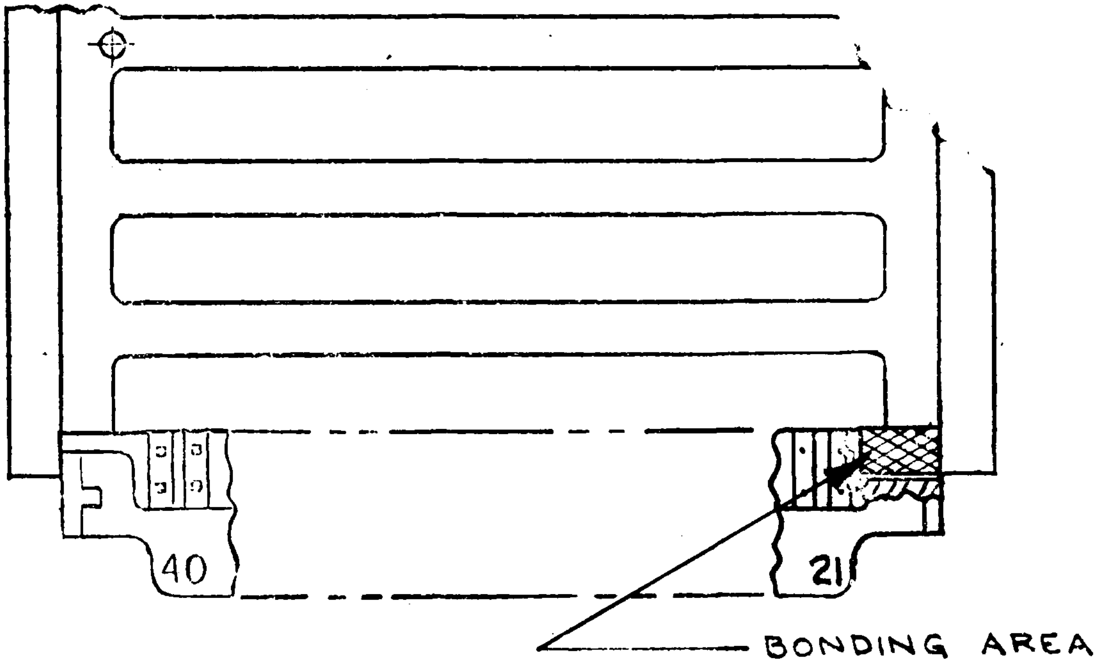

TAB BONDING AREA = (2 x .195 x .110) + (.05 x .195) = .053 IN^2

2A CENTER TAB BONDING AREA = (2 x .10 x .08) + (.05 x .10) = .021 IN^2

SHEAR STRENGTH FOR ADHESIVE (C1, 200AS179-1) = 1500 PSI MIN

2A MODULE'S FRAME/CONNECTOR BONDING STRENGTH

(.053 + .053 + .021) 1500 = 190.5 lb_f

MAXIMUM REQUIRED EXTRACTION/INSERTION FORCE = 62.5 lb_f

1A MODULE'S FRAME/CONNECTOR BONDING STRENGTH

(.053 + .053) 1500 = 159 lb_f

MAXIMUM REQUIRED EXTRACTION/INSERTION FORCE = 25 lb_f

CALCULATION OF FRAME TAB STRENGTH

FIGURE V-8

NAC TR-2217

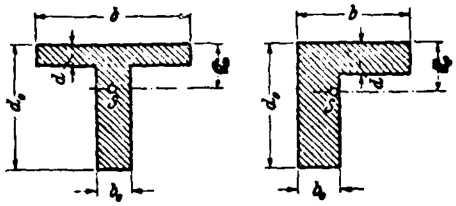

Fig. 1
T-Beam Cross Sections

$b = .275$ in.
$d = .05$ in.
$b_c = .05$ in.
$d_c = .10$ in.

$B = b_c/b = .05/.275 = .182$
$Q = d/d_c = .05/.10 = .50$

$N = 1/2\{[B + (1-B)Q^2] / [B + (1-B)Q]\}$
$N = .327$
$U = 4[N^3 - (1-B)(N-Q)^3 + B(1-N)^3]$
$U = .379$

c = distance to the neutral axis $= N \times d_c = .327 \times .10 = .033$ inch

I = moment of inertial $= U\,(b\,d_c^3)/12 = (.379 \times .275 \times .10^3)/12$

$I = .00000869$ in^4

THE FLEXIAL STRESS $= F = Mc/I$

M = moment for a fixed beam $= PL/8$

therefore: $F = PLc/8I$
substituting c and I: $F = .033\,PL/\,8(.00000869) = 475\,PL$

The force, P, required to exceed the elastic limits of the "T" top assuming the frame material is AL 6061 (yield strength = 28 ksi) is:

2A (no center support; L = 5.16 in.) $P > 28000/475(5.16) = 11.5$ lbs

2A (with center support; L = 2.5 in.) $P > 28000/475(2.5) = 23.6$ lbs

1A (L = 2.16 in.) $P > 28000/475(2.16) = 27.6$ lbs

The calculation above for the 2A dip frame shows a 2 to 1 increase in the amount of force required to deform the frame. Of course, the calculation assumes that the center support will not buckle. This is a good assumption when the frame is assembled with a printed circuit board.

"T" TOP FRAME DEFLECTION

FIGURE V-9

VI. PRODUCIBILITY

A. FRAME PRODUCIBILITY

1. An item of major concern in the production of the frame is the fabrication method of the "T" top.

The SEM frame is a sheet metal piece with a bent over lip at the top. Thus, the use of forming in fabricating the frame can be easily incorporated. In the case of the ISEM, the requirement for the top to be in a shape of a "T" changed the whole prospective in fabrication techniques. Forming, in this case, is still possible but the method in forming the top must be considered carefully. This forming method consists of bending a .025 inch thick AL 5052 90 degrees to form one edge of the "T," then bending 180 degress in the opposite direction to obtain the "T." This method does not form a true "T," but it does give the top surface area as does the "T" top. Problems involved in using this technique are mainly due to the small bend radius required and the production of a dip frame with a thickness of .05 inch.

Other methods investigated were machining, brazing-on of the "T" top, extruding, forging, and impact extrusion. Due to the cost and difficulty in maintaining the required flatness of the top, impact extrusion was evaluated to be the optimum fabrication technique for production.

The method for using impact extrusion varies with the type of frame. In the case of the Center frame, impact extrusion of the frame is the only step required to fabricate the complete frame. In the case of the DIP frame, the "T" is impact extruded first, then the configuration for forming is blanked out, and finally, the frame is formed. Cost for producing the DIP frame will be higher than for the Center frame, but the cost for both frames would not be much greater than the equivalent SEM frames.

Accurate tooling cost and parts cost are not available for analysis, since the fabrication technique is fairly new. Parts usually impact extruded are not as small as the frames, and the fabrication can be done only by a few commercial vendors. Therefore, it is recommended that more vendor sources be developed.

2. Tables VI-1 and VI-2 contain the calculated maximum device population for existing SEM modules and ISEM modules. These calculated values disregard tolerances, manufacturing processes such as automatic insertion tools, and producibility in a production run. These calculations are also based on the package sizes denoted in Table VI-1 and VI-2 and the maximum circuit mounting area given in Table V-1.

The problems of production tolerances, tolerances required for use of automatic insertion tool, and producibility are taken into consideration in Figure VI-1. The analysis is only for the DIP frame, since orientation and length of the cutouts on the frame determines the maximum device population. There is no special orientation or position required of the flatpacks for the center fin module.

The 2A rib length is 2.53 inches. For three fourteen-pin DIPS at .796 inch length, the minimum rib length requirement is 2.438 inches. This means that the module can accommodate three rows by three columns of DIPS per half of a 2A DIP frame. This totals out to be eighteen DIPS per module, as indicated in Table VI-1. Figure VI-2 shows this configuration.

Likewise, the required rib length for a sixteen-pin DIP is 2.738 inches. This means only twelve of these packages can be fitted into a 2A frame. Figure VI-3 shows the module.

Figure VI-3 also shows that an eighteen- and twenty-pin DIP have basically the same package length, (.875 inch long) as the sixteen-pin DIP. Therefore, the same number of these DIPS will fit a 2A frame.

TABLE VI-1

MAXIMUM DEVICE POPULATIONS

DUAL IN-LINES	EXISTING SEM		IMPROVED SEM		IMPROVED/EXISTING	
	1A	2A	1A	2A	1A	2A
16 PIN (.75 LG)	6	12	9	18	1.50	1.50
16 PIN (.875 LG)	5*	12*	6	12	1.20	1.00
18 PIN	4	8	6	12	1.50	1.50
20 PIN	4	8	6	12	1.50	1.50
22 PIN	2+	4+	5*	12*	2.50	3.00
24 PIN	1	4	1+	4+	1.00+	1.00+
28 PIN	1	3	1+	3+	1.00+	1.00+
40 PIN	1	2	1+	2+	1.00+	1.00+

* DENOTES VERTICAL DIP MOUNTING ORIENTATION FOR MAX DENSITY

+ DENOTES THAT MODULE CAN ACCOMODATE AN ADDITIONAL HORIZONTAL ROW OF 0.3 INCH CENTER DIPS WHEN MIXING IS CONSIDERED

TABLE VI-2

MAXIMUM DEVICE POPULATIONS

FLATPACKS	EXISTING SEM		IMPROVED SEM		IMPROVED/EXISTING	
	1A	2A	1A	2A	1A	2A
14 PIN (.25 X .25)	16	40	24	60	1.50	1.50
16 PIN (.25 X .375)	16	40	24	60	1.50	1.50
24 PIN (.375 X .625)	6	14	12	28	2.00	2.00
40 PIN (MOT 621-01)	2	8*	4	12	2.00	1.50

* DENOTES UNDESIRABLE FLATPACK LEAD MOUNTING ORIENTATION (AXIS OF FLATPACKS LEADS PARALLEL TO GUIDE RIB HEIGHT DIMENSION)

CALCULATED MAXIMUM DEVICE POPULATION

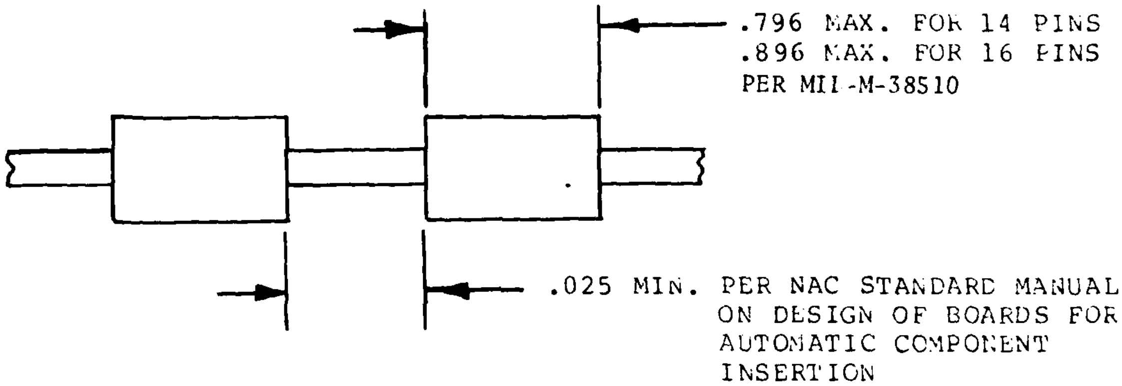

THEREFORE:

	NO. OF DIPS	LENGTH REQUIRED OF RIB
16 PIN DIP	1	.896 MIN
	2	1.817 MIN
	3	2.738 MIN
14 PIN DIP	1	.796 MIN
	2	1.617 MIN
	3	2.438 MIN

FIGURE VI-1

IMPROVED SEM 2A OUTLINE

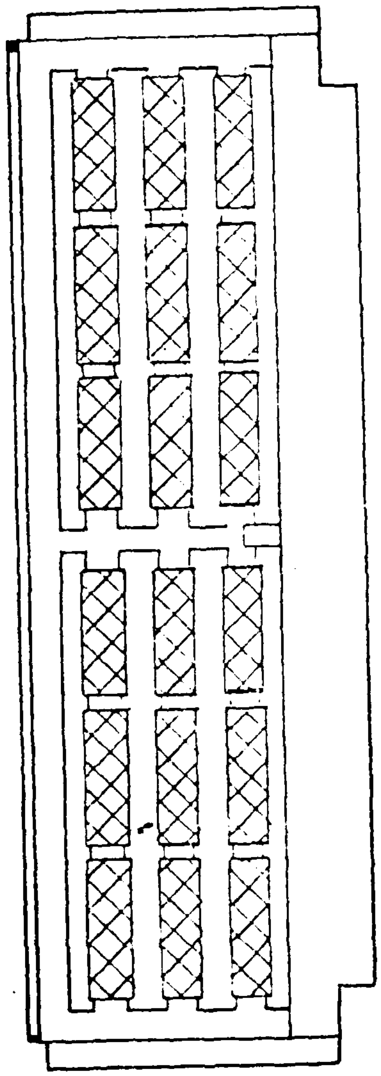

SHOWN: EIGHTEEN 16-PIN DUAL IN-LINES (.750" LONG)

FIGURE VI-2

IMPROVED SEM 2A OUTLINE

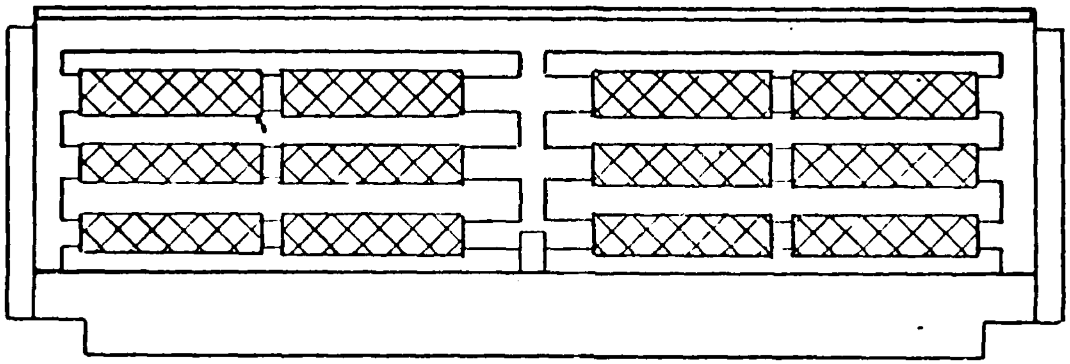

SHOWN: TWELVE 20-PIN DUAL IN-LINES

LAYOUT QUANTITY APPLICABLE FOR:

16-PIN DUAL IN-LINES (.875" LONG)

18-PIN DUAL IN-LINES

20-PIN DUAL IN-LINES

FIGURE VI-3

For a 1A DIP frame, the rib length is 2.16 inches. Even though the total allowable width is 2.44 inches, .160 inch is used for the transition of the bend on the side guides. This leaves 2.28 inches for the total span. Since this 2.28 inches is still less than the 2.438 inches minimum rib length requirement for three DIPS, the rib length of 2.16 inches was chosen to match the 2.16 inch span for the locational rivet holes. This saves an extra step required to locate the cutout.

The figures indicate that only three rows by two columns of DIPS are possible. The discrepancy with Table VI-1 is due to the fact that a .750 inch package butted end for end gives 2.250 inches. If .01 inch is allowed between the DIPS, the total space required, in addition to the 2.250 inches, is .020 inch. The total required becomes 2.270 inches, which is less than the 2.28 inch maximum span of the module.

Figure VI-4 shows the frame configuration for DIP components which are .300 inch centers between rows of lead holes. The rib spacing is .400 inch.

The minimum possible rib spacing is given in Figure VI-5 for the ISEM DIP frame.

The ribs are grouped as close to the top of the module as possible. This is to allow for the maximum amount of circuit paths to run between the bottom row of DIPS and the connector for input/output lines.

B. CONNECTOR

1. The analysis will only deal with the 2A DIP connector. The 1A DIP frame, 1A center frame, and 2A center frame were all made compatible with existing SEM connectors. Therefore, the only connector design necessary was for the 2A DIP frame.

The connector design would like to achieve two goals:

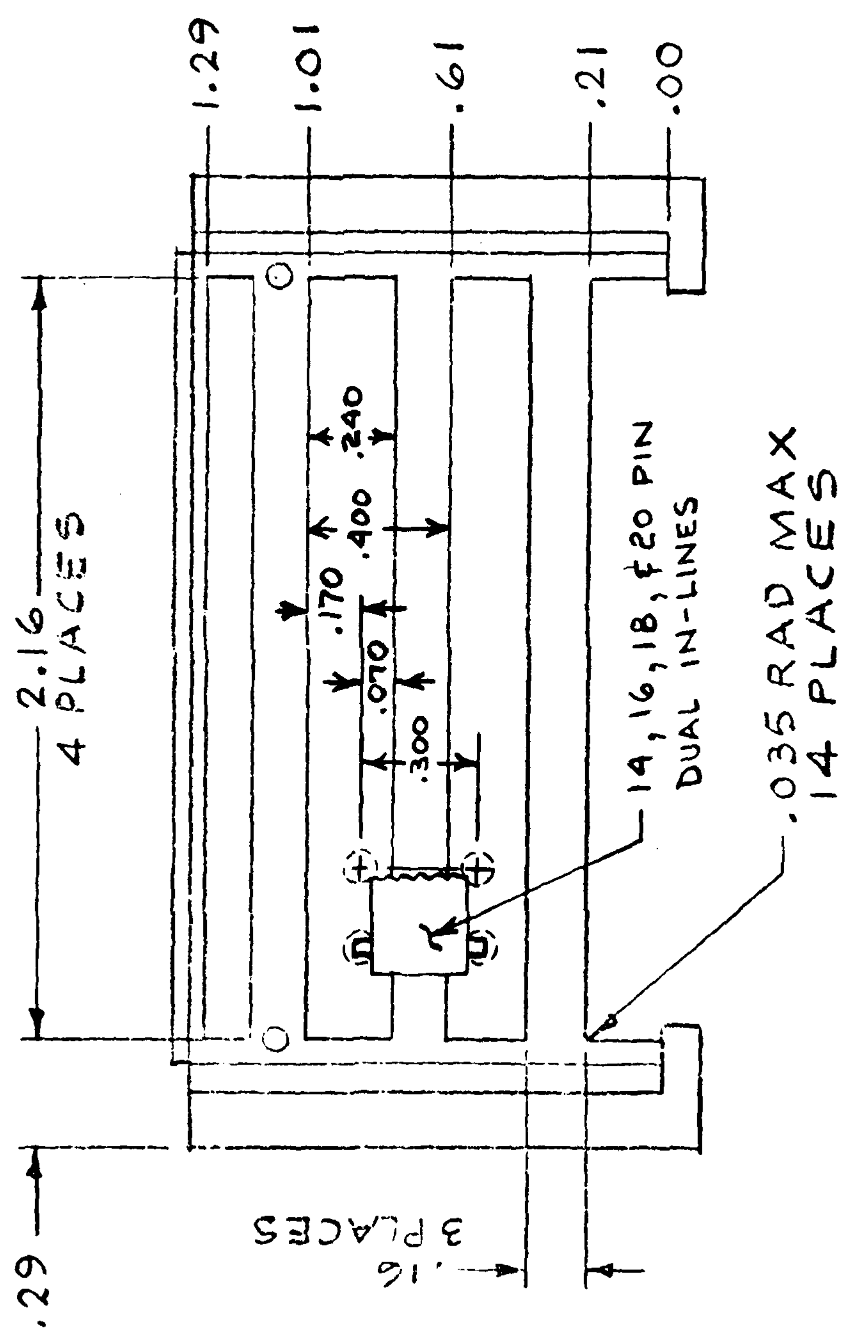

DIP FRAME RIB LAYOUT

FIGURE VI-4

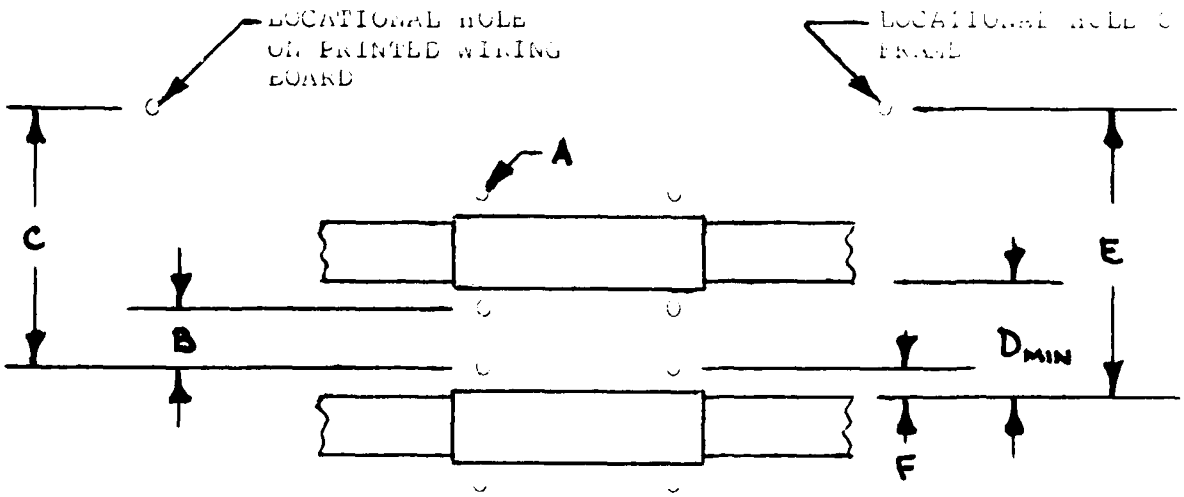

$D_{min} = 2F + E$ = MIN. RIB SPACING

$F = E - C$

$E = A + .010$

FOR .300 WIDE DIP:

$A = .062$ DIA

$E - C = .034$

THEREFORE:

$D_{min} = 2(E-C) + A + .01$

$D_{min} = 2(.034) + .062 + .01$

$D_{min} = .240$

CALCULATION FOR MINIMUM RIB SPACING

FIGURE VI-5

a. Keep the method of attachment between 1A and 2A SEM and ISEM DIP frames and connectors as similar as possible. Doing this would simplify assembly, setups and eliminate the need for assembly learning curve.

b. Minimize the assembly time required for keying pin insertion and pin shield assembly.

The attachment of the frame to the connector is accomplished by bonding tabs on the side guides of the frame, similar to the 1A DIP frame, to the connector and bonding a third tab into a grooved base at the center of the connector. Figure VI-6 shows the attachment of the module. Figure VI-7 shows the attachment of the center tab.

The option of whether to use an insert in the connector for pressing the keying pins in, rather than bonding, was analyzed. From calculations shown in Figure VI-8, the true positional tolerance required for the insert would be .0029 inch. This is much too tight for the connector vendors to hold. Because of this, the keying pins for the connector for the 2A DIP frame will be bonded.

As for the pin shields, it was found that the bonded-on pin shields had a tendency to fall off the connector during wave soldering. Because of this, different pin shield configurations were investigated. These configurations consisted of:

(1) Wrap-around pin shields;

(2) Molded pin shields;

(3) Metal molded pin shields.

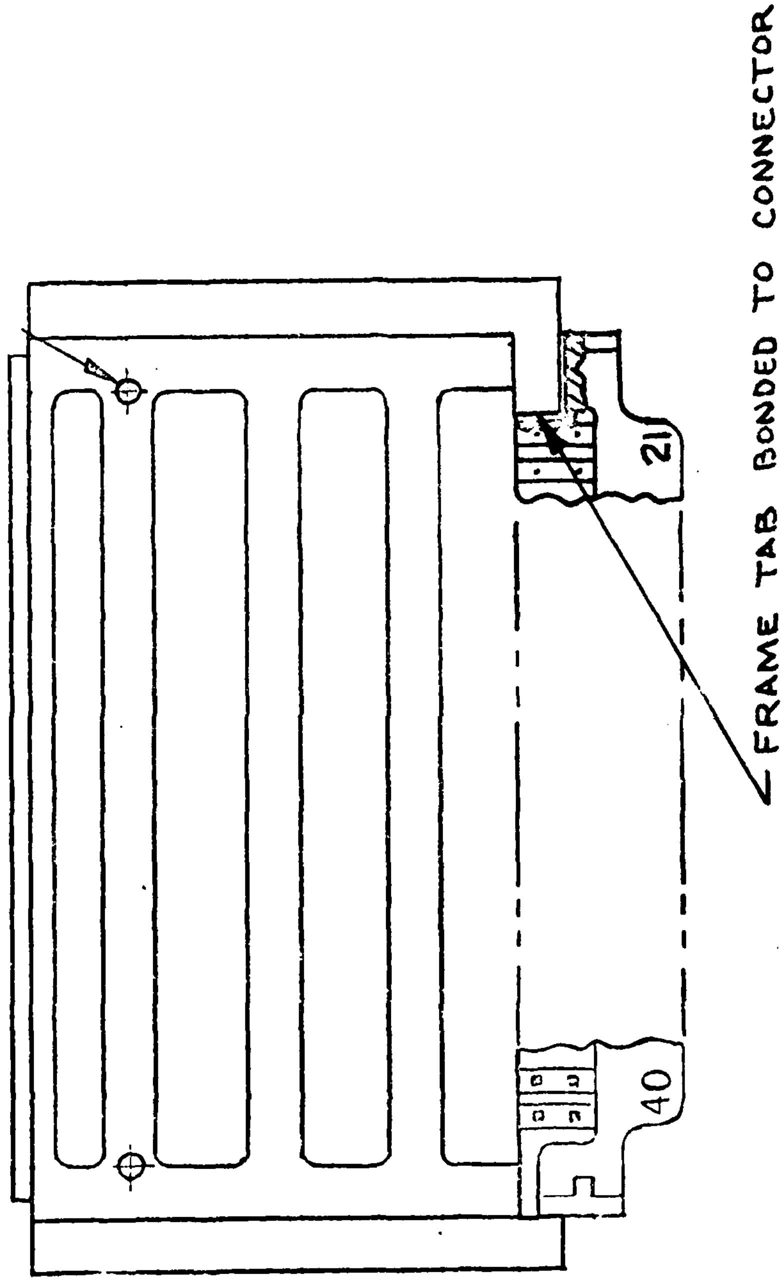

1A DIP FRAME MODULE

FIGURE VI-6

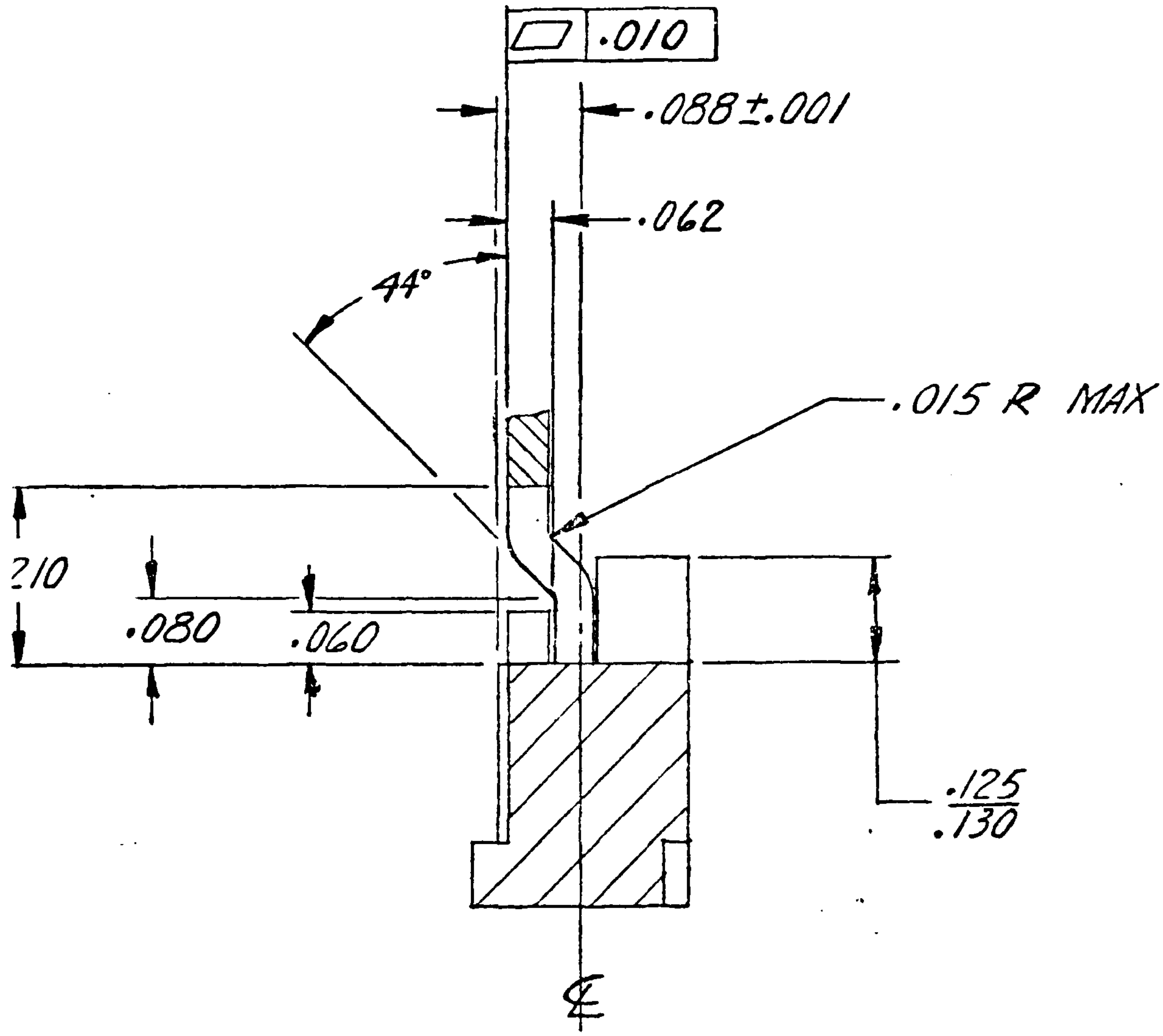

CENTER ATTACHMENT METHOD FOR ISEM 2A LIT FRAME

FIGURE VI-7

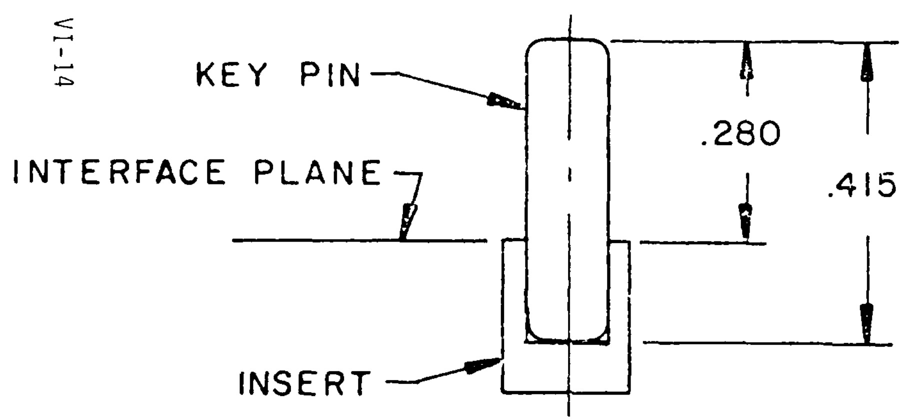

$X = \oplus$ INSERT

$.007 = \oplus$ TIP OF KEYING PIN

$$X = \frac{.007}{.280}(.415 - .280)$$

$$X = .0034$$

$$\circledcirc_{\text{KEY PIN}} = .0005$$

$$\therefore X_{REQ} = .0034 - .0005$$

$$= .0029$$

CALCULATION OF TRUE POSITIONAL TOLERANCE
REQUIRED OF CONNECTOR KEYING INSERTS

FIGURE VI-8

The wrap-around pin shield is a metal shield which wraps around the connector. Difficulty of assembly and reliability of attachment makes this an undesirable part to use.

The molded shield is a shield made of plastic, molded as part of the connector. There is no assembly required since it is part of the connector. The drawback to this method is that the thickness required for the molded shield may require a connector, greater than .290 wide. If the shield thickness is reduced to .030 inch thick, the straightness requirement of the shield could not be met, because of the 5.20 inch length of the 2A shield. Figure VI-9 shows the shield requirements. An additional problem would be warpage during wave solder should the shield thickness be reduced to .030 inch or less.

The metal molded pin shield consists of a metal shield which is molded into the connector. This part increases the cost of the connector. Additionally, there is no assurance that the shield would be as straight as required, or would remain intact during wave solder.

A process change, instead of a connector pin shield redesign, might hold some possibility. The existing SEM pin shield would still be used. During wave solder, the pin shield would be protected by a plastic booty slipped on the connector. This would not only solve the problem of the new connector design, but the existing connector designs as well. The process has not been tested as yet, and should be further investigated.

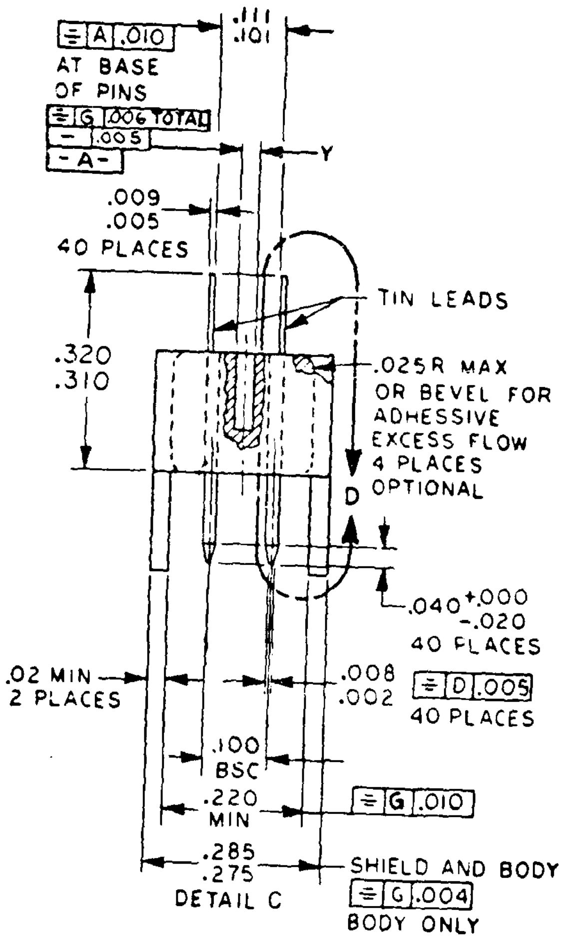

CONNECTOR PIN SHIELD DIMENSIONAL REQUIREMENTS

FIGURE VI-9

VII. COMPATIBILITY

A. COMPATIBILITY ANALYSES

In the analyses of compatibility between existing SEM and improved SEM, the major parameters to consider are card cage compatibility, thermal compatibility, and wire wrap plate compatibility.

1. With respect to card cage compatibility, Table V-1 shows a summary of SEM and ISEM characteristics and dimensional outlines. One of the most significant differences between the SEM and the ISEM in Table V-1 is the span of the module. In increasing the total surface area of the side guides, for a better thermal interface, the overall span of the module changes from 5.620 inches, for the SEM 2A, to 5.740 inches, for ISEM 2A. For the SEM 1A, the span was changed from 2.620 inches to 2.740 inches. As a result of this, card cages for the existing SEM modules will not accept ISEM modules. However, card cages made for the ISEM modules will accept both SEM and ISEM modules.

As also evident from Table V-1, ISEM modules are also designed for .300 inch pitch. Even though this pitch presents problems of short component lead length projections for soldering, restrictions on component heights and restriction of air flow for direct air impingement, the advantages outweigh the disadvantages. In a systems application, a .300 inch pitch card cage means less volume for a given amount of circuitry versus a larger module pitch. In addition, if any effort in mixing existing SEM with ISEM modules in a card cage other than at .300 pitch was attempted, the result would be either volume inefficient packaging or a nonstandard card cage. These factors lead to a conclusion that .300 pitch is best suited for an ISEM module.

2. The increased span of the ISEM module also has an effect on the thermal capability of the ISEM card cage. It is desirable to have an ISEM card cage with the same envelope as the SEM card cage. Therefore, the center to center width of the ISEM card cage should be six inches. Since the ISEM module is 5.74 inches wide, less than .130 inch is left on either side of the card cage for water or air channels to dissipate the heat from the modules. Appendix D analyzes the different possible card cage cooling configurations and their thermal capability, taking into account the possible types and size of channels possible.

The thermal compatibility is comprised of three parts.

a. Compatibility with the side guide interfaces to the card cage;

b. Compatibility for top plate cooling;

c. Compatibility for forced convection over the fin.

The side guide interfaces to the card cage consist of clips and wedges. These interfaces are described in greater detail in Section IX. The side guide for the ISEM is .150 inch wide versus .090 for existing SEM. Even though there is mechanical compatibility with the clips and wedges, the effectiveness is greater for ISEM than for existing SEM in thermal conduction to the card cage.

Likewise for top plate cooling, the ISEM "T" top offers more contact area than the SEM "L" top. This increases the effectiveness of top plate cooling. Another factor which increases the effectiveness of top plate cooling is the use of Belleville washers. They offset the dimensional tolerances in the height of the modules and increase the contact pressure between the top of the modules and the cold plate. Unfortunately, the Belleville washers can only be used with ISEM modules. A

SEM module will fit in a slot with accommodations for the Belleville washers, but the washers will have no effect.

Only certain SEM configurations lend themselves to direct air impingement. The ISEM allows all configurations to be cooled by this method.

As can be seen, the side guide of the SEM module has a .280 inch wide shoulder to border the printed wiring board. The ISEM makes a direct transition from a .050 inch side guide to the area the printed circuit board is mounted. This eliminates the barrier to the components for direct air impingement. For increased thermal efficiency of the ISEM versus SEM, see Section IV.

3. Wire wrap plate compatibility of the SEM and ISEM is centered around the 100-pin connector. The 1A existing SEM and ISEM modules use identical 40-pin connectors. Thus, either a 1A SEM or ISEM module would fit the same wire wrap plate.

For the 2A modules, the existing SEM DIP frame uses two 40-pin connectors, while the ISEM uses a 100-pin connector. See Appendix B for ISEM module and frame drawings. With the addition of the extra twenty pins, the wrap plate loses the center support rail. Figure VII-1 shows a 2A SEM wrap plate versus a 2A ISEM wrap plate. The loss of this center support rail weakens the wrap plate, and allows for deflection of the plate upon insertion of a module. In Appendix C is an evaluation of the deflection of the wrap plate.

The conclusions drawn from the calculations in Appendix C are:

a. The unbraced wrapost plate, 20 x 6 inches, will not support the maxinum insertion force without deflection beyond the .020 inch imposed limit.

b. A support spacing of 3.6 inches is required for the wrapost plate.

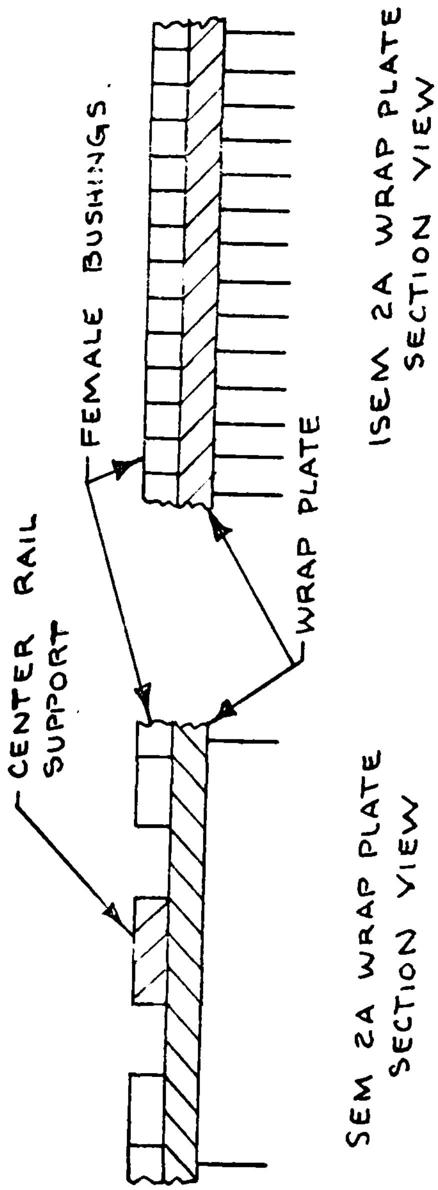

SEM VERSUS ISEM 2A CARD CAGE WRAP PLATE

FIGURE VII-1

VIII. EXTRACTOR

A. MECHANICAL DESIGN

1. An extractor was designed which was compatible with both existing SEM and ISEM modules in an ISEM card cage. The existing SEM extractor was not considered for the ISEM because:

a. The holes required on the frame take up possible circuit area.

b. The extractor interferes with component location on the modules.

c. The extractor gives no mechanical advantage, making the extraction of the 100-pin connector difficult.

d. The extractor is bulky and hard to use.

e. Redesigr would have been required, because of the "T" top on the ISEM modules.

The proposed extractor design works on the principle of prying the top lip of the module, using the card cage guide rails as the pivot point. This is shown in Figure VIII-1.

The amount of travel the module requires in the Y direction as shown in Figure VIII-1, to be fully disengaged from the female connector on the wrap plate, is .150 inch. This means that point A in Figure VIII-1 must travel a distance of .150 inch in the Y direction to extract the module.

Figure VIII-2 shows the rotation of the extractor arm and the angles which it goes through. From Figure VIII-2, the calculation of the amount of rotation required of the extractor to move point A .150 inch in the Y direction is as follows:

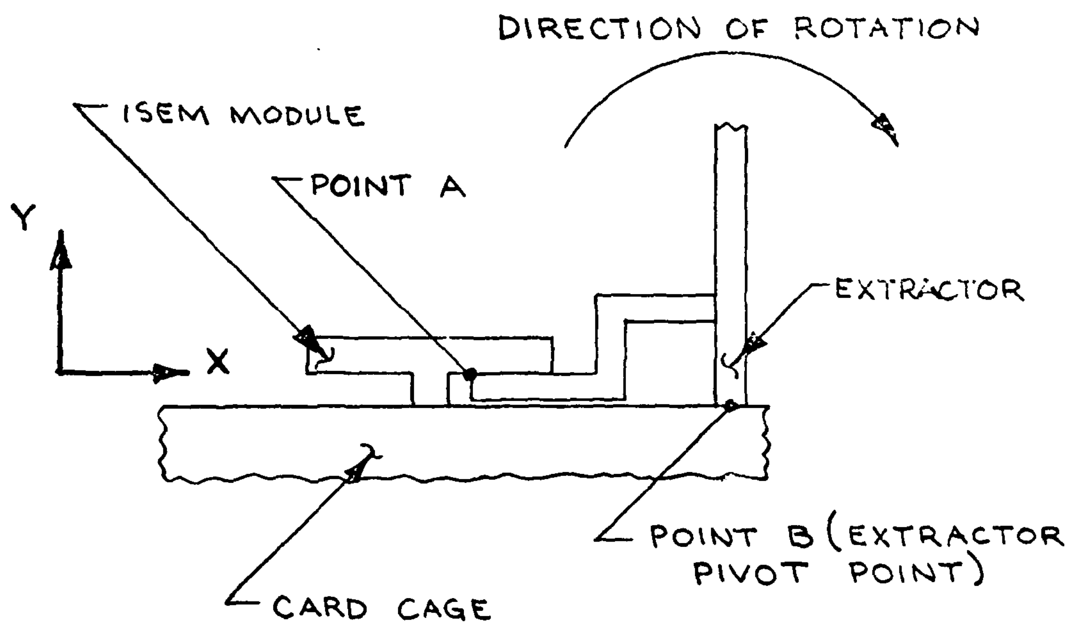

EXTRACTOR ILLUSTRATION

FIGURE VIII-1

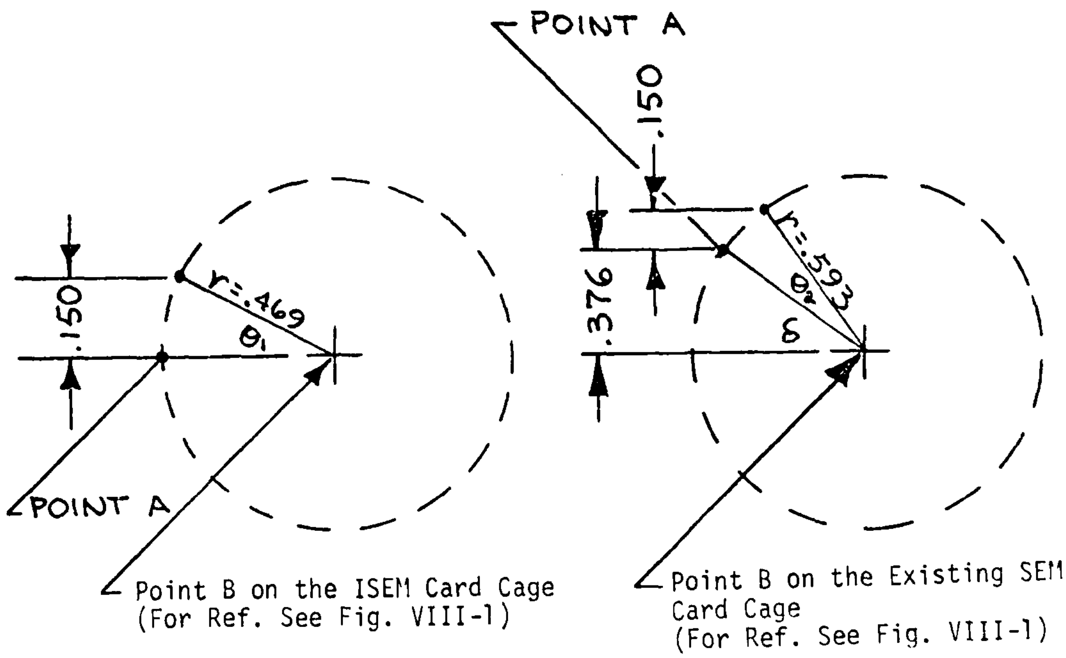

EXTRACTOR ROTATIONAL MOVEMENT

FIGURE VIII-2

r = distance from point A to point B

θ_1 = angle required to move point A a distance of .150 inch in the Y direction for an ISEM card cage.

θ_2 = angle required to move point A a distance of .150 inch in the Y direction for an existing SEM card cage.

For the ISEM card cage:

$$\theta_1 = \sin^{-1}\frac{(.150)}{r} = \sin^{-1}\frac{(.150)}{(.469)}$$

$$\theta_1 = 18.66°$$

For the existing SEM card cage:

$$\theta_2 = \sin^{-1}\left(\frac{.376 + .150}{.593}\right) - \delta = 62.5° - \delta$$

$$\delta = \sin^{-1}\left(\frac{.376}{.593}\right) = 39.35°$$

$$\theta_2 = 62.5° - 39.35° = 23.15°$$

The calculations indicate that a greater angle of rotation is required to extract a module in an existing card cage, than in an ISEM card cage.

If a force analysis is done, the mechanical advantage of the extractor can be calculated. Figure VIII-3 shows the force breakdown.

Where: F1 = force exerted at the top of the extractor (operator's force)

F2 = frictional force

F3 = vertical component of F2 (force required to extract the module)

r1 = lever arm from the top of the extractor to the pivot point B

r2 = distance from point A to point B (see figure VIII-1)

θ = sweep angle for the extractor

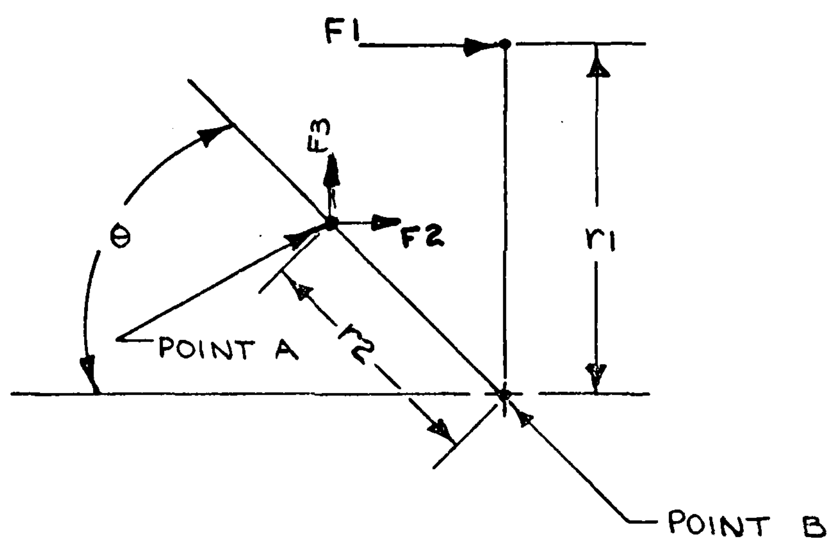

EXTRACTOR FORCE ANALYSIS

FIGURE VIII-3

Neglecting any frictional forces, the forces at point B balance out to be:

$$(F1)(r1) = (F3)(R2)\cos\theta$$

Relating the force by the operator to the force on the module results in the following equation:

$$F3/_{F1} = \frac{(r1)}{r2\ (\cos\theta)}$$

The variables r1 and r2 are dependent on the extractor design. The angle θ is dependent on the card cage configuration; existing SEM or ISEM card cage. At present, there are two extractor designs, one for the existing SEM card cage and one for the ISEM card cage.

For the existing SEM card cage, the ratio of extraction force to operator's force required for extraction ($^{F3/}F1$) is as follows:

$$r1 = 1.63$$
$$r2 = .593$$
$$\theta = 39.35^{o}$$

$$F3/_{F1} = \frac{(r1)}{r2\ (\cos\theta)} = \frac{(1.63)}{.593\ (\cos 39.35)} = 3.55$$

For an ISEM card cage:

$$r1 = 1.63$$
$$r2 = .469$$
$$\theta = 0^{o} \text{ (from figure VIII-2)}$$

$$F3/_{F1} = \frac{(r1)}{r2\ (\cos\theta)} = \frac{(1.63)}{.469\ (\cos\theta)} = 3.49$$

The reason that the angle θ was chosen to be at the initial point of extraction was because as θ approached 90°, cos θ approached 0. This indicate that the vertical force increases as the angle θ increases. Therefore, a small angle θ, as in the initial point of extraction, gives the smallest vertical force by the extractor. This is the worse-case condition.

The force required to extract a module depends on the number of pins contained by the connector. As defined by MIL-C-28754, the maximum insertic force per pin is 10 ounces, while the minimum withdrawal force per pin is 2 ounces. Assuming that the withdrawal force would never exceed the maximum insertion force, the worse-case condition for the withdrawal force would be 10 ounces per pin. Relating this to the connectors, a 1A module, with a forty-pin connector, would require a 25 pound force to extract the module. A 2A module, with a one hundred-pin connector, would require a 62.5 pound force to extract the module.

Using the designed extractor, the force required by the operator (F1) to extract a 1A module would then be 7.0 pound force in an existing SEM carc cage, and 7.2 pound force in an ISEM card cage. For a 2A module, the force required would be 17.6 pound force in an existing card cage, and 17.9 pound force in an ISEM card cage.

To lower the force required by the operator to extract a module, the following can be done:

1. Decrease the number of connector pins.

2. Increase r1.

3. Decrease r2.

4. Have the angle θ as large as possible.

5. Decrease the maximum withdrawal force.

Decreasing the number of connector pins is not desirable, since higher component density, one of the main goals of this task, dictates higher input/output capability. As for changes to r1, r2, and θ, they are closely linked to the card cage design. Plus, it is desirable to have an extractor with the capability of being stored as a module. This storage capability and the existing SEM and ISEM card cage design determined r1, r2, and θ. This leaves decreasing the withdrawal force as the best alternative.

The different methods of decreasing the withdrawal force are as follows:

1. Increase the tuning fork gap (increase A in figure VIII-4).

2. Decrease the tuning fork thickness (decrease B in figure VIII-4).

3. Improve the finish of the plating of the blade and the mating surfaces of the tuning fork.

Changing the physical dimensions on the tuning fork to decrease the amount of contact pressure between the fork and the blade has already been incorporated by certain commercial vendors for low insertion force connectors. The application of this method for lower insertion/withdrawal forces is frowned upon, since it is felt that degradation of electrical contact would result from the weaker tuning fork. A more widely accepted means of lowering the insertion/withdrawal forces is by improving the finish of the blade and tuning fork. The finishes range from 50 micro inches, for medium insertion force, to 27 micro inches, for low insertion force. Amp Incorporated has a blade which is graphite impregnated to reduce the coefficient of friction. This method is desirable because it eliminates the need for fine polishing to attain the 27 micro inch finish. The graphite impregnated blade requires further investigation into possible corrosion effect due to graphite transfer to other surfaces.

Further study into the possible use of low insertion/extraction force tuning fork and blade should be investigated, since the trend is toward

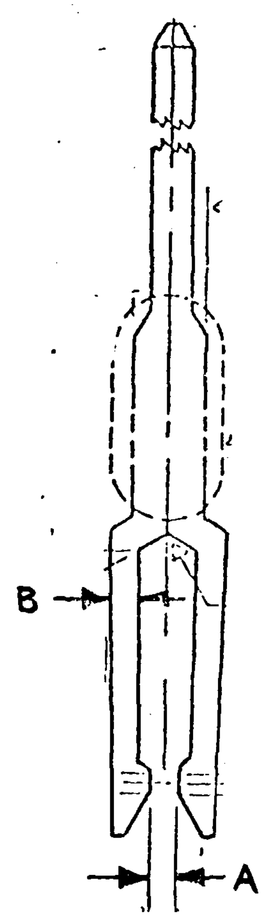

WRAP PLATE FORK

FIGURE VIII-4

modules with higher component density, which leads to higher input/output capabilities which increases the insertion/extraction forces required per module.

B. STRUCTURAL ANALYSIS

The complication of the "T" top on the ISEM modules also added difficulty in the design of the extractor. The "T" top is .270 inch wide. The module pitch is .300. This leaves a possible gap of .030 inch between modules at nominal conditions, leaving little tolerance for straightness of the "T" top or tolerances in the card cage and module.

The required force to extract a module ranges from a 25 pound force to a 62.5 pound force, depending on whether it is a 1A or a 2A module. Since the reason for going to a "T" top was to increase the amount of surface area at the top of the module for top plate cooling and increase the cross sectional area at the top for heat flow to the side guides, reducing the width of the "T" top from .270 inch is not desirable. But, to extract by prying on the top lip with a .030 inch or less thick extractor presents a structural problem for the extractor, when the force required can be as much as 62.5 pound force. To alleviate this problem, notches (.100 x .030) were cut out at the four corners of the "T" top. The corners were chosen because they would not interfere with the module circuitry. The extractor was designed with tabs which fit the notches on the module. Figure VIII-6 shows a module being extracted. Figure VIII-7 shows the use of the module extractor in extracting an end module. Figure VIII-8 shows a module extractor stored in a card cage.

With the .030 inch notch cut in the "T" top, the nominal gap between modules is now .090 inch. Since the extractor is to be stored as a module, the thickness of the extractor should be approximately .050 inch for compatibility with module/card cage interfaces which may be present in the storage slot. At this thickness, there is a tolerance clearance of .040 inch. As a result, the module extractor was chosen to be .042 inch thick, since this is a common stock thickness.

For the strength required by the tab, the flexural stress at the extreme fiber is: $f = MC/I = M/S$

Where: M = bending moment = + FL

I = moment of inertia = $bd^3/12$

$S = I/C$ = section modulus = $bd^2/6$

C = distance to extreme fiber = $d/2$

Using the parameters given in Figure VIII-5 and on page VIII-10, the flexural stress is:

$$f = M/S = \frac{+\,FL}{bd^2/6} = \frac{(31.2\ \text{lb})\ (.098)}{(.150)\ (.042)^2/6}$$

$$f = 6.93 \times 10^4 \text{ PSI}$$

The yield strength for AL 5052 is 2.8×10^4 PSI, which is inadequate. The yield strength for stainless steel, Class 302/304, annealed is 6.8×10^4 PSI, which is marginal. The best suited would be to use either half-hard stainless steel, Class 302/304, with a yeild of 1.50×10^5 PSI, or heat-treated condition RH 950 solution annealed 17-7 PH stainless steel.

C. PRODUCIBILITY

The extractor will be a formed part. Tooling will be required to form it, but there is no other operation required after forming. Therefore, there is initial tooling cost, but the piece part would be fairly inexpensive.

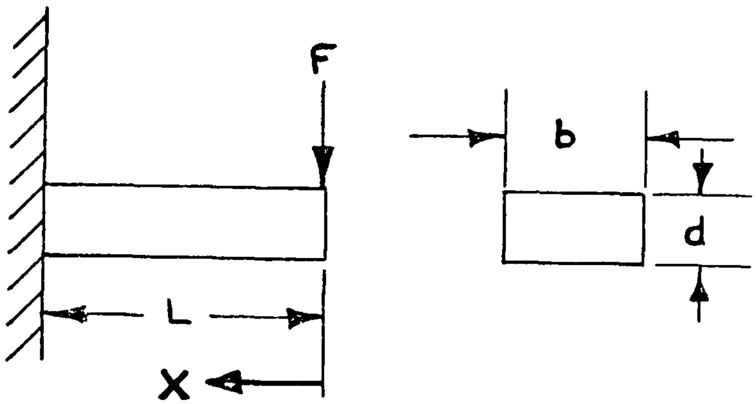

FOR THE ISEM EXTRACTOR:

b = .150 INCH
d = .042 INCH
L = .098 INCH

EXTRACTOR LIP DETAIL

FIGURE VIII-5

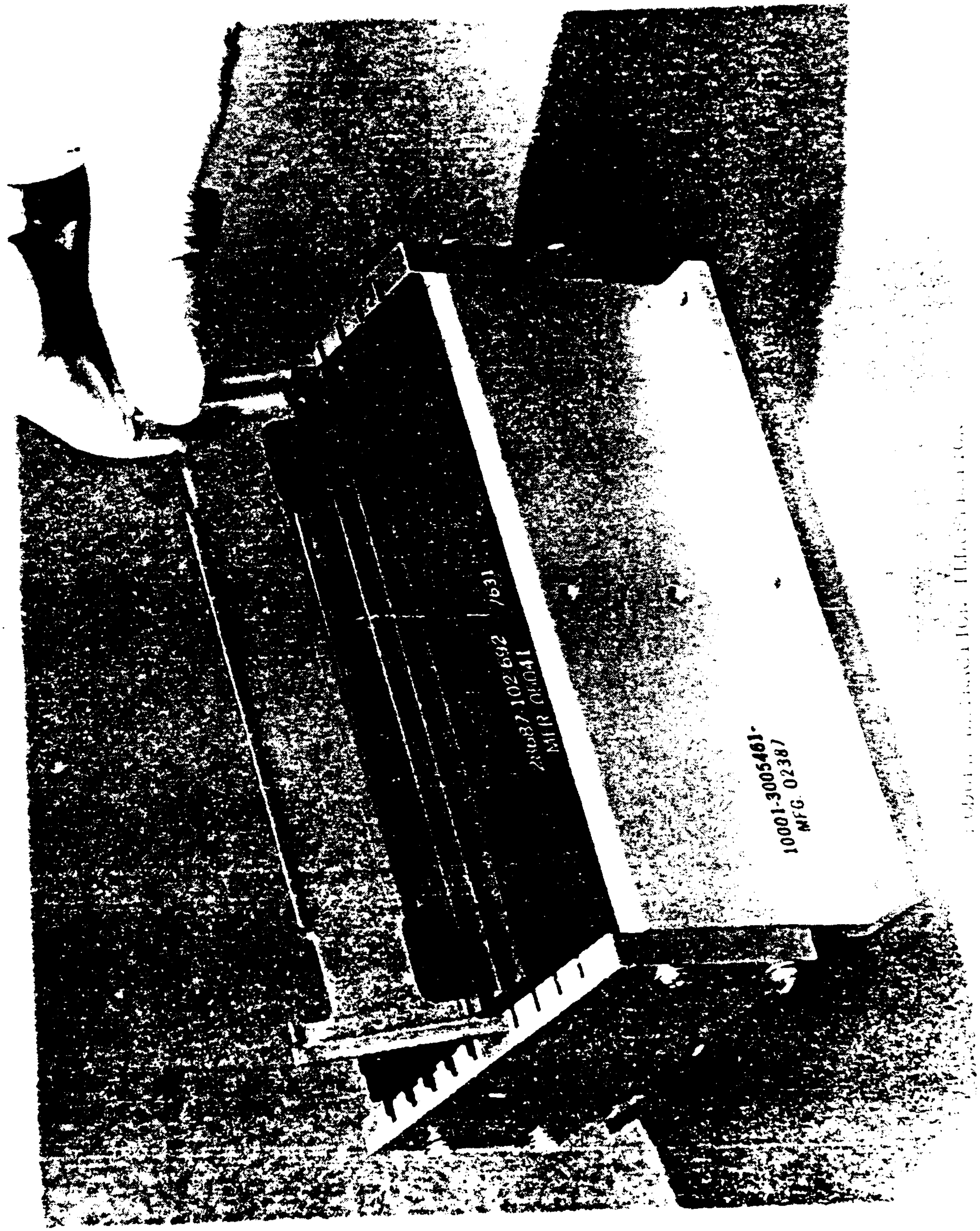

FIGURE VIII-6 [illegible]

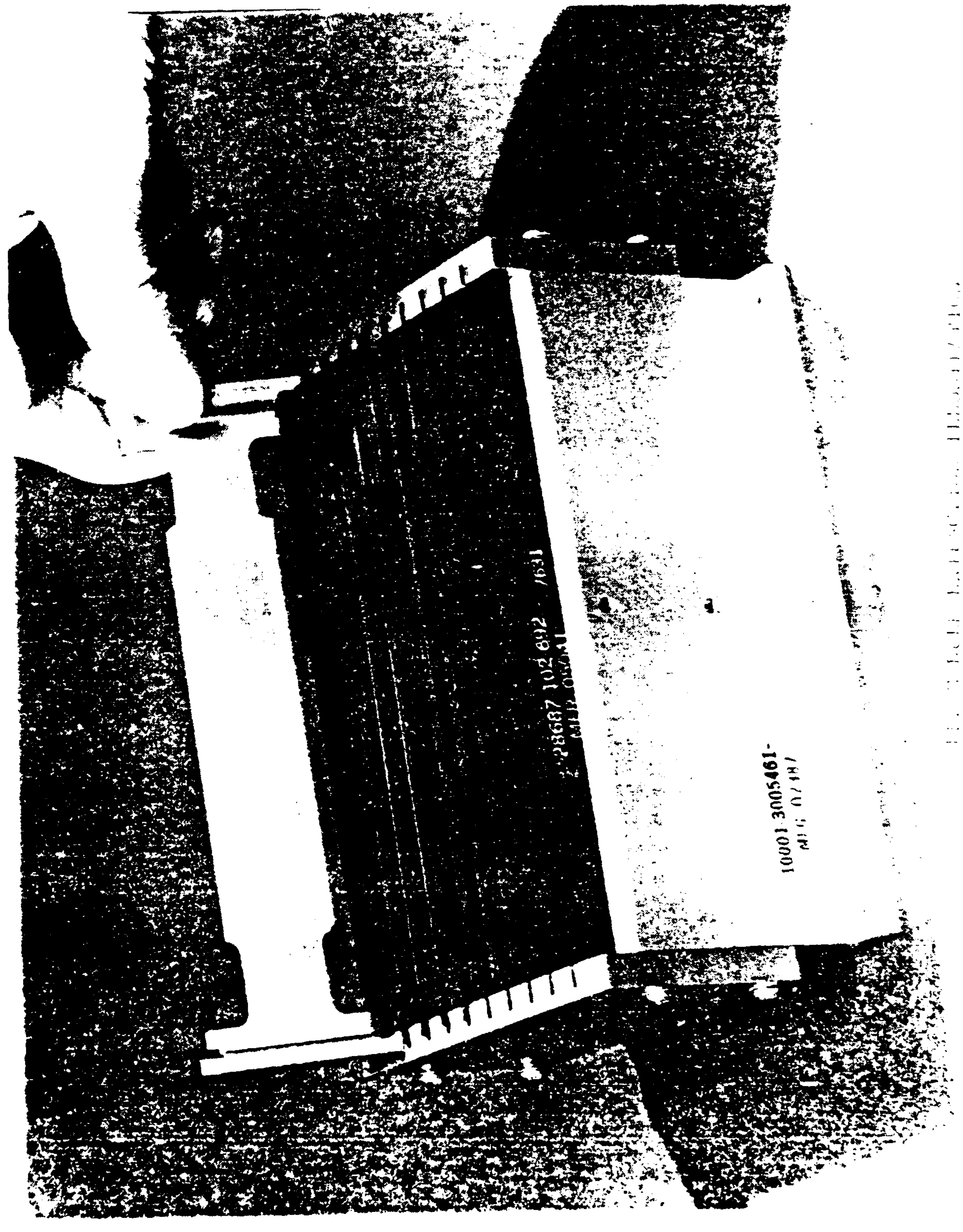
10001 3005461-

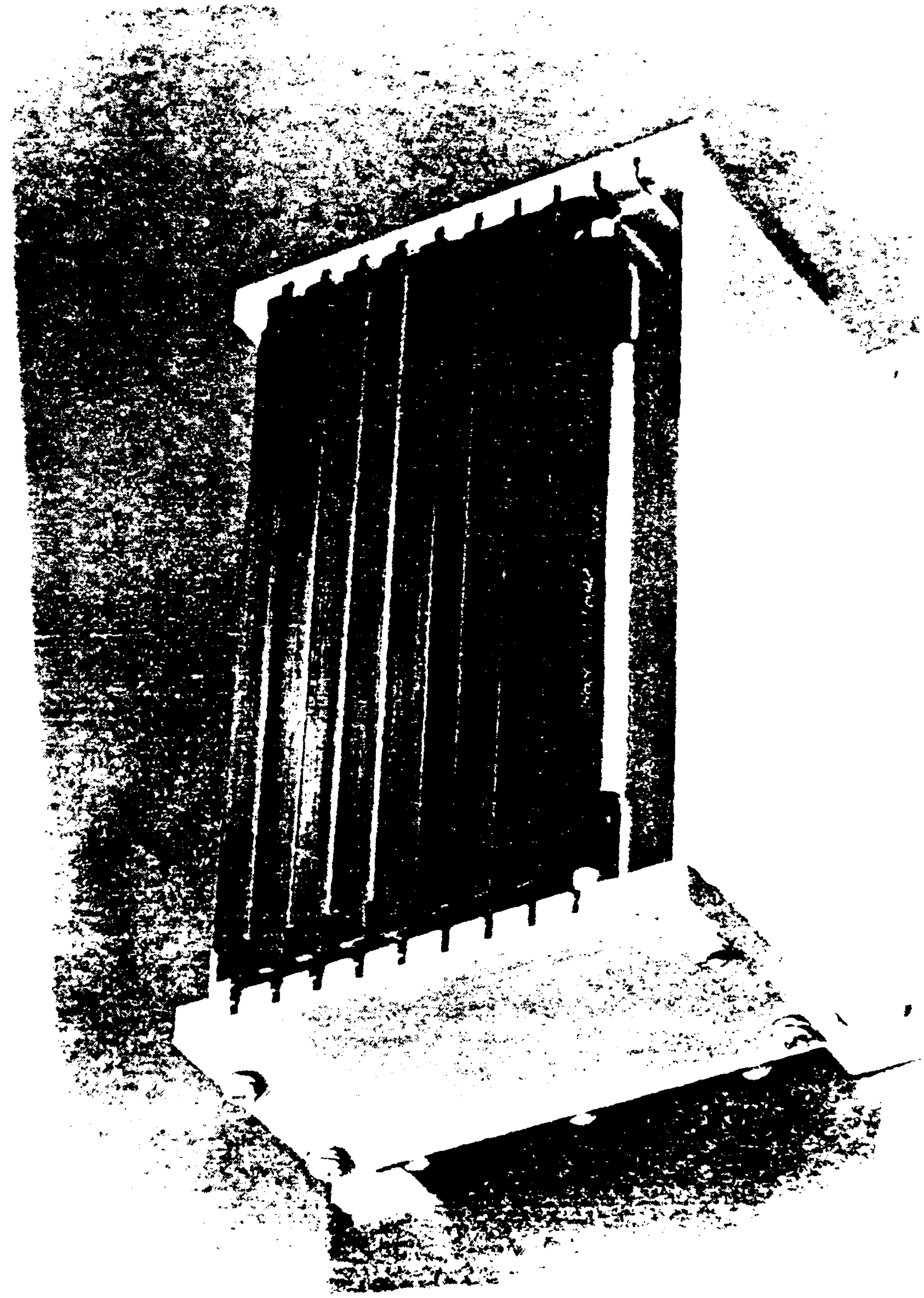

IX. CARD CAGE/MODULE INTERFACES

A. INTERFACES

1. A major obstacle in using conduction cooling is the high thermal resistance at the interface between the module and the cold plate. As pointed out in Section V, the thermal resistance at the interfaces between the module and the cold plate is a function of the contact area. Irregularities between mating surfaces of the module and cold plate decrease the amount of contact area and increase the amount of thermal resistance. The interface retainers come into play in forcing the mating surfaces of the module and cold plate together to conform to each other's irregularities to increase the contact area. The interface retainers investigated consist of:

   a. Belleville washers for top plate cooling.

   b. Standard Bircher clip for card cage cooling.

   c. The Wedge concept for card cage cooling.

   d. Improved three convolution IERC clip for card cage cooling.

   Since Belleville washers are discussed only in Section V and this section deals only with card cage interfaces, just the last three types of interface retainers are discussed.

2. The standard Bircher clip and the IERC clip are both spring clips fabricated from beryllium-copper. They both use the spring tension of the material to apply the force required to push the side guide of the module against a heatsink. In the case of the Bircher clip, the module side guides are wedged between two springs. The heat is then transferred from the module to the clip to the card cage. In the case of

the IERC clip, the springs are used to push the module side guides directly against the card cage walls. Figure IX-1 shows a Bircher clip mounted in a card cage. Figure IX-2 shows a IERC clip mounted in a card cage.

The wedge is as the name implies. It consists of two wedge-like pieces which are mated together at the center by a screw. Upon turning the screw, the bottom piece and top piece are pulled together. This forces the two pieces to split sideways, which is against the module side guide. Figure IX-3 shows a wedge mounted in a card cage.

B. CONCLUSION

1. In comparing the three types of interfaces, the standard Bircher clip proved to be the least effective thermally, giving a thermal resistance of 6.2^{0} C/W. The IERC clip had a thermal resistance of 2.0^{0} C/W. The wedge was the most effective thermally, giving a thermal resistance of 1.7^{0} C/W. The thermal resistances are for the two module interfaces in parallel. Even though the wedge has the lowest thermal resistance of the three types of interfaces, it has the following disadvantages:

a. It requires a large amount of volume for mounting.

b. The size of the wedge causes a significant increase in unit weight.

c. It requires individual fastening and loosening of each wedge per module when inserting or extracting modules. This would increase the MTTR (Mean Time To Repair) of the system.

d. It requires a complicated card cage design to accommodate the wedge. Part of this design must also insure that the wedge would be activated before the system can be energized, since an open wedge could cause module failure from thermal overload.

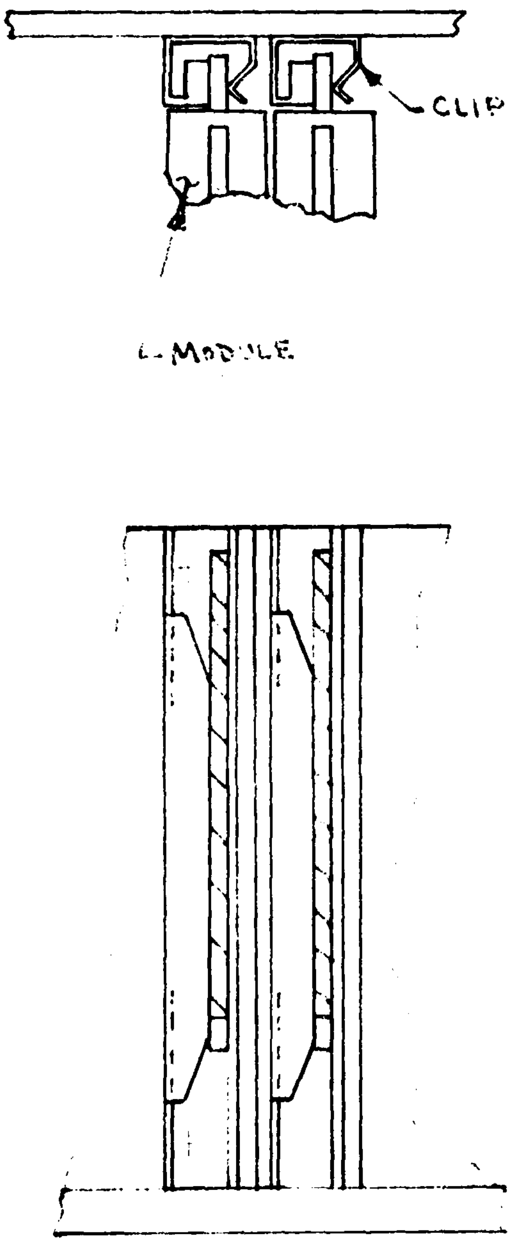

BIRCHER CLIP

FIGURE IX-1

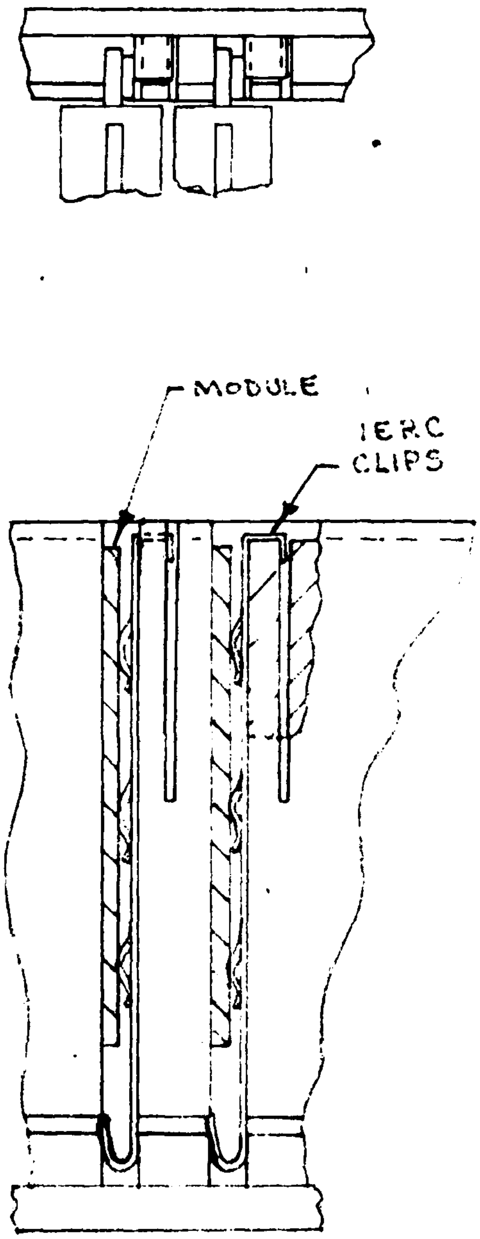

SPRING CLIP

FIGURE IX-2

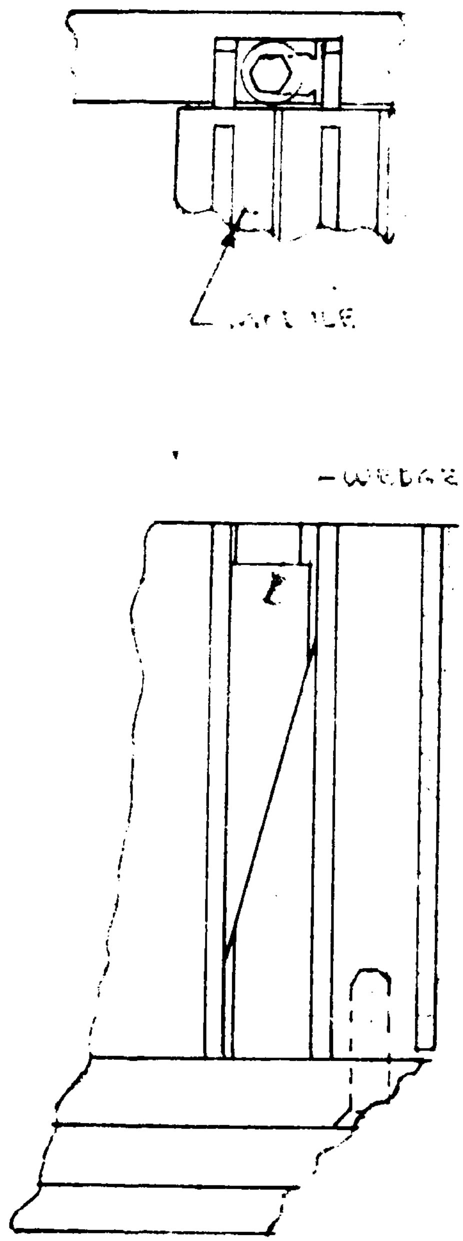

WEDGE

FIGURE IX-3

e. The pressure due to the wedge can possibly cause fusing between the side guide of the module and the wedge over a long period of time.

The advantages to using the wedge are:

a. There is a predictable and positive contact pressure force applied to the module side guide.

b. The presence of the wedge holds and gives structural strength to the module/card cage assembly in shock and vibration.

c. No increase in module insertion or extraction force.

For the IERC clips, the disadvantages to using them are:

a. The positional tolerances of the clip (relative to the module), the module side guide thickness, and the fabricational tolerances of the clip are very critical to the amount of contact pressure which would be applied to the module side guides. As a result, consistent contact pressure is difficult to attain.

b. The beryllium-copper is brittle and is subject to breakage when the module is inserted or extracted at an angle.

c. Insertion and extraction of the module over a prolonged period can cause partial inelastic deformation of the clips, resulting in loss of contact pressure.

d. Increase in module insertion and extraction force.

The advantages to using the IERC clip are:

a. It consumes very little volume, which allows f
on a .30 pitch.

b. It adds little to the unit weight.

c. There is no manual manipulation required to activate the clip.

d. Installation requirements are simple.

e. Fabrication of the clips is simple and inexpensive.

The thermal resistance of the standard Bircher clip is too high and was not considered for use with the ISEM. The wedge and the IERC clip have nearly the same thermal resistance. Considering the tradeoffs between the two, the IERC clips seem to be best suited for production usage.

Experimental data on the design and thermal testing of a light weight card cage which included module interfaces was compiled by the *Raytheon Company* (SSD), Portsmouth, Rhode Island. For detail on the experimental data, refer to LIGHTWEIGHT CARD CAGE ASSEMBLY, prepared under contract number N00163-77-C-0063 for Naval Avionics Center. Final report was released in Aug 1978.

Naval Avionics Center, Indianapolis, Indiana (NAC TR-2217)
Improved Standard Electronic Modules Thermal and Mechanical Analyses and Design (UNCLASSIFIED)
By: William Taw Pages: 163
Dated: 1 September 1978
This report covers the design, development, and thermal modeling, and testing of a new module family, the Improved Standard Electronic Modules (ISEM), which is compatible with the existing SEM Program modules.

1. Improved Standard Electronic Modules Program

I. Taw, William

II. Work Request N00095377WR 09153

Naval Avionics Center, Indianapolis, Indiana (NAC TR-2217)
Improved Standard Electronic Modules Thermal and Mechanical Analyses and Design (UNCLASSIFIED)
By: William Taw Pages: 163
Dated: 1 September 1978
This report covers the design, development, and thermal modeling, and testing of a new module family, the Improved Standard Electronic Modules (ISEM), which is compatible with the existing SEM Program modules.

1. Improved Standard Electronic Modules Program

I. Taw, William

II. Work Request N00095377WR09153

Naval Avionics Center, Indianapolis, Indiana (NAC TR-2217)
Improved Standard Electronic Modules Thermal and Mechanical Analyses and Design (UNCLASSIFIED)
By: William Taw Pages: 163
Dated: 1 September 1978
This report covers the design, development, and thermal modeling, and testing of a new module family, the Improved Standard Electronic Modules (ISEM), which is compatible with the existing SEM Program modules.

1. Improved Standard Electronic Modules Program

I. Taw, William

II. Work Request N00095377WR 09153

Naval Avionics Center, Indianapolis, Indiana (NAC TR-2217)
Improved Standard Electronic Modules Thermal and Mechanical Analyses and Design (UNCLASSIFIED)
By: William Taw Pages: 163
Dated: 1 September 1978
This report covers the design, development, and thermal modeling, and testing of a new module family, the Improved Standard Electronic Modules (ISEM), which is compatible with the existing SEM Program modules.

1. Improved Standard Electronic Modules Program

I. Taw, William

II. Work Request N00095377WR09153

Naval Avionics Center, Indianapolis, Indiana (NAC TR-2217)
Improved Standard Electronic Modules Thermal and Mechanical Analyses and Design (UNCLASSIFIED)
By: William Taw   Pages: 163
Dated: 1 September 1978
This report covers the design, development, and thermal modeling, and testing of a new module family, the Improved Standard Electronic Modules (ISEM), which is compatible with the existing SEM Program modules.

1. Improved Standard Electronic Modules Program

I. Taw, William

II. Work Request N00095377WR09153

Naval Avionics Center, Indianapolis, Indiana (NAC TR-2217)
Improved Standard Electronic Modules Thermal and Mechanical Analyses and Design (UNCLASSIFIED)
By: William Taw   Pages: 163
Dated: 1 September 1978
This report covers the design, development, and thermal modeling, and testing of a new module family, the Improved Standard Electronic Modules (ISEM), which is compatible with the existing SEM Program modules.

1. Improved Standard Electronic Modules Program

I. Taw, William

II. Work Request N00095377WR09153

Naval Avionics Center, Indianapolis, Indiana (NAC TR-2217)
Improved Standard Electronic Modules Thermal and Mechanical Analyses and Design (UNCLASSIFIED)
By: William Taw   Pages: 163
Dated: 1 September 1978
This report covers the design, development, and thermal modeling, and testing of a new module family, the Improved Standard Electronic Modules (ISEM), which is compatible with the existing SEM Program modules.

1. Improved Standard Electronic Modules Program

I. Taw, William

II. Work Request N00095377WR09153

Naval Avionics Center, Indianapolis, Indiana (NAC TR-2217)
Improved Standard Electronic Modules Thermal and Mechanical Analyses and Design (UNCLASSIFIED)
By: William Taw   Pages: 163
Dated: 1 September 1978
This report covers the design, development, and thermal modeling, and testing of a new module family, the Improved Standard Electronic Modules (ISEM), which is compatible with the existing SEM Program modules.

1. Improved Standard Electronic Modules Program

I. Taw, William

II. Work Request N00095377WR09153

APPENDIX A

THERMAL TEST RESULTS

APPENDIX A

THERMAL TEST RESULTS

A. FORCED AIR CONVECTION OVER THE FIN

1. Forced convection was evaluated for two different card cage heights. One height represents present card cage systems, whereas the second represents an extended card cage height designed for optimum conduction through an ISEM card guide. The extended height test was performed to evaluate supplemental cooling by forced convection over the fin. Figure A-1 illustrates the profile geometries of the two test models (labeled A & B). Both models contained 15 (3 rows of 5 modules each) 2A load modules in a 1/4" thick plexiglass duct. (See Figure A-2.) The duct was encased in approximately 4 inches of styrofoam insulation.

The module array duct (Figure A-2) was connected to a 24-inch long transition duct, a 6" x 6" mixing box, a 24" long x 1-1/2" DIA pipe, a differential pressure flow meter, a 12" long x 1-1/2" DIA pipe, and finally attached to the air moving device. Air at various velocities was drawn through the system, as described above, and monitored by the flow meter.

A listing of test equipment is as follows:

Flow Meter - Meriam Instruments Model 50MW20
Flow Meter Manometer - Meriam Instruments Type WM
Module Array Duct Manometer - Meriam Instruments Type TM
Air Moving Device - Dayton Model 2Z-563

Each load module contained twelve (12) 16-pin DIP resistors capable of dissipating 2.5 watts per package. Fenwal Uni-Curve thermistors were mounted on nine of the resistors and two were embedded in the vertical

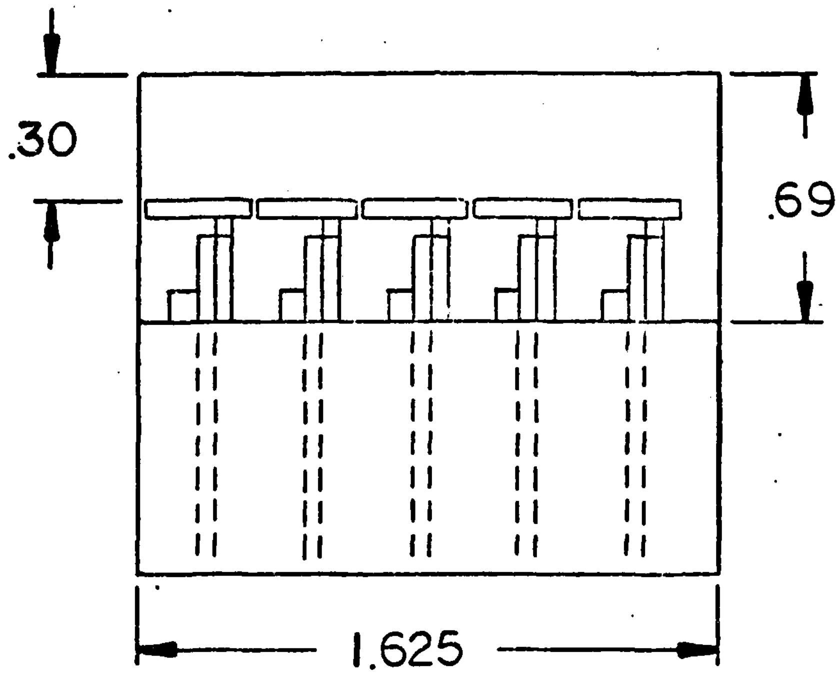

TEST MODEL "A"

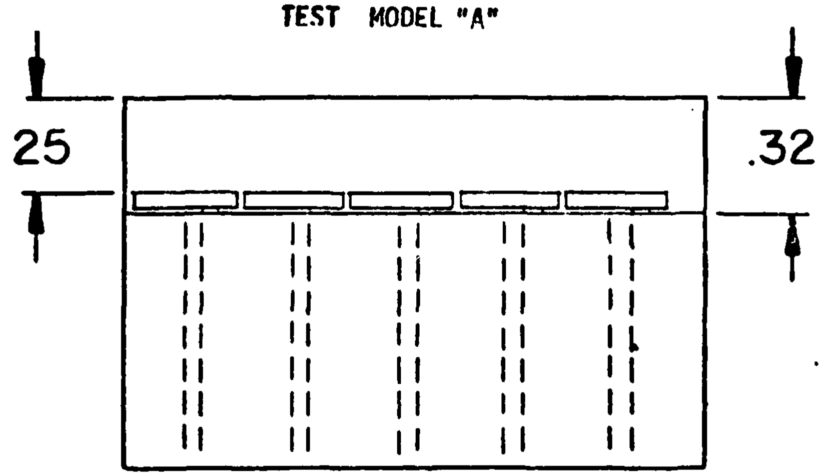

TEST MODEL "B"

FIGURE A-1

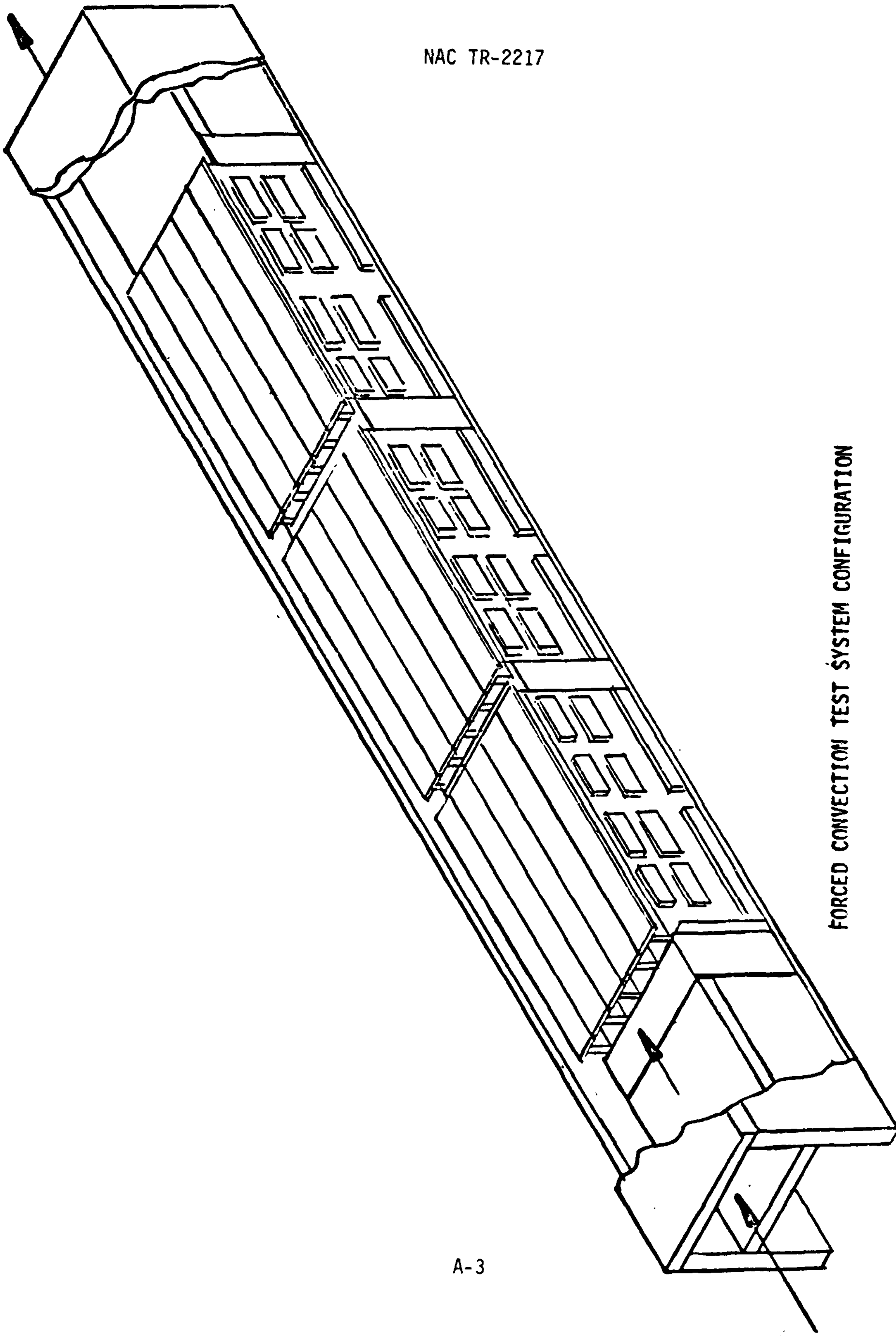

FORCED CONVECTION TEST SYSTEM CONFIGURATION

FIGURE A-2

portion of the fin. Thermistor locations are shown in Figure A-3. This load module configuration was used for all testing.

Table A-1 contains thermal test results for both the "T" and "L" fins. The indicated thermal resistances are for the middle row of modules, and they are an average value of the three center modules of that row.

Calculated thermal resistance values (air-fin) are based on inlet air conditions to that particular row of modules. Air velocities were calculated using the profile free-flow area, and are not the velocities in the fin area. Resistance values, therefore, will not be valid for all duct heights.

Table A-2 contains calculated module power capacities. Calculations are based on Table A-1 resistances and module frame thermal modeling results. Note all conditions stated in the table for each particular frame type.

B. DIRECT AIR IMPINGEMENT

1. Direct air impingement testing was performed with the modules on .3" and .4" centers. The test model card cage configuration is shown in Figure A-7. As with the forced air convection testing, the model contained 15 load modules and was insulated with styrofoam. Air at various velocities was drawn through the system and component case temperatures recorded for each condition.

Table A-3 contains the thermal data and Table A-4 contains projected module power capacities for the two different center spacings.

Calculated thermal resistance values (component case-air) are based on the inlet air conditions to the particular row of modules and the component power dissipation. Comparisons between the two different

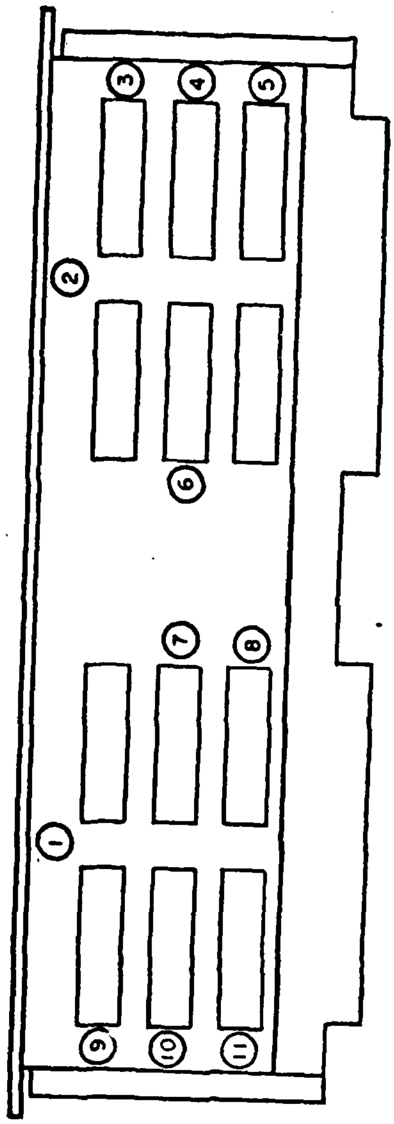

THERMISTOR ARRANGEMENT

FIGURE A-3

TABLE A-1

FORCED CONVECTION FIN-AIR RESISTANCE

TEST MODEL "A"

INTERFACE	AVERAGE DUCT VEL. (FT/SEC)	THERMAL RESISTANCE (°C/WATT) *
T FIN TO AIR	10	7.3
(0.280" Wide)	15	5.3
	20	4.2
	25	3.3
L FIN TO AIR	10	8.6
(0.180" Wide)	15	6.5
	20	4.3
	25	3.2

TEST MODEL "B"

INTERFACE	AVERAGE DUCT VEL. (FT/SEC)	THERMAL RESISTANCE (°C/WATT)
T FIN TO AIR	10	15.1
(0.280 WIDE)	15	13.1
	20	11.5
	25	10

*All values for 2A Size Modules

TABLE A-2

FORCED CONVECTION FIN POWER CAPACITIES

TEST MODEL "A"

DIP FRAME

MODULE	AVERAGE DUCT VEL. (FT/SEC)	MODULE RIB ORIENTATION	MODULE POWER (WATTS)
SEM 1A	10	VERTICAL	2.1
ISEM 1A		VERTICAL	2.5
		HORIZONTAL	2.1
SEM 2A		VERTICAL	4.3
ISEM 2A		VERTICAL	5.1
		HORIZONTAL	4.0
SEM 1A	15	VERTICAL	2.5
ISEM 1A		VERTICAL	3.0
		HORIZONTAL	2.4
SEM 2A		VERTICAL	5.1
ISEM 2A		VERTICAL	6.2
		HORIZONTAL	4.6
SEM 1A	20	VERTICAL	3.0
ISEM 1A		VERTICAL	3.3
		HORIZONTAL	2.6
SEM 2A		VERTICAL	6.2
ISEM 2A		VERTICAL	6.9
		HORIZONTAL	5.0
SEM 1A	25	VERTICAL	3.4
ISEM 1A		VERTICAL	3.7
		HORIZONTAL	2.8
SEM 2A		VERTICAL	7.1
ISEM 2A		VERTICAL	7.7
		HORIZONTAL	5.5

TABLE A-2 (Continued)

CONDITIONS

45°C Inlet Temp, 105°C Max. Jct. Temp.

ISEM - 6101 AL, SEM 5052 AL

Uniform Power Distribution

25°C/Watt Jct. to Case for Dip

SEM 1A: (5) 16 Pin Dips

SEM 2A: (12) 16 Pin Dips

ISEM 1A: Vertical - (5) 16 Pin Dips; Horizontal - (9) 16 Pin Dips

ISEM 2A: Vertical -(12) 16 Pin Dips; Horizontal - (16)16 Pin Dips

TABLE A-2 (Continued)

FORCED CONVECTION FIN POWER CAPACITIES

TEST MODEL "A"

CENTER FRAME

MODULE	AVERAGE DUCT VEL. (FT/SEC)	MODULE POWER (WATTS)
SEM 1A	10	2.6
ISEM 1A		3.3
SEM 2A		5.5
ISEM 2A		6.5
SEM 1A	15	3.2
ISEM 1A		4.3
SEM 2A		6.8
ISEM 2A		8.3
SEM 1A	20	4.3
ISEM 1A		5.0
SEM 2A		9.0
ISEM 2A		9.9
SEM 1A	25	5.1
ISEM 1A		5.9
SEM 2A		10.8
ISEM 2A		11.6

TABLE A-2 (Continued)

CONDITIONS

45°C Inlet Temp, 105°C Max. Jct. Temp.

ISEM - 6101 AL, SEM 5052 AL

Uniform Power Distribution

45°C/W Jct. to Case for Flatpack

ISEM 1A: 12 - 16 Pin Flatpacks Per Side

ISEM 2A: 24 - 16 Pin Flatpacks Per Side

SEM 1A: 8 - 16 Pin Flatpacks Per Side

SEM 2A: 20 - 16 Pin Flatpacks Per Side

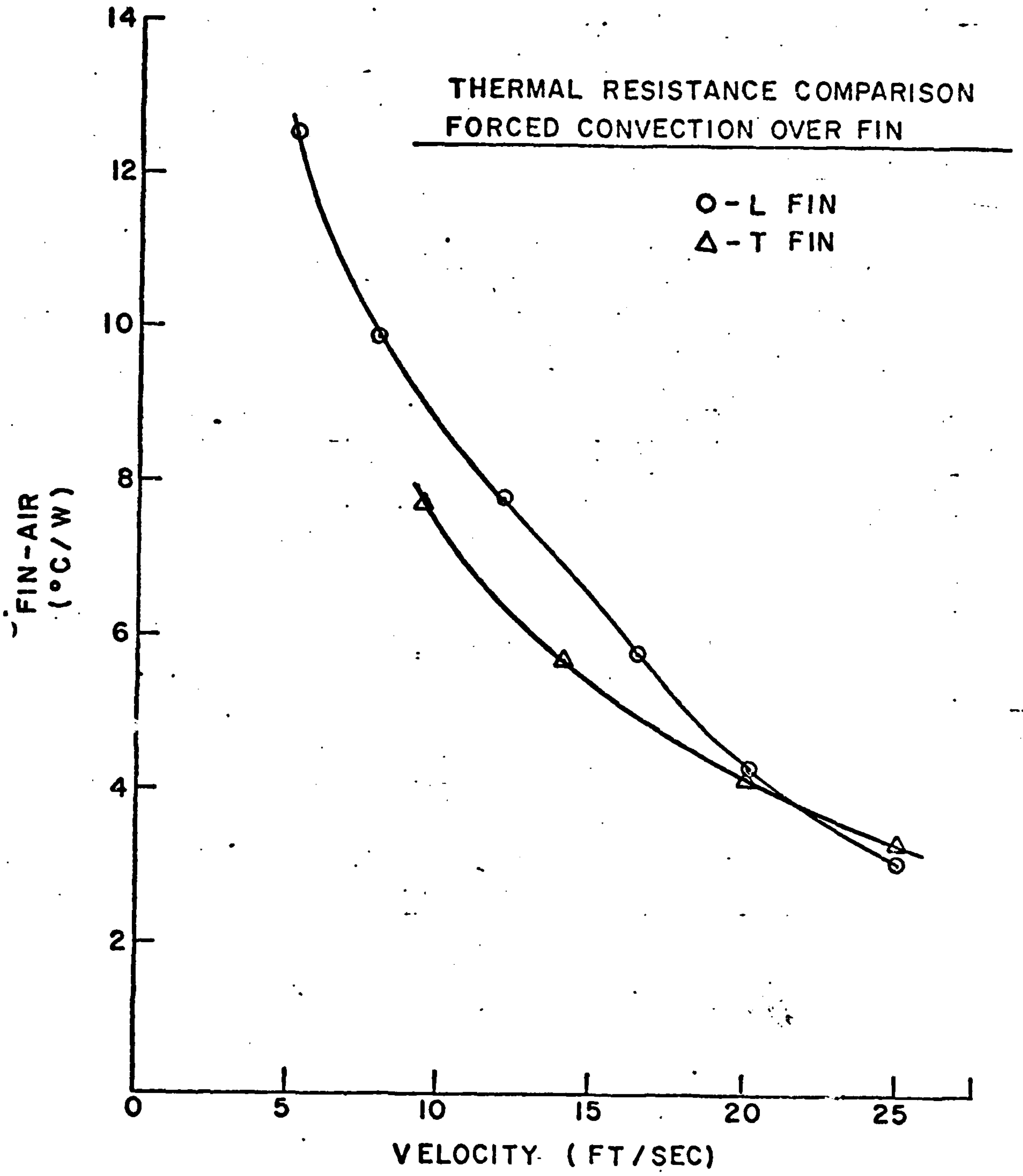
THERMAL RESISTANCE COMPARISON
FORCED CONVECTION OVER FIN
O - L FIN
Δ - T FIN
FIN-AIR (°C/W)
14
12
10
8
6
4
2
0
5
10
15
20
25
VELOCITY (FT/SEC)

FIGURE A-4

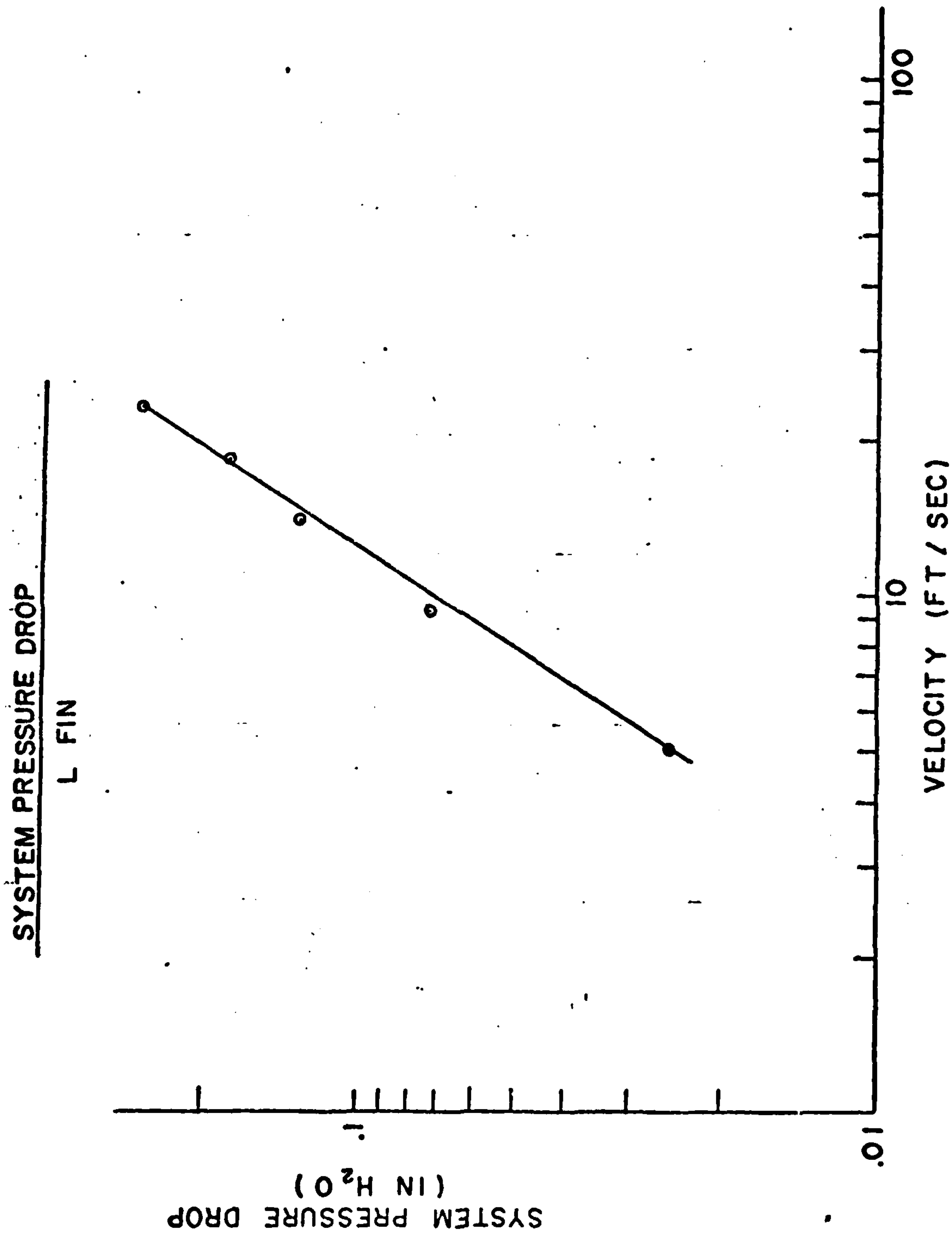
SYSTEM PRESSURE DROP
L FIN
SYSTEM PRESSURE DROP
(IN H_2O)
.01
.1
10
100
VELOCITY (FT/SEC)

FIGURE A-5

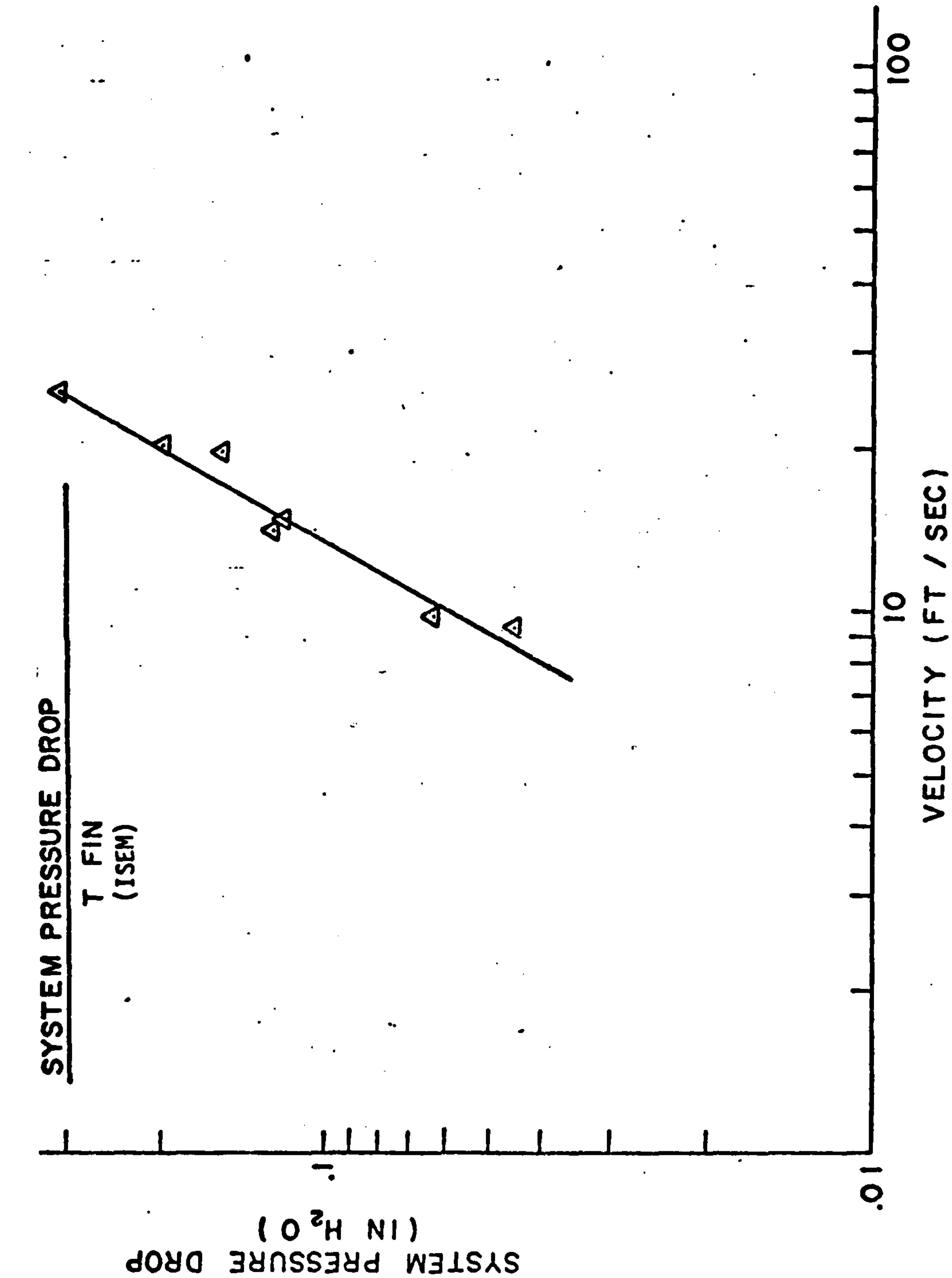
SYSTEM PRESSURE DROP
T FIN
(ISEM)
SYSTEM PRESSURE DROP
(IN H_2O)
.1
.01
10
100
VELOCITY (FT / SEC)

FIGURE A-6

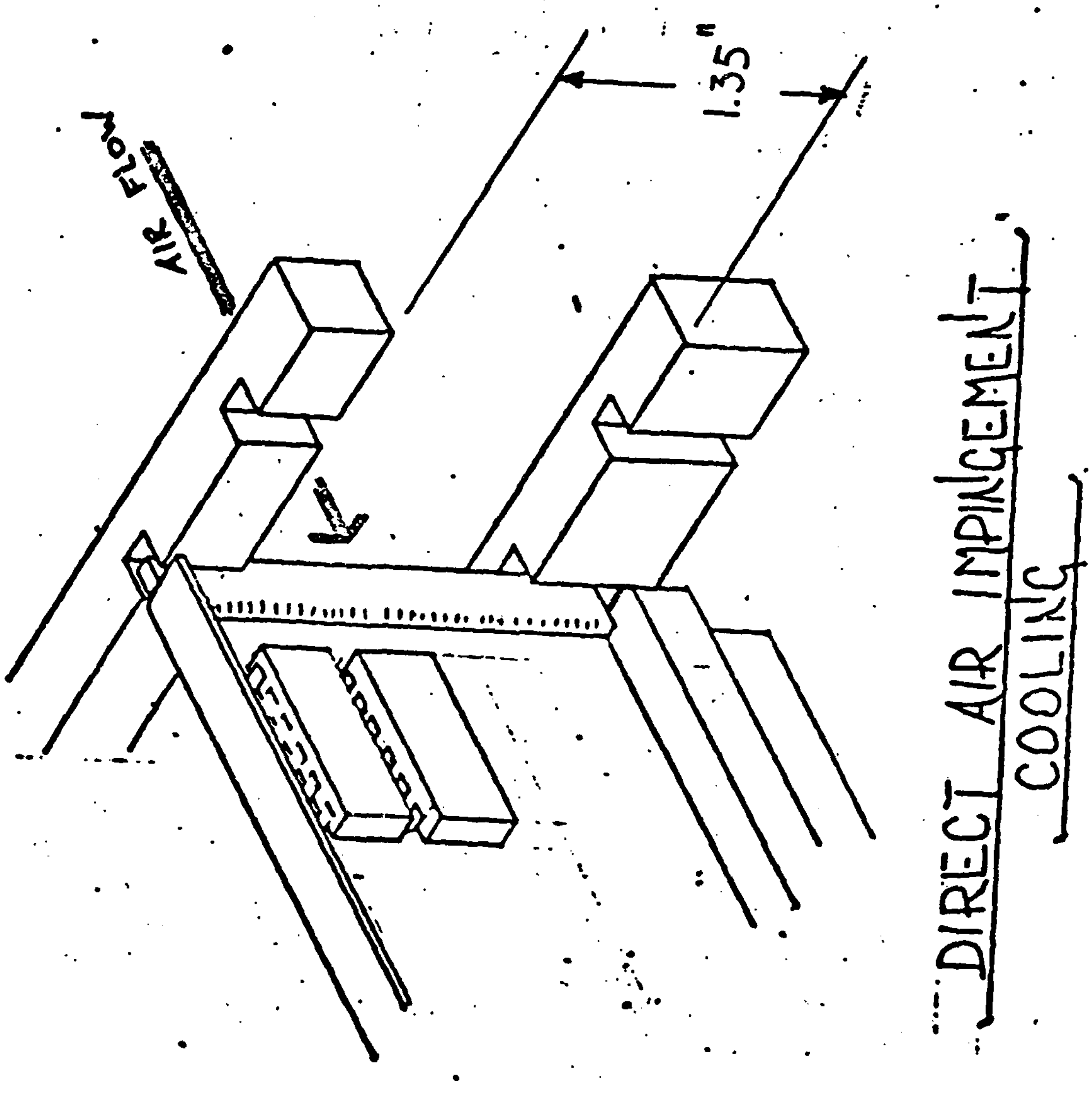

FIGURE A-7

TABLE A-3

DIRECT AIR IMPINGEMENT

FY77 SEM R&D THERMAL TESTING RESULTS

INTERFACE	MTG. PITCH	THERMAL RESISTANCE (°C WATT)
COMP CASE-AIR (5 FT/SEC)	0.3"	82
COMP CASE-AIR (10 FT/SEC)	0.3"	60
COMP CASE-AIR (15 FT/SEC)	0.3"	42
COMP CASE-AIR (20 FT/SEC)	0.3"	36
COMP CASE-AIR (25 FT/SEC)	0.3"	31
COMP CASE-AIR (10 FT/SEC)	0.4"	37
COMP CASE-AIR (15 FT/SEC)	0.4"	29
COMP CASE-AIR (20 FT/SEC)	0.4"	26
COMP CASE-AIR (25 FT/SEC)	0.4"	22

* BASED ON COMPONENT POWER OF 16 PIN DIP UNIFORMLY POWERED

* VALUE RELATIVE TO INLET AIR TO MODULE AT COMPONENT HOTSPOT

TABLE A-4

ISEM DIRECT AIR IMPINGEMENT POWER CAPACITIES

.3" MODULE CENTERS

MODULE	AVE DUCT VEL. (FT/SEC)	MODULE POWER (WATTS)
1A Dip	5	5.0
1A C.F.		6.8
2A Dip		9.0
2A C.F.		17.2
1A Dip	10	6.4
1A C.F.		8.7
2A Dip		11.3
2A C.F.		21.8
1A Dip	15	8.1
1A C.F.		11.2
2A Dip		14.3
2A C.F.		27.9
1A Dip	20	8.6
1A C.F		12.3
2A Dip		15.7
2A C.F.		30.8
1A Dip	25	9.6
1A C.F.		13.5
2A Dip		17.1
2A C.F.		33.6

TABLE A-4 (Continued)

ISEM DIRECT AIR IMPINGEMENT POWER CAPACITIES

.4 MODULE CENTERS

MODULE	AVE DUCT VEL (FT/SEC)	MODULE POWER (WATTS)
1A Dip	10	8.7
1A C.F.		12.1
2A Dip		15.5
2A C.F.		30.3
1A Dip	15	10.0
1A C.F.		14.0
2A Dip		17.8
2A C.F.		35.0
1A Dip	20	10.6
1A C.F.		14.8
2A Dip		18.8
2A C.F.		37.1
1A Dip	25	11.5
1A C.F.		16.2
2A Dip		20.4
2A C.F.		40.5

TABLE A-4 (Continued)

CONDITIONS

45°C Inlet Air to Module, 105°C Max Jct. Temp.

Uniform Power Distribution

25°C/W Jct. to Case for Dip

45°C/W Jct. to Case for Flat Pack

1A Dip: (9) 16 Pin Dips

2A Dip: (16) 16 Pin Dips

1A C.F.: (12) 16 Pin Flatpacks Per Side

2A C.F.: (30) 16 Pin Flatpacks Per Side

center spacings are based on equal air velocities and do not consider the differing mass flow rates.

Figure A-8 is a plot of thermal resistance versus air flow velocity. Data points are worst-case thermal resistances (i.e., based on hottest module component case) at each velocity, again based on module inlet conditions. A small error factor may be introduced, due to the fact that the thermistor is located on the end of the DIP instead of the top. Air velocities were calculated using the free-flow areas of the module profile.

Test model system pressure drop curves are shown in Figure A-9. This is a total drop across the 15-module array (3 rows of 5 modules each).

C. "T" FIN "EAR" CONDUCTION

1. The "ear" refers to the extension of the "T" fin beyond the module side guides. The "ear" has two semi-circular holes on each edge to accommodate hold-down devices.

The card cage consisted of three water cooled card guides, accommodating a total of ten 2A load modules (2 rows of 5 modules each). Each card guide contained a .375" diameter water passage. The flow rate through the three card guides, which were in parallel, was 3 GPM. This resulted in a very small temperature rise across the card cage. This small rise was neglected in all thermal resistance calculations.

Data was collected for three different conditions: Condition 1, with the "ears" held down to the card cage with 4-40 screws torqued to a value of two inch-pounds; Condition 2, with the "ears" insulated from the card cage and with no hold downs; and Condition 3, with the modules randomly inserted with no insulation or hold-down screws. Figure A-10 shows the test configuration for Condition 1. The thermal resistance

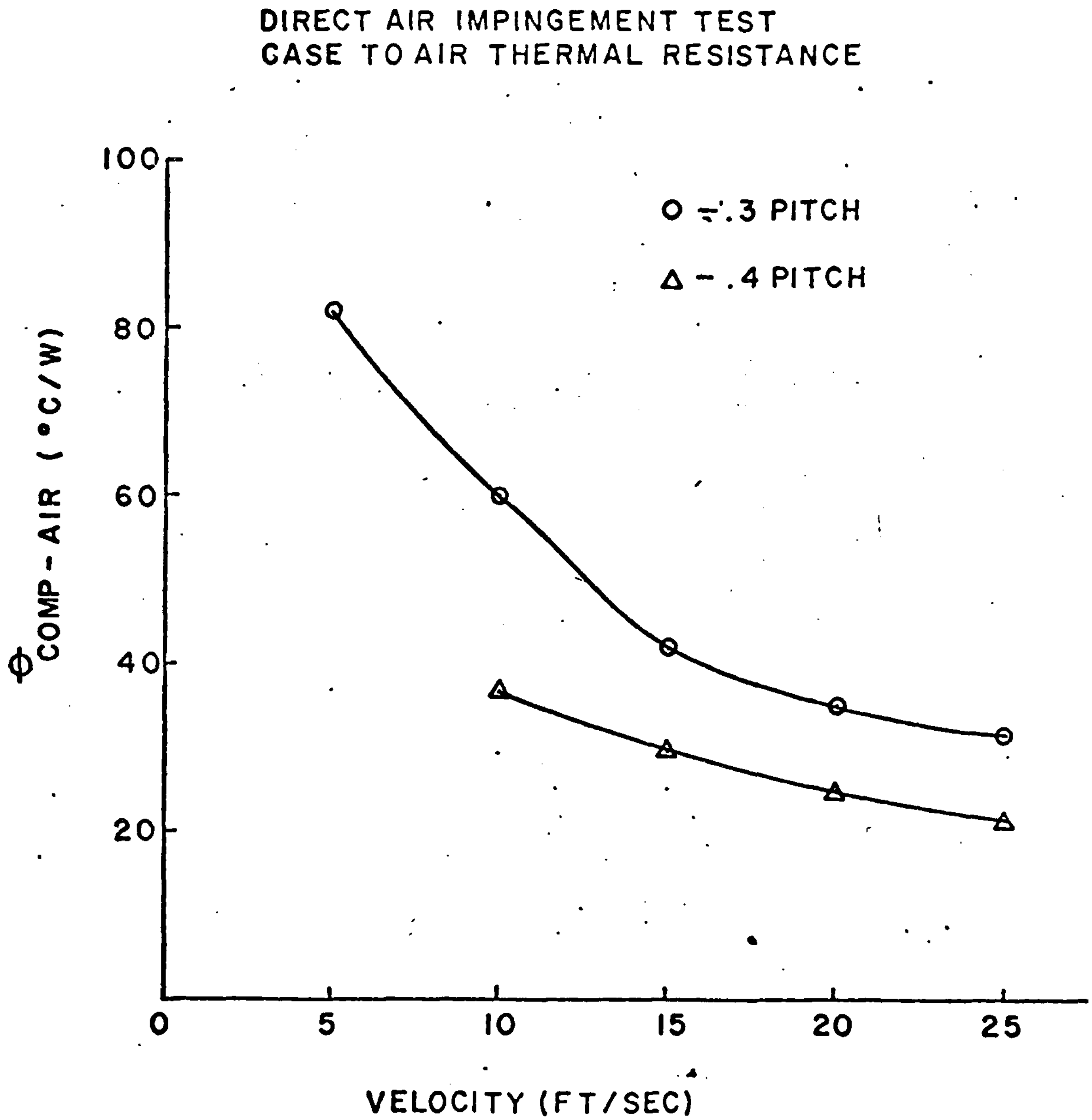
DIRECT AIR IMPINGEMENT TEST
CASE TO AIR THERMAL RESISTANCE
O - .3 PITCH
Δ - .4 PITCH
$\phi_{COMP-AIR}$ (°C/W)
100
80
60
40
20
0
5
10
15
20
25
VELOCITY (FT/SEC)

FIGURE A-8

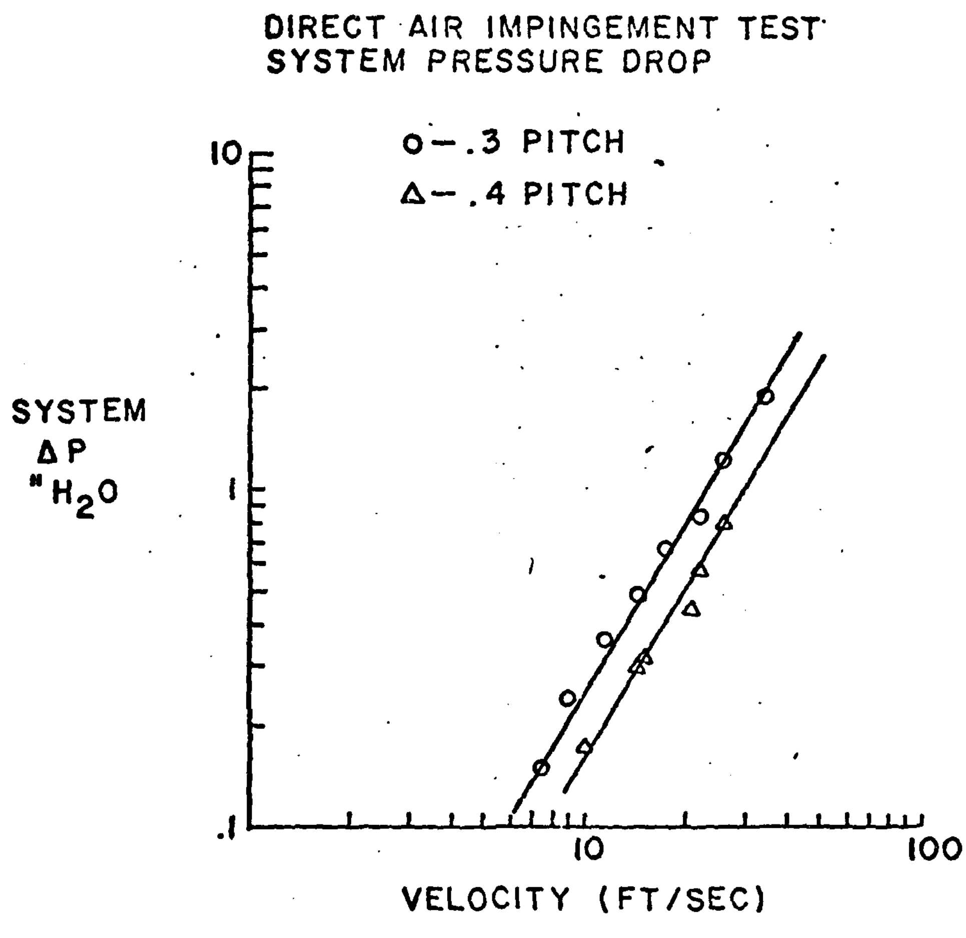
DIRECT AIR IMPINGEMENT TEST
SYSTEM PRESSURE DROP
o — .3 PITCH
Δ — .4 PITCH
SYSTEM
ΔP
"H_2O
10
1
.1
10
100
VELOCITY (FT/SEC)

FIGURE A-9

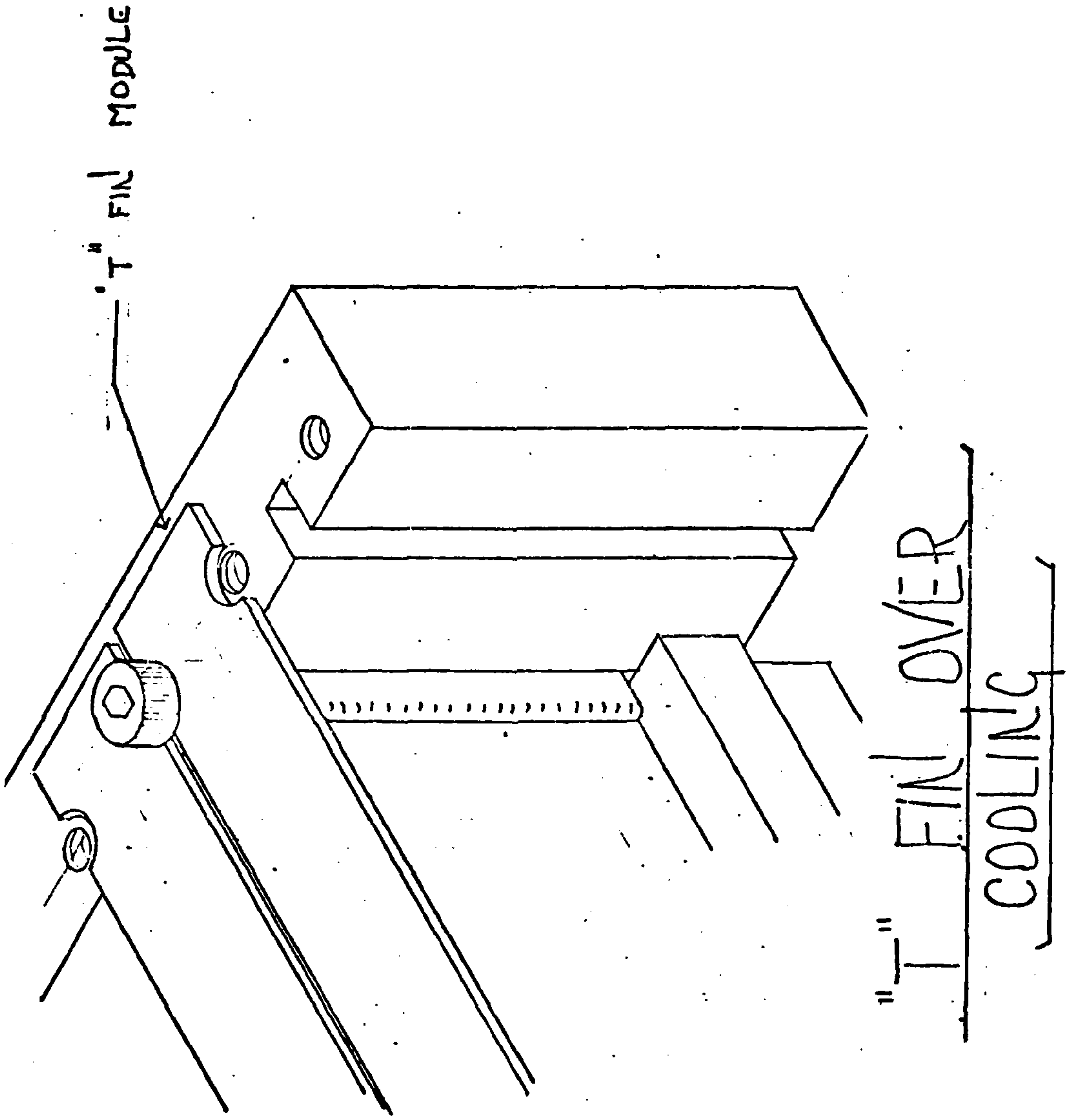

FIGURE A-10

between the module and system for each system for each condition is as follows:

Condition 1: $\Theta = 4.9°C/W$ (Θ_{M+E-cc})
Condition 2: $\Theta = 8.9°C/W$ (Θ_{M-cc})
Condition 3: $\Theta = 8.2°C/W$

Condition 3 would simulate a case where the hold-down devices were inadvertently not engaged. To determine the thermal resistance of the ear-card guide interface (Θ_{E-cg}), the data for Conditions 1 and 2 was used in the following fashion:

Unknown: Θ_{E-cg}
Known: Θ_{M-cc}
Θ_{M+E-cc}

Where Θ_{M-cc} is the thermal resistance between the module (excluding the ear) and the total card cage, including wire wrap plate, and Θ_{M+E-cc} is the thermal resistance between the module (including the ear) and the total card cage. We can reasonably assume that Θ_{M+E-cc} is nothing more than Θ_{E-cg} in parallel with Θ_{M-cc}.

$$\Theta_{M+E-cc} = \Theta\ E = cg \quad \Theta M-cc$$

$$\Theta M+C-cc = \frac{\Theta E-cg \qquad \Theta M-cc}{\Theta E-cg + \Theta M-cc}$$

$$4.9°C/W = \frac{8.9°C/W\ \Theta E-cg}{8.9°C/W + \Theta E-cg}$$

Therefore: $\Theta E-cg = 10.9°C/W$

D. FIN CONDUCTION

1. Fin conduction testing utilized a water cooled cold plate covering an array of 10 2A load modules (2 rows of 5 modules each). The internal cold plate design was such that the two rows of 5 modules were in parallel. The flow rate was held constant at 3 GPM to minimize the temperature rise across the cold plate. For the purpose of determining thermal resistances, this small temperature rise was neglected.

The interface between the module fin and the cold plate was developed by pressing the cold plate onto the modules. This was accomplished by passing eighteen 4-40 screws through the cold plate into the card guides and torquing each screw to a value of two inch-pounds. The modules were individually pressed up against the cold plate by Bellville washer energy cartridges located within the card guides. The net upward force was approximately 100 pounds per 2A load module. See Figure A-11 for the test configuration.

Both the .280" "T" fin and the conventional "L" fin were tested for comparison purposes. The thermal resistance between the water and the fin for the .280" "T" was .53°C/W, compared with 2.14°C/W for the conventional "L". Table A-5 contains a summary of projected power capacities for various module configurations.

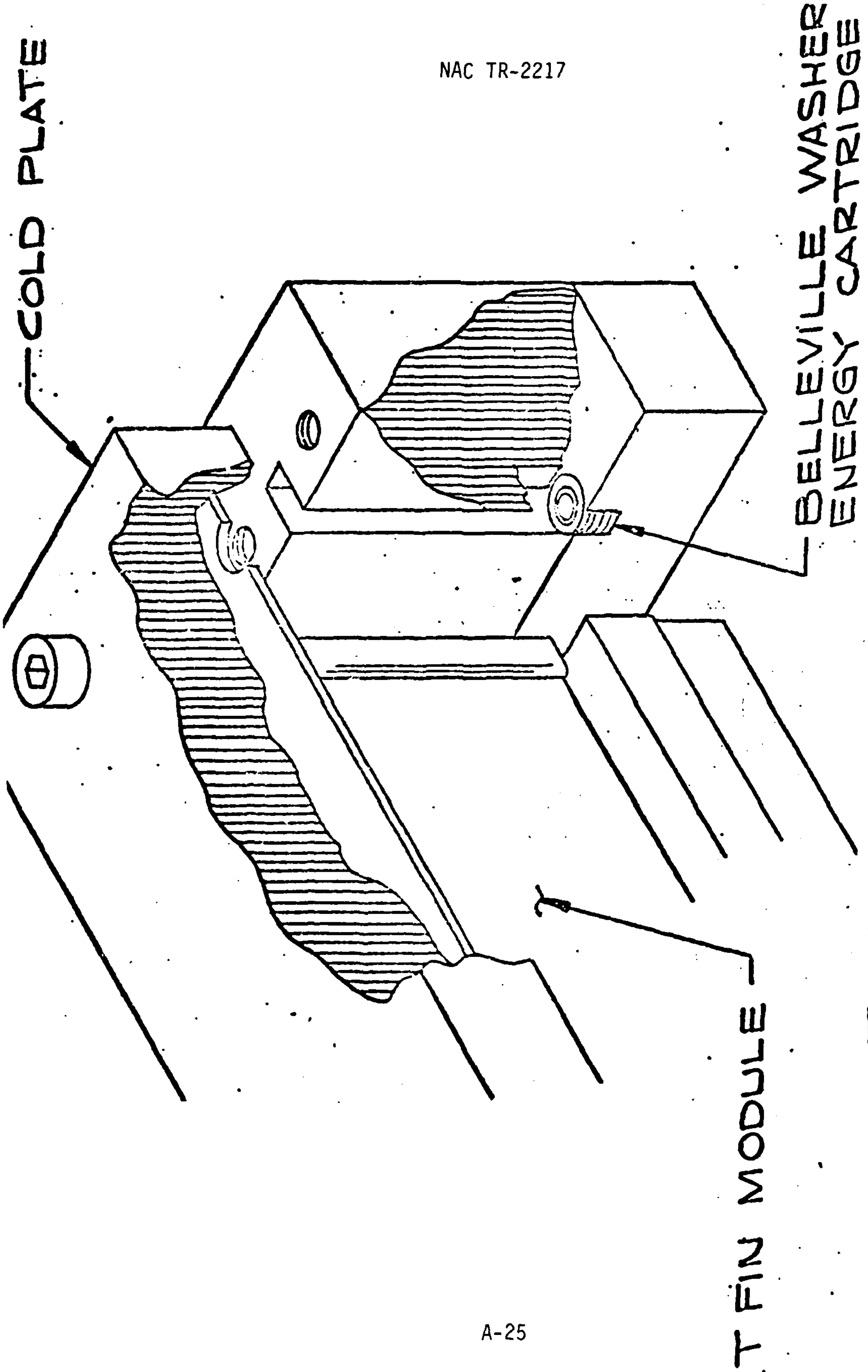

TOP COOLING

FIGURE A-11

TABLE A-5

FIN CONDUCTION POWER CAPACITIES

MODULE	RIB ORIENTATION	MODULE POWER
SEM 1A Dip	VERTICAL	4.5
ISEM 1A Dip	VERTICAL	6.4
ISEM 1A Dip	HORIZONTAL	4.5
SEM 1A C.F.		7.2
ISEM 1A C.F.		14.9
SEM 2A Dip	VERTICAL	9.3
ISEM 2A Dip	VERTICAL	13.8
ISEM 2A Dip	HORIZONTAL	8.4
SEM 2A C.F.		15.6
ISEM 2A C.F.		30.0

CONDITIONS

35°C Inlet Water, 105°C Max Jct Temp.

Uniforma Power Distribution

ISEM-6101 AL, SEM 5052 AL

SEM 1A Dip and ISEM 1A Dip W/Vert Ribs: (5) - 16 Pin Dips

ISEM 1A Dip: (9) - 16 Pin Dips

SEM 2A Dip & ISEM 2A Dip W/Vert Ribs: (12) - 16 Pin Dips

ISEM 2A Dip: (16) - 16 Pin Dips

ISEM 1A C.F.: (12) - 16 Pin Flatpacks Per Side,

SEM 1A C.F.: (8) - 16 Pin Flatpacks Per Side

ISEM 2A C.F.: (24) - 16 Pin Flatpacks Per Side, 25°C/W Jct to Case for Dip

SEM 2A C.F.: (20) - 16 Pin Flatpacks Per Side 45°C.W Jct to Case for Flatpac

APPENDIX B

MECHANICAL DESIGN DRAWINGS

NOTE: THE DRAWINGS CONTAINED HEREIN ARE ENGINEERING DESIGN QUALITY ONLY AND SHOULD NOT BE USED FOR PROCUREMENT PURPOSES. CONTACT THE NAVAL AVIONICS CENTER, CODE 924, FOR LATEST REVISION OF ISEM PROCUREMENT DRAWINGS.

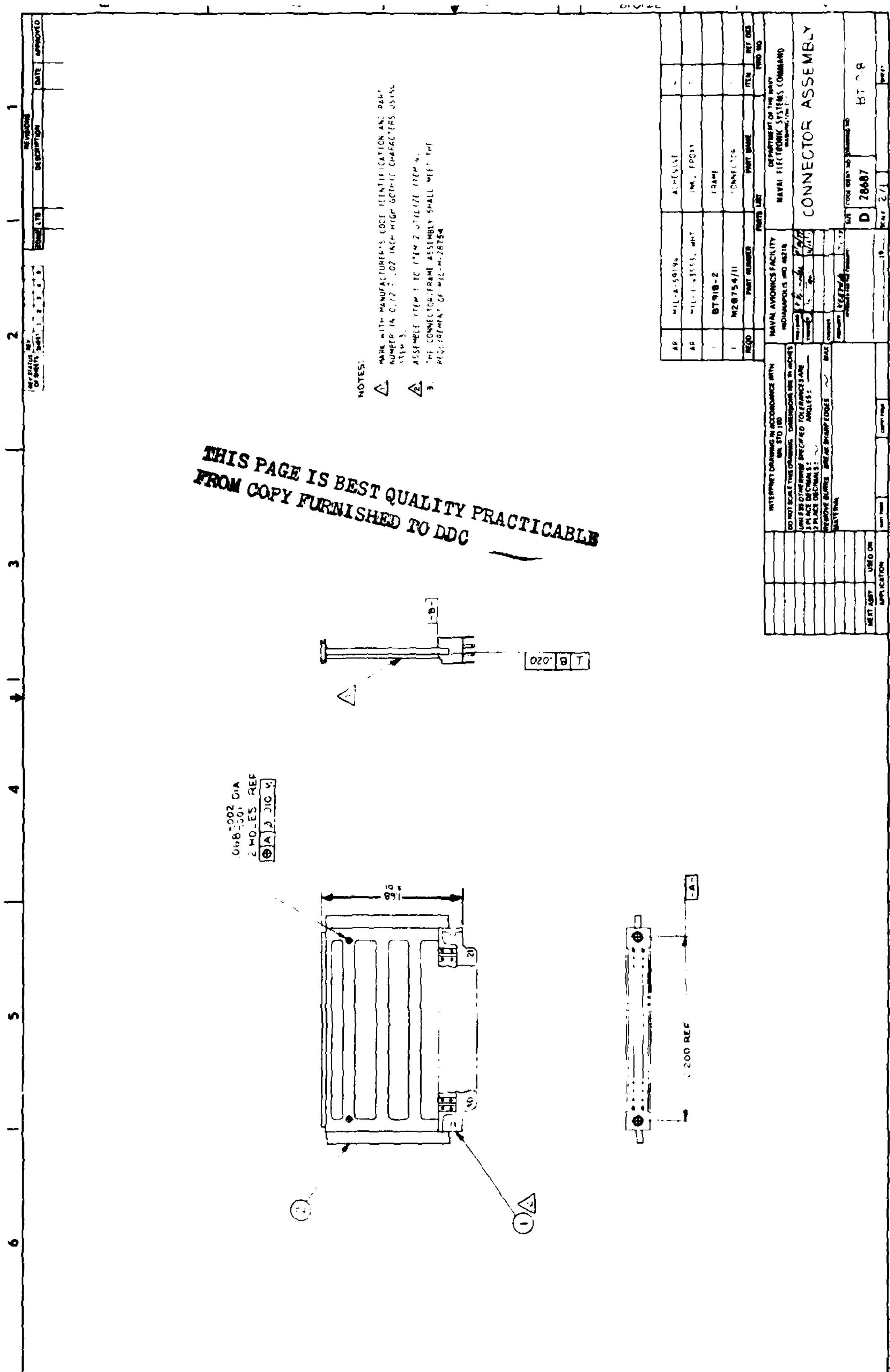
CONNECTOR ASSEMBLY
DEPARTMENT OF THE NAVY
NAVAL ELECTRONIC SYSTEMS COMMAND
NAVAL AVIONICS FACILITY
INDIANAPOLIS IND 46218
D 28687
NOTES:
M28754/11
BT918-2
CONNECTOR
FRAME
ADHESIVE
1.200 REF

Figure B-1

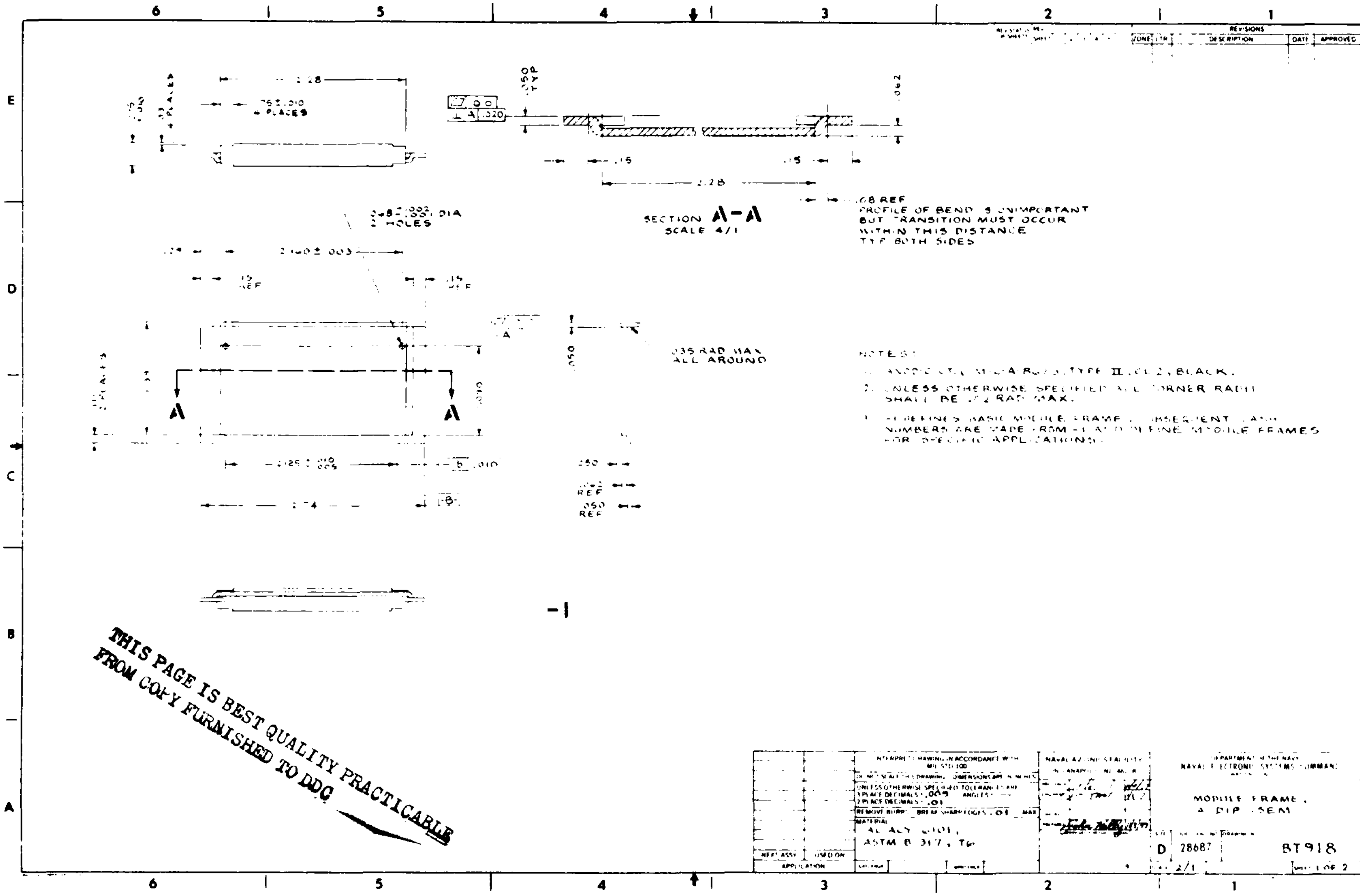

Figure B-2 (Sheet 1 of 2)

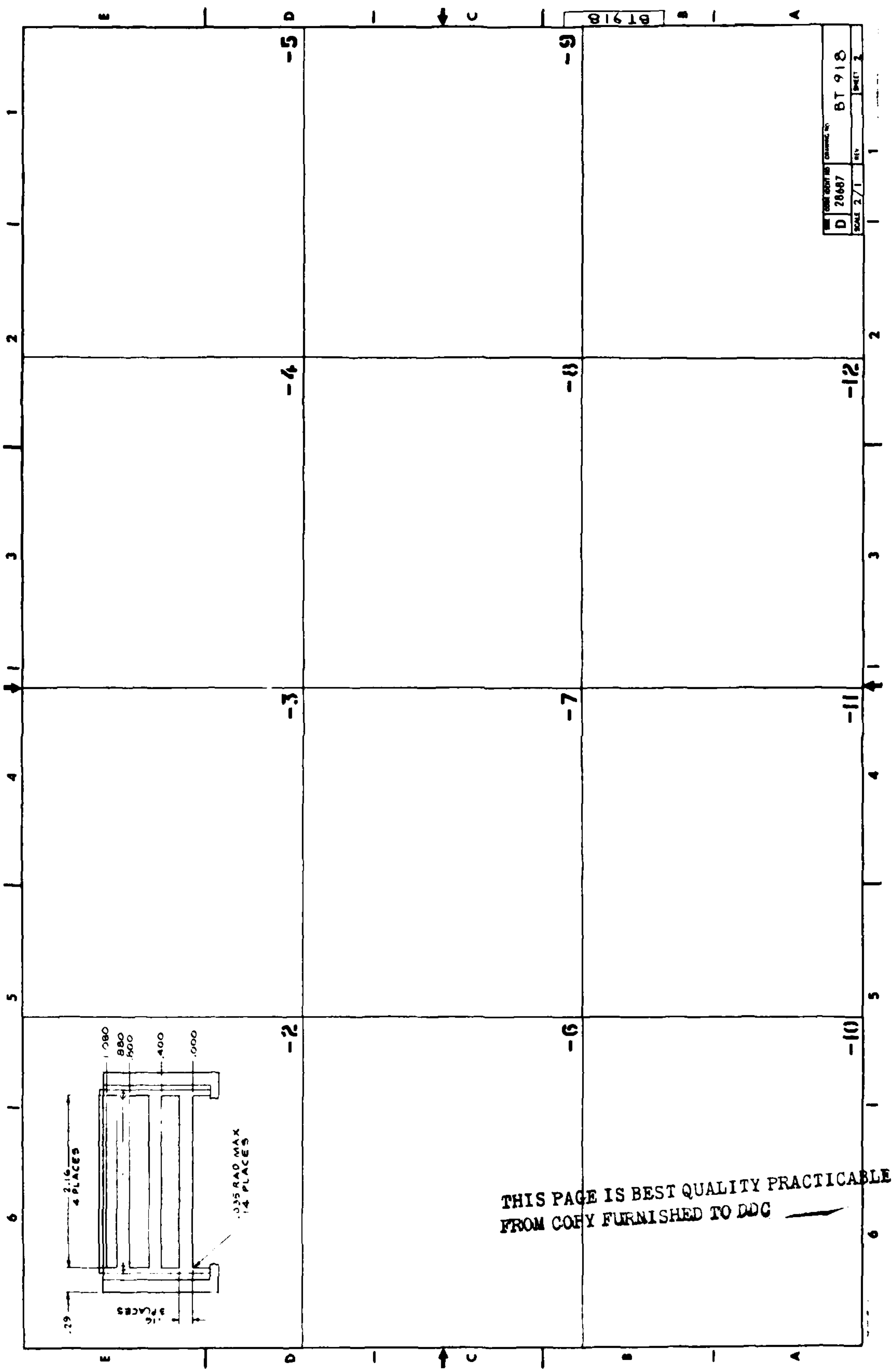

Figure B-2 (Sheet 2 of 2)

THIS PAGE IS BEST QUALITY PRACTICABLE
FROM COPY FURNISHED TO DDC

REV STATUS OF SHEETS	REV					
	SHEET	1	2	3	4	5

BT1102

REVISIONS			
LTR	DESCRIPTION	DATE	APPROVED

REQUIREMENTS

1. THE FINISHED PRINTED WIRING BOARD SHALL [illegible] WITH THE REQUIREMENTS SPECIFIED HEREIN AND SPECIFICATION [illegible]

A. MINIMUM [illegible] COPPER THICKNESS [illegible]

B. MINIMUM CONDUCTOR [illegible]

C. MINIMUM [illegible] SPACING [illegible]

D. MINIMUM AN[illegible]

MATERIAL [illegible]

[illegible]

MASTER PATTERN [illegible]

A. A RIGHT READING [illegible]

B. PHOTO[illegible] MEASUREMENTS FOR REFERENCE ON[illegible]

MINIMUM CONDUCTOR WIDTH [illegible]

MINIMUM CONDUCTOR SPACING [illegible]

NEXT ASSY	USED ON
APPLICATION	

BT1102

Figure B-3 (Sheet 1 of 2)

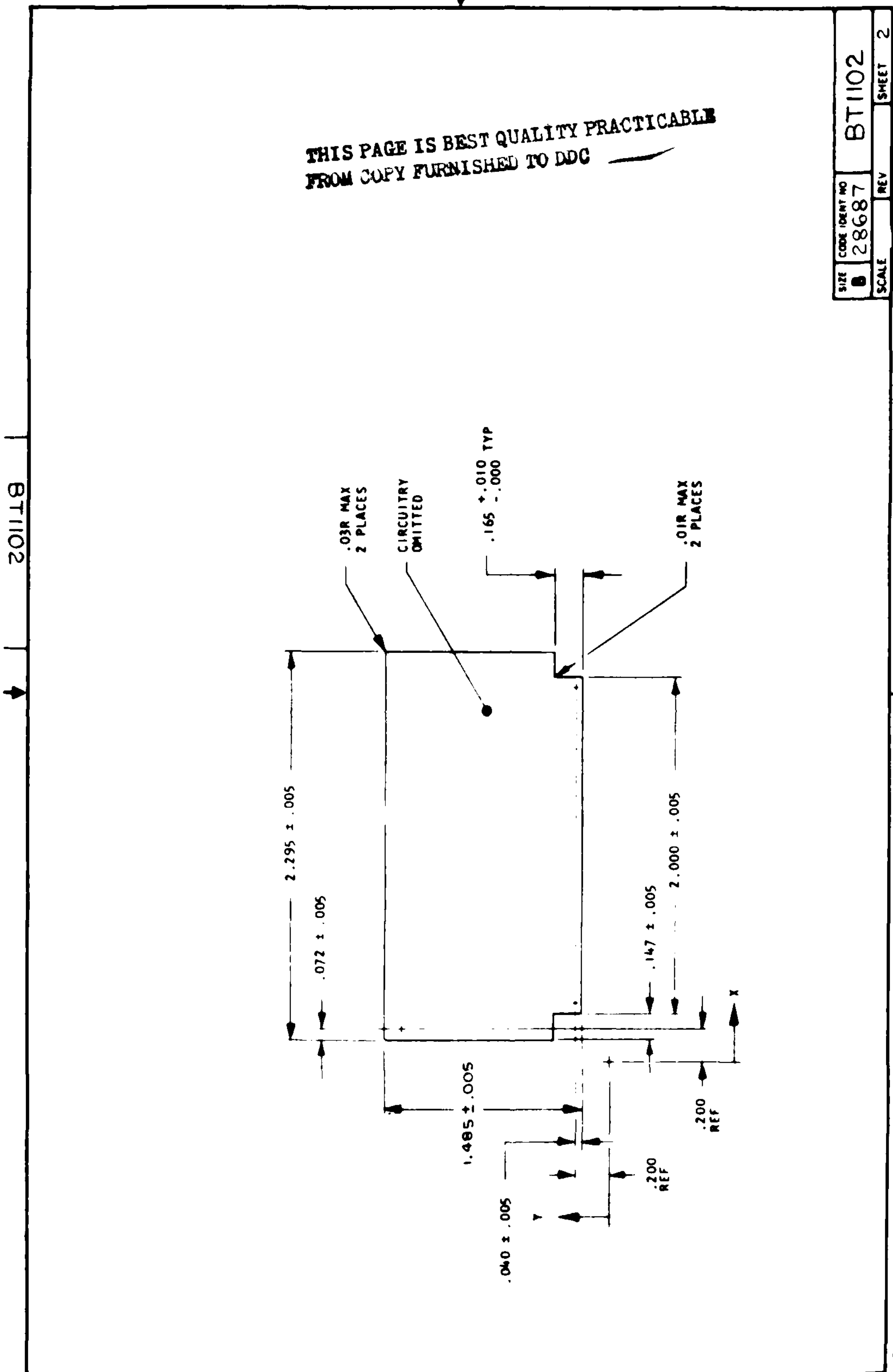

Figure B-3 (Sheet 2 of 2)

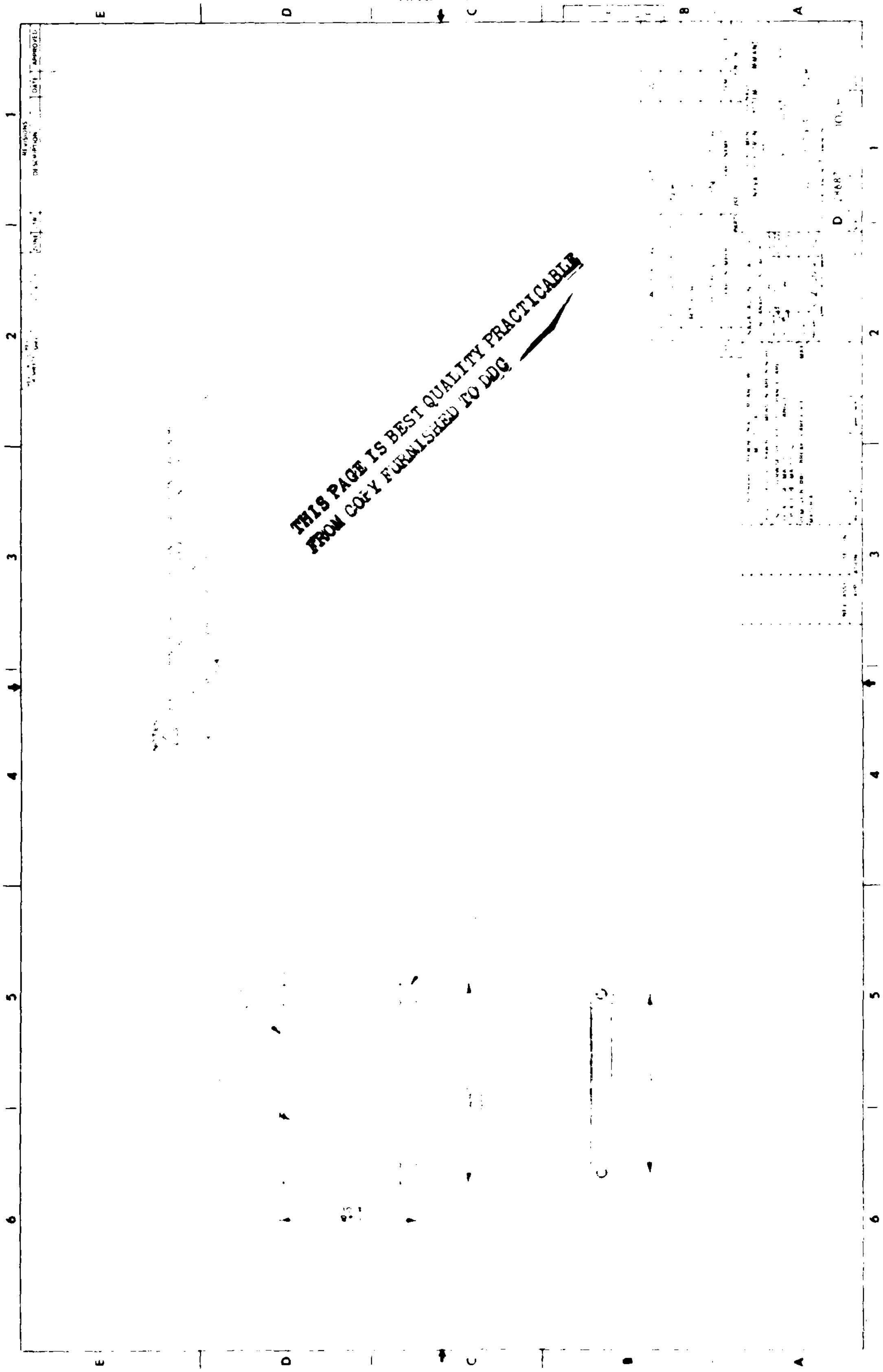

Figure B-1

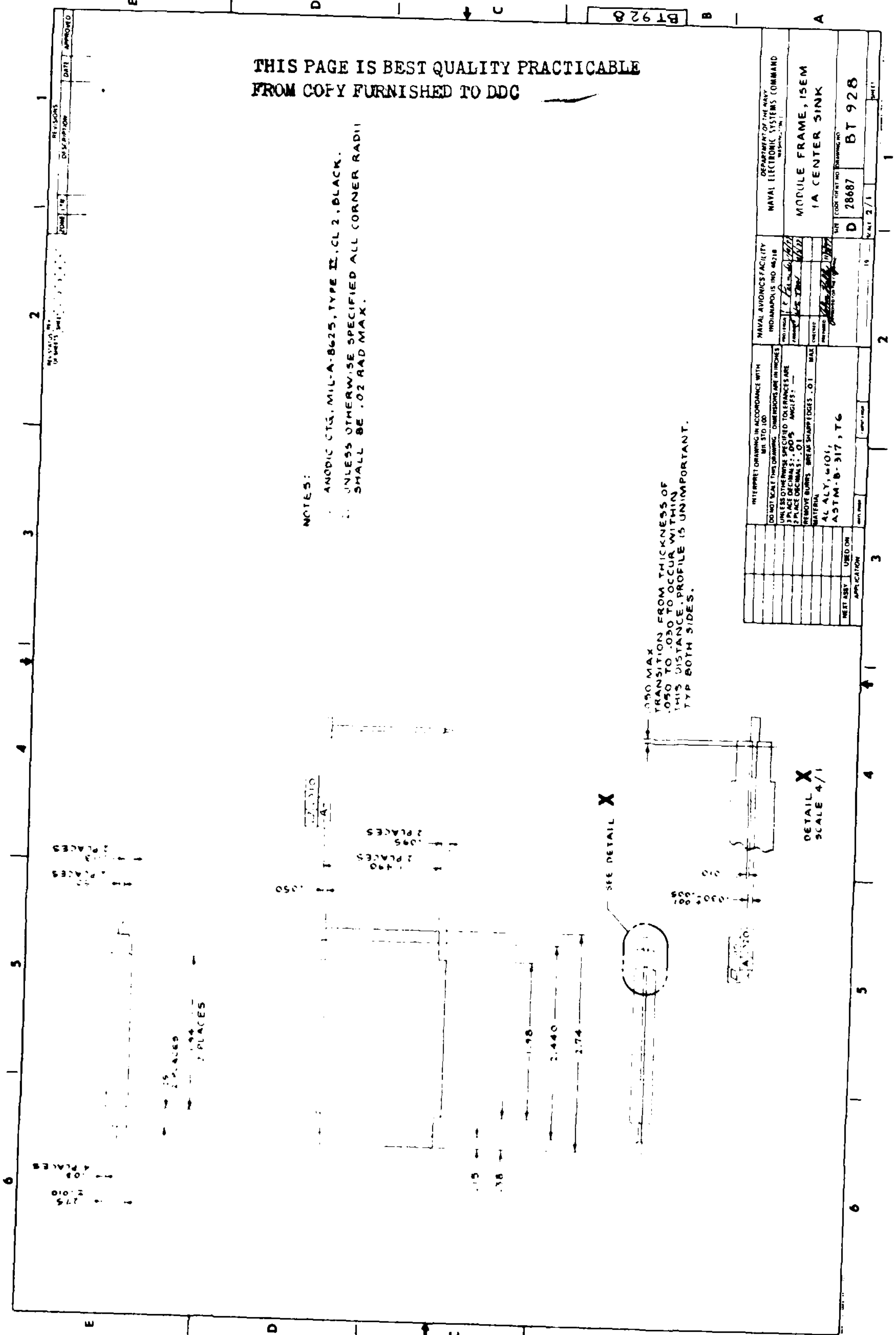
BT 928
NOTES:
1. ANODIC CTG, MIL-A-8625, TYPE II, CL 2, BLACK.
2. UNLESS OTHERWISE SPECIFIED ALL CORNER RADII SHALL BE .02 RAD MAX.
.030 MAX TRANSITION FROM THICKNESS OF .050 TO .030 TO OCCUR WITHIN THIS DISTANCE. PROFILE IS UNIMPORTANT. TYP BOTH SIDES.
SEE DETAIL X
DETAIL X SCALE 4/1
1.98
2.440
2.74
.050
DEPARTMENT OF THE NAVY
NAVAL ELECTRONIC SYSTEMS COMMAND
MODULE FRAME, ISEM
1A CENTER SINK
D 28687 BT 928
SCALE 2/1
NAVAL AVIONICS FACILITY
INDIANAPOLIS IND 46218
MATERIAL
AL ALY, 6101,
ASTM-B-317, T6

Figure B-5

REV STATUS OF SHEETS	REV					
	SHEET	1	2	3	4	5

BT1104

REVISIONS			
LTR	DESCRIPTION	DATE	APPROVED

REQUIREMENTS

1. THE FINISHED PRINTED WIRING BOARD SHALL COMPLY WITH THE REQUIREMENTS SPECIFIED HEREIN AND SPECIFICATION WS6137
   A. MINIMUM FINISHED COPPER THICKNESS 0.0025
   B. MINIMUM CONDUCTOR WIDTH 0
   C. MINIMUM CONDUCTOR SPACING 0
   D. MINIMUM ANNULAR RING 0
2. MATERIAL 0.0
   PLASTIC SH. THIN LAM. MET-CLAD, MIL-P-55617, TYPE (CY B)
   STARTING COPPER THICKNESS OPTIONAL (SEE 1 A ABOVE)
3. PLATING. TIN-LEAD PLATING SHALL BE IN ACCORDANCE WITH SPECIFICATION MIL-P-81728.
4. FOR HOLE PROCESSING REQUIREMENTS SEE
5. THE DELINEATIONS ON SHEET ARE FOR ORIENTATION ONLY
6. MASTER PATTERN (PHOTOTOOLS):
   A. A RIGHT READING BASE SIDE (MULTI IMAGE) DIAZO FILM SET WILL BE SUPPLIED UPON REQUEST BY NAVAL AVIONICS FACILITY, INDIANAPOLIS, INDIANA 46218 AND SHALL BE USED TO PRODUCE THE PRINTED WIRING BOARD. THE REQUEST FOR THE PHOTOTOOLS SHALL INDICATE THE IDENTIFICATION AND APPLICABLE REVISION LETTER AS INDICATED ON SHEET
   B. PHOTOTOOL MEASUREMENTS FOR REFERENCE ONLY
   MINIMUM CONDUCTOR WIDTH . . . .
   MINIMUM CONDUCTOR SPACING . . . .

THIS PAGE IS BEST QUALITY PRACTICABLE FROM COPY FURNISHED TO DDC

NEXT ASSY	USED ON	INTERPRET DRAWING IN ACCORDANCE WITH MIL-STD-100	NAVAL AVIONICS FACILITY INDIANAPOLIS IND 46218	DEPARTMENT OF THE NAVY ... COMMAND WASHINGTON D.C.
APPLICATION		DO NOT SCALE THIS DRAWING. DIMENSIONS ARE IN INCHES. UNLESS OTHERWISE SPECIFIED TOLERANCES ARE 3 PLACE DECIMALS ± 2 PLACE DECIMALS ± ANGLES ±	ENGINEER / CHECKED / PREPARED	PRINTED WIRE BOARD
		REMOVE BURRS BREAK SHARP EDGES MAX		SIZE B / CODE IDENT NO 28687 / DRAWING NO BT1104
		MATERIAL:	19	SCALE / SHEET 1 OF 2
		MATL ENGR		

Figure B-6 (Sheet 1 of 2)

BT1104

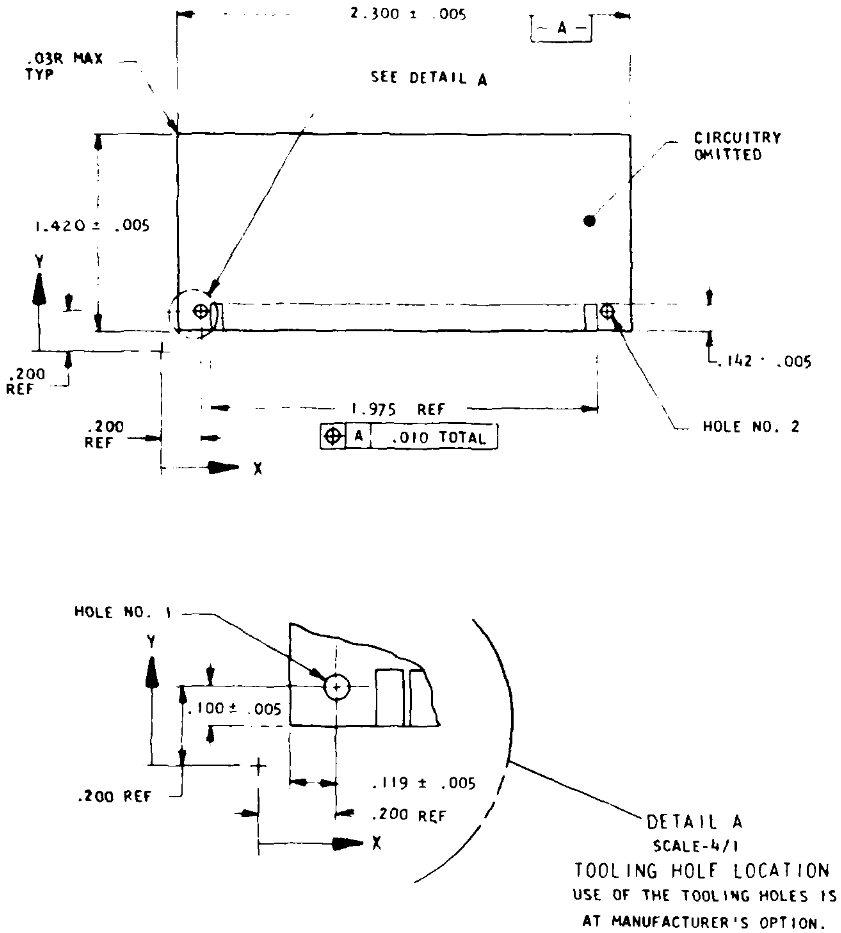

HOLE CHART

HOLE NO.	X → BSC	Y ↑ BSC	HOLE SIZE	LOCATION TOL.
1 SEE DETAIL A	.200	.200	.062 ± .001 DIA	⊕ .005 DIA
2 SEE DETAIL A	2.262	.200	.062 ± .001 DIA	⊕ .005 DIA

SIZE	CODE IDENT NO	
B	28687	BT1104
SCALE	REV	SHEET 2

9ND NAFI 4122/9 (9-73)

Figure B-6 (Sheet 2 of 2)

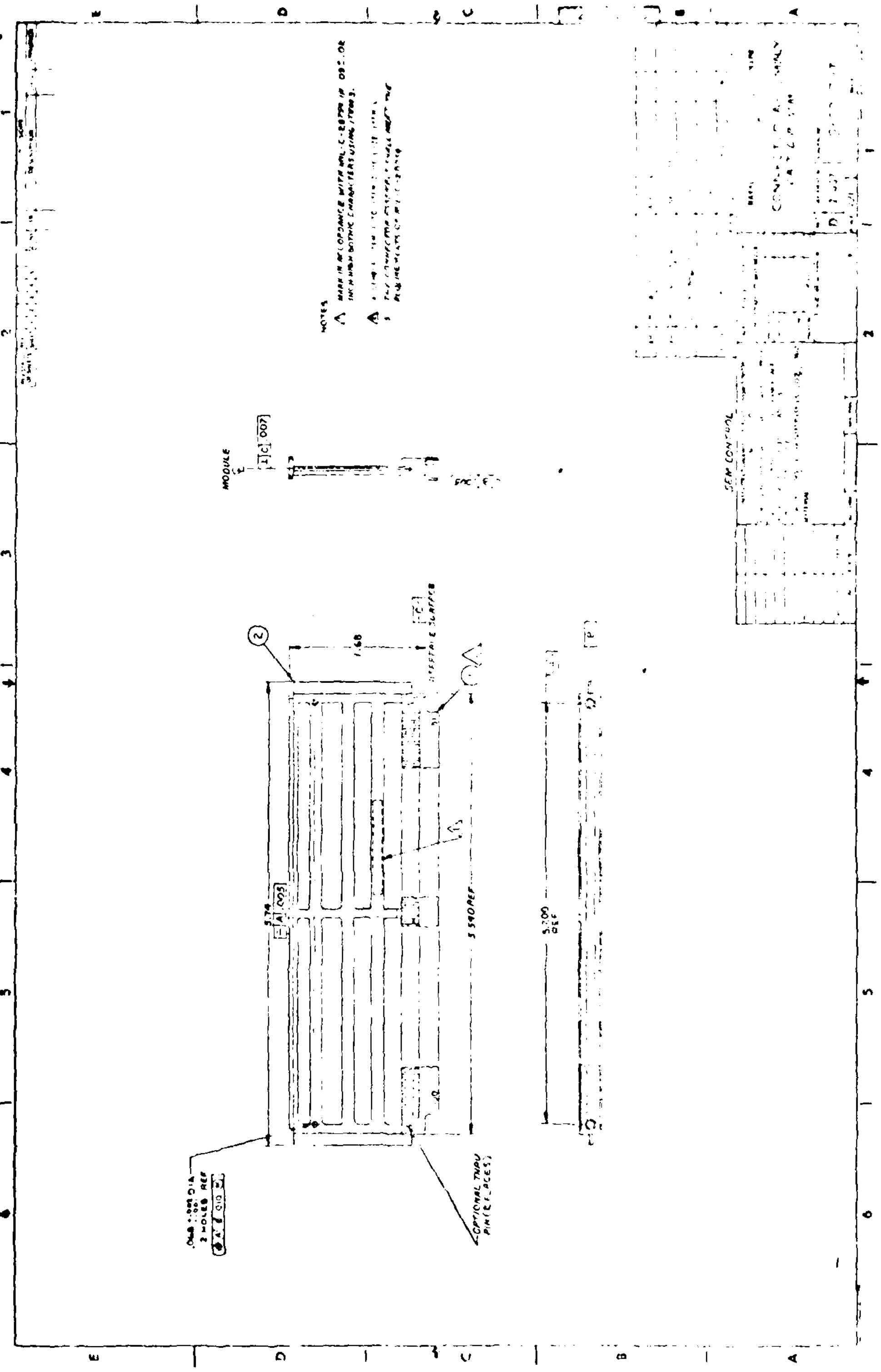

Figure B-7

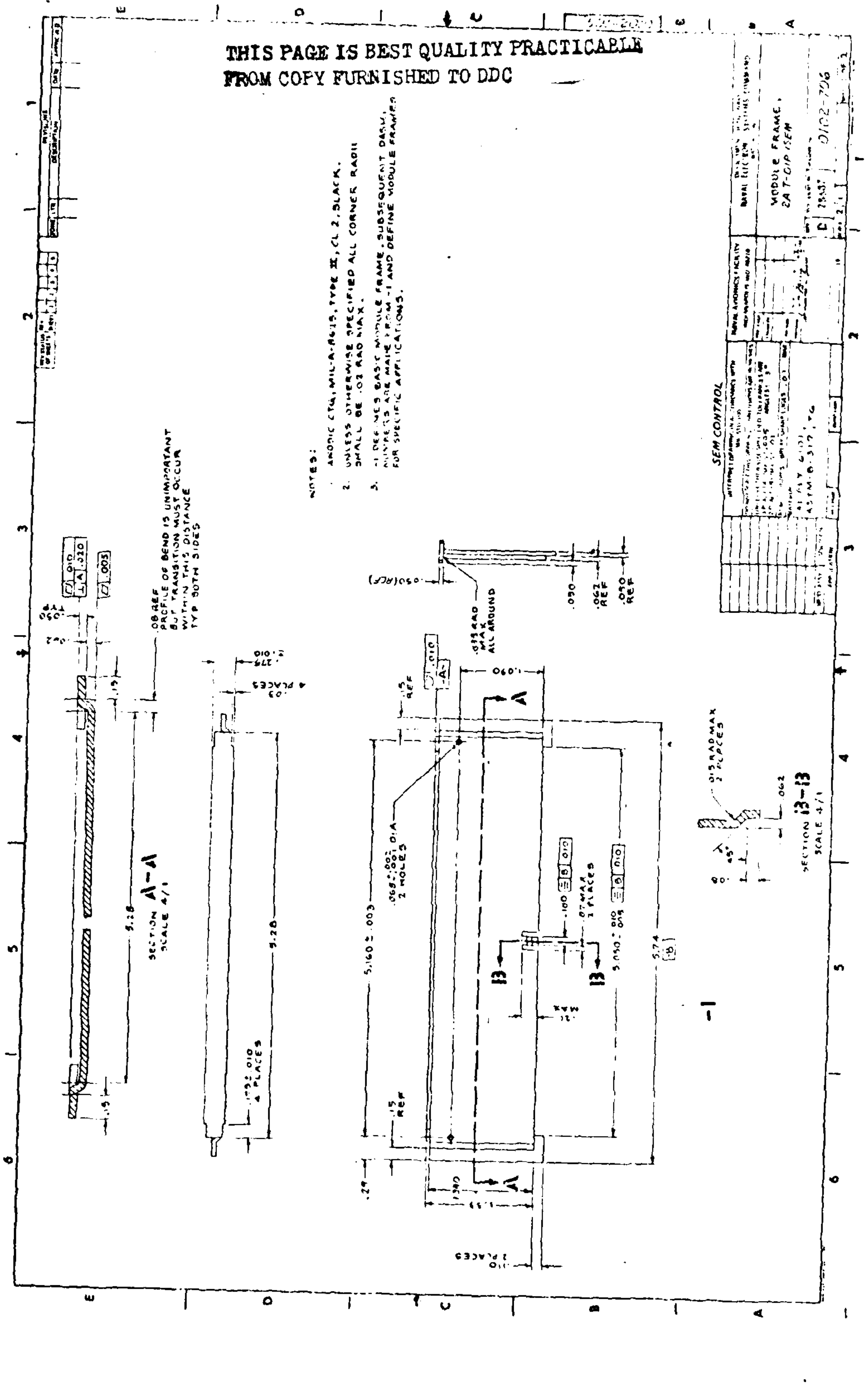

Figure B-8 (Sheet 1 of 2)

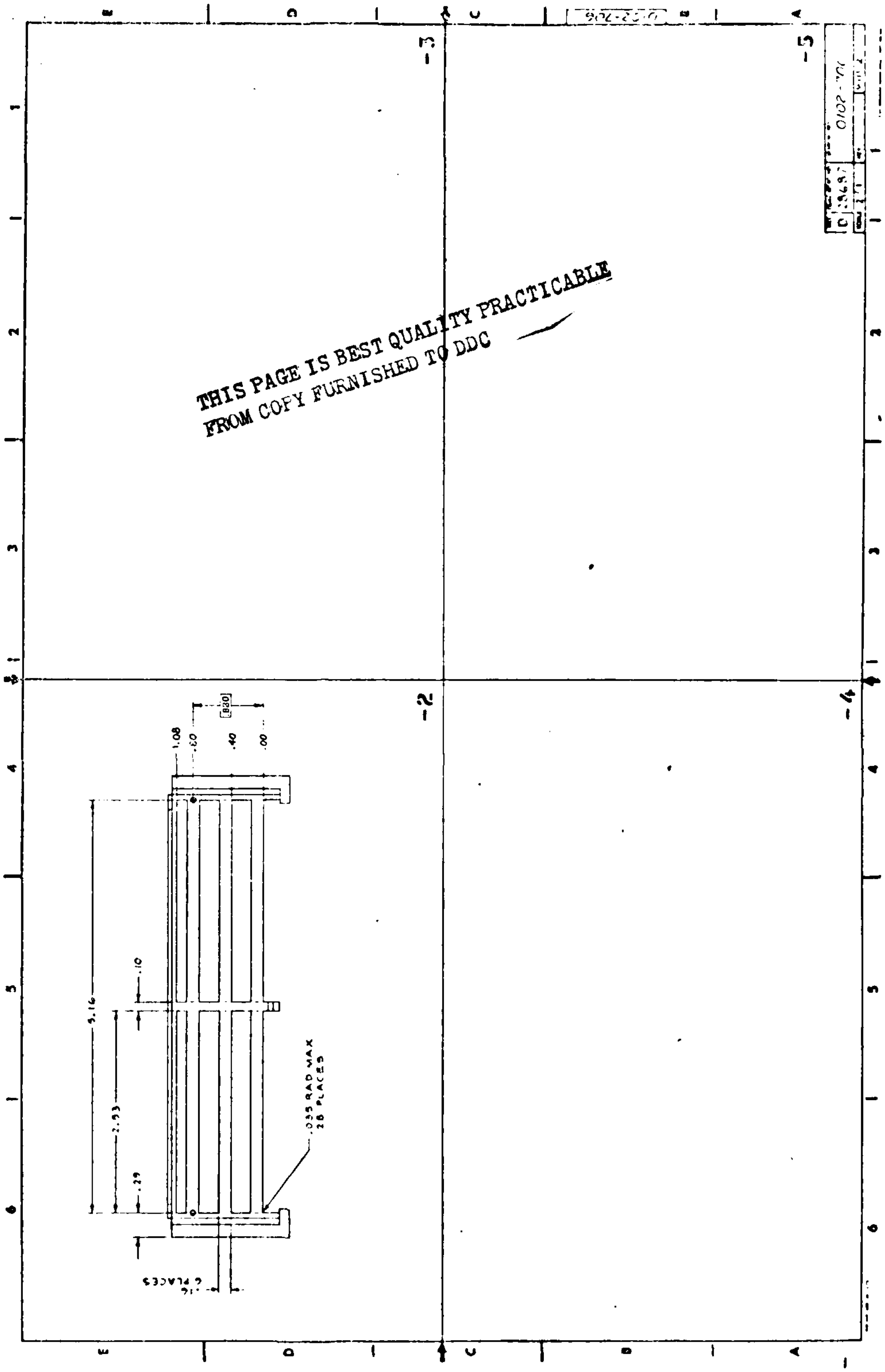

Figure B-8 (Sheet 2 of 2)

THIS PAGE IS BEST QUALITY PRACTICABLE
FROM COPY FURNISHED TO DDC

BT1101

REV STATUS OF SHEETS	REV					
	SHEET	1	2	3	4	5

REVISIONS			
LTR	DESCRIPTION	DATE	APPROVED

REQUIREMENTS:

1. THE FINISHED PRINTED WIRING BOARD SHALL COMPLY WITH THE REQUIREMENTS SPECIFIED HEREIN AND SPECIFICATION WS6137
   - A MINIMUM FINISHED COPPER THICKNESS 0.0025
   - B MINIMUM CONDUCTOR WIDTH 0
   - C MINIMUM CONDUCTOR SPACING 0
   - D MINIMUM ANNULAR RING 0.0
2. MATERIAL:
   PLSTC SH, THIN LAM, MET-CLAD, MIL-P-55617, TL-GE C*/ B1
   * STARTING COPPER THICKNESS OPTIONAL (SEE 1 A ABOVE)
3. PLATING: TIN-LEAD PLATING SHALL BE IN ACCORDANCE WITH SPECIFICATION MIL-P-81728.
4. FOR HOLE PROCESSING REQUIREMENTS SEE
5. THE DELINEATIONS ON SHEET ARE FOR ORIENTATION ONLY
6. MASTER PATTERN (PHOTOTOOLS)
   - A A RIGHT READING BASE SIDE (MULTI-IMAGE) DIAZO FILM SET WILL BE SUPPLIED UPON REQUEST BY NAVAL AVIONICS FACILITY, INDIANAPOLIS, INDIANA 46218, AND SHALL BE USED TO PRODUCE THE PRINTED WIRING BOARD. THE REQUEST FOR THE PHOTOTOOLS SHALL INDICATE THE IDENTIFICATION AND APPLICABLE REVISION LETTER AS INDICATED ON SHEET
   - B. PHOTOTOOL MEASUREMENTS FOR REFERENCE ONLY
     - MINIMUM CONDUCTOR WIDTH 0
     - MINIMUM CONDUCTOR SPACING . . . . 0.

NEXT ASSY	USED ON
APPLICATION	

INTERPRET DRAWING IN ACCORDANCE WITH MIL-STD-100
DO NOT SCALE THIS DRAWING. DIMENSIONS ARE IN INCHES
UNLESS OTHERWISE SPECIFIED TOLERANCES ARE
3 PLACE DECIMALS ± ANGLES ±
2 PLACE DECIMALS ±
REMOVE BURRS BREAK SHARP EDGES MAX
MATERIAL: 2
MATL ENGR | CMPNT ENGR

NAVAL AVIONICS FACILITY
INDIANAPOLIS, IND. 46218

PROJ ENGR		
ENGINEER		
CHECKED		
PREPARED	Butler	11/10/77

APPROVED FOR THE COMMAND
19

DEPARTMENT OF THE NAVY
NAVAL [illegible] COMMAND
WASHINGTON, D.C. 20360

PRINTED WIRE BOARD

SIZE	CODE IDENT NO.	DRAWING NO.
B	28687	BT1101
SCALE		SHEET 1 OF 2

Figure B-9 (Sheet 1 of 2)

NAC TR-2217

THIS PAGE IS BEST QUALITY PRACTICABLE
FROM COPY FURNISHED TO DDC

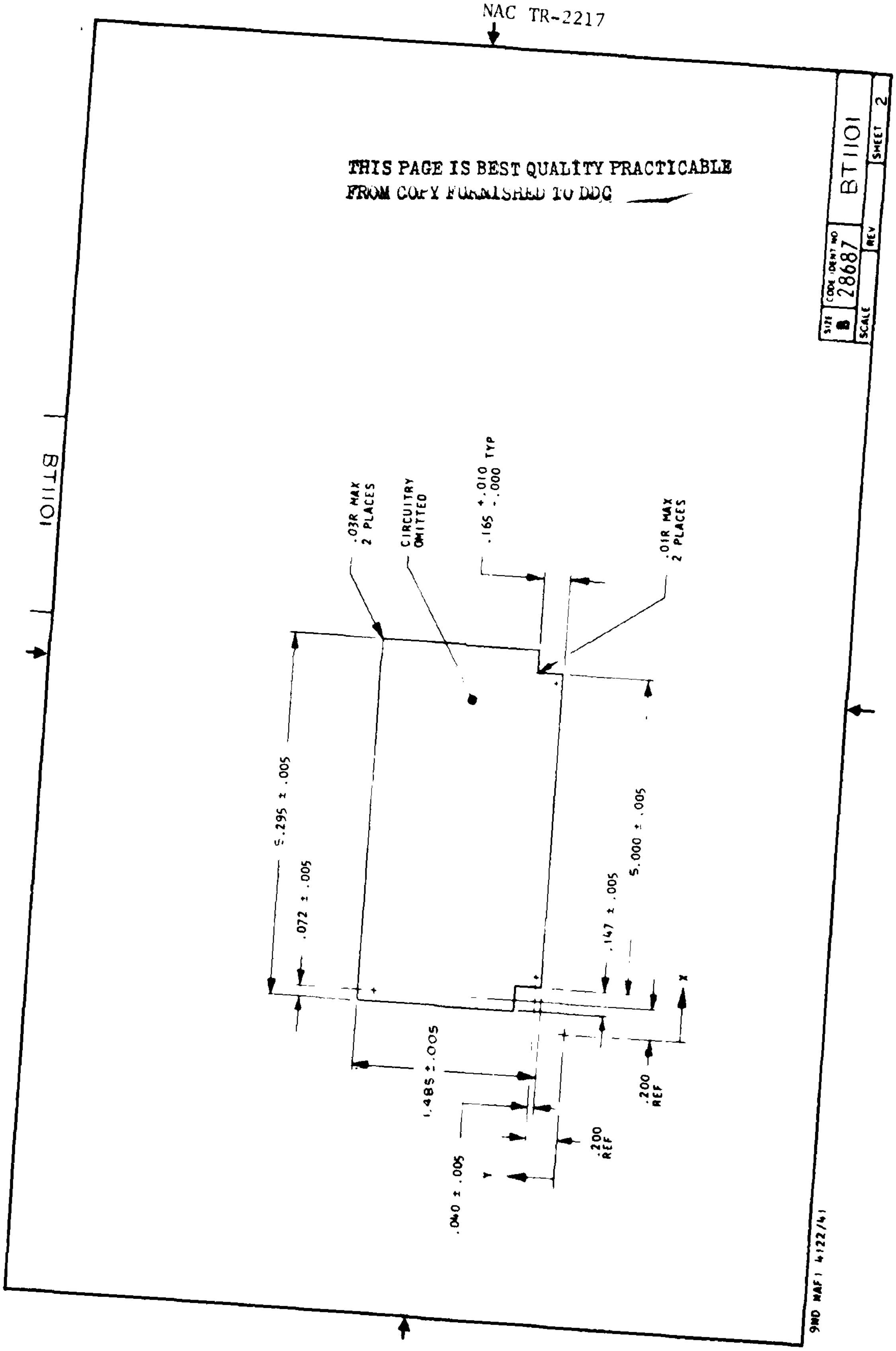

Figure B-9 (Sheet 2 of 2)

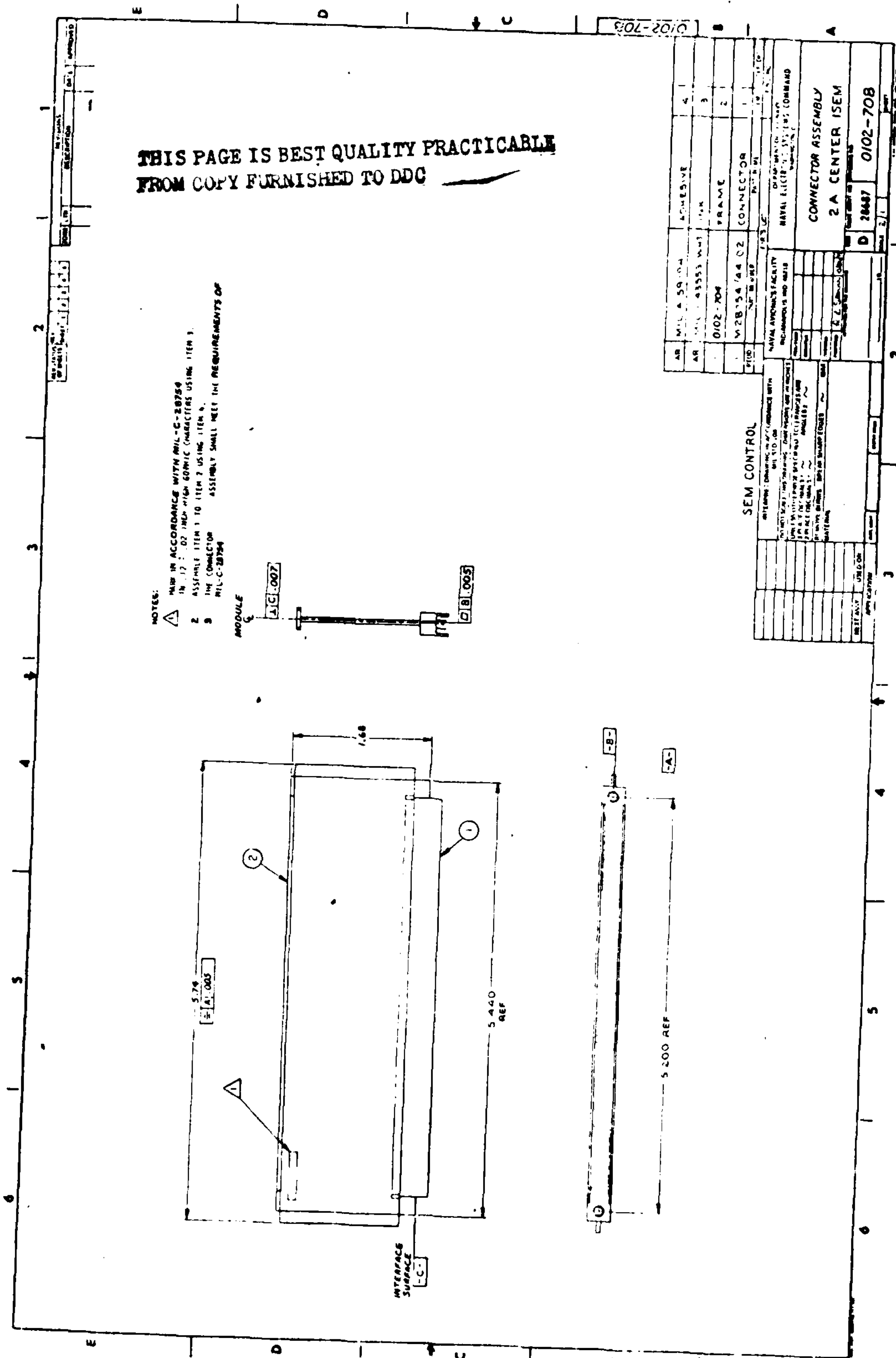
CONNECTOR ASSEMBLY
2A CENTER ISEM
0102-708
SEM CONTROL
0102-703
MODULE
INTERFACE SURFACE
5.440 REF
5.200 REF
1.68

Figure B-10

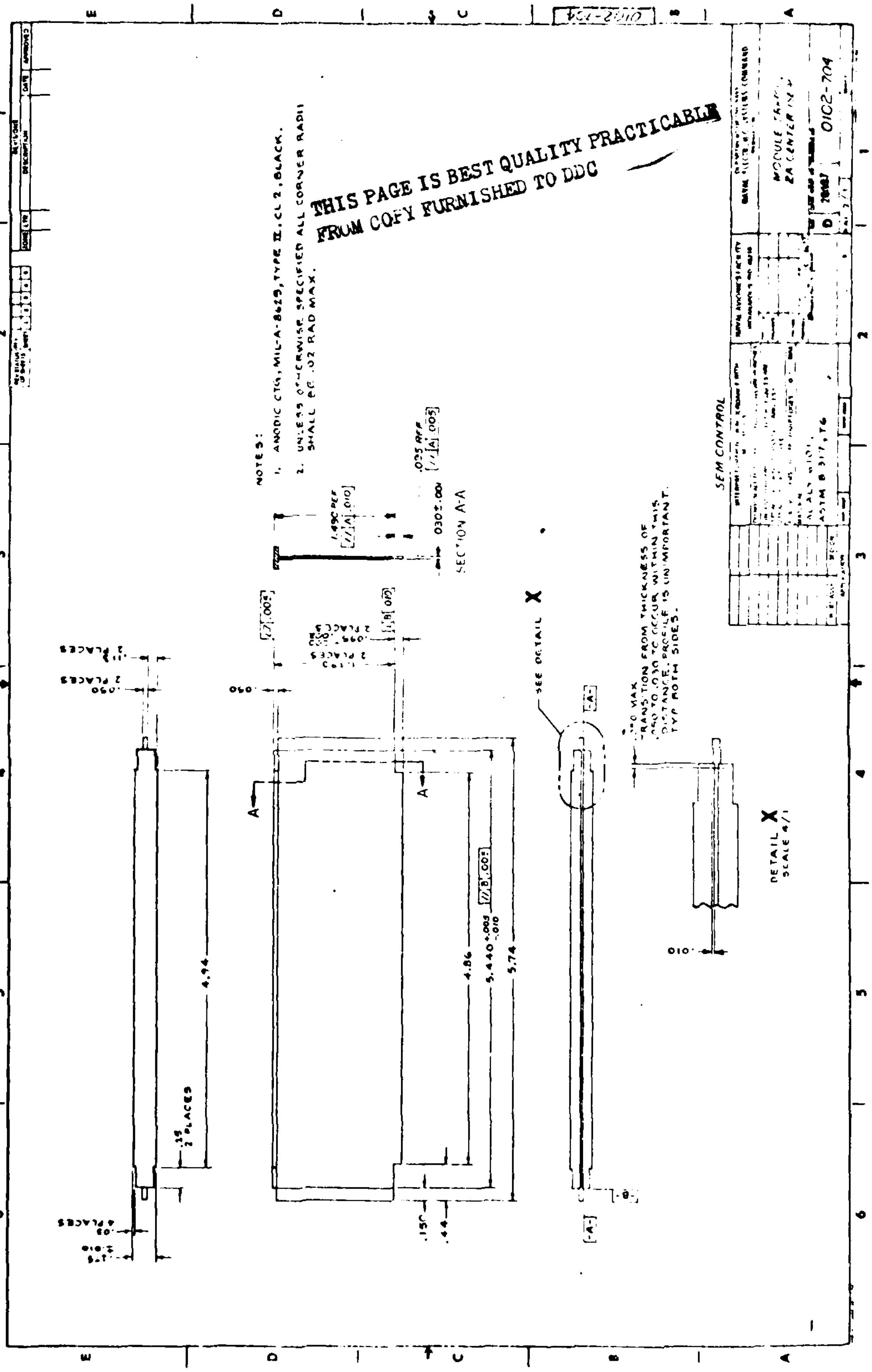
NOTES:
1. ANODIC CTG, MIL-A-8625, TYPE II, CL 2, BLACK.
2. UNLESS OTHERWISE SPECIFIED ALL CORNER RADII SHALL BE .02 RAD MAX.
SECTION A-A
SEE DETAIL X
DETAIL X SCALE 4/1
SEM CONTROL
01C2-704
THIS PAGE IS BEST QUALITY PRACTICABLE
FROM COPY FURNISHED TO DDC

Figure B-11

REV STATUS OF SHEETS	REV					
	SHEET	1	2	3	4	5

BT1103

REVISIONS			
LTR	DESCRIPTION	DATE	APPROVED

REQUIREMENTS

1 THE FINISHED PRINTED WIRING BOARD SHALL COMPLY WITH THE REQUIREMENTS SPECIFIED HEREIN AND SPECIFICATION WS6137

A MINIMUM FINISHED COPPER THICKNESS - - - - - - - 0.0025

B MINIMUM CONDUCTOR WIDTH - - - - - - - - - - - - 0

C MINIMUM CONDUCTOR SPACING - - - - - - - - - - - 0

D MINIMUM ANNULAR RING - - - - - - - - - - - - 0.C

2 MATERIAL

PLSTC SH. THIN LAM. MET-CLAD. MIL-P-55617. TI-GE C*/ B!

* STARTING COPPER THICKNESS OPTIONAL (SEE 1 A ABOVE)

3 PLATING TIN-LEAD PLATING SHALL BE IN ACCORDANCE WITH SPECIFICATION MIL-P-81728.

4 FOR HOLE PROCESSING REQUIREMENTS SEE

THE DELINEA... ON SHEET ARE FOR ORIENTATION ONLY

MASTER PATTERN (PHOTOTOOLS)

A A RIGHT READING BASE SIDE (MULTI IMAGE) DIAZO FILM SET WILL BE SUPPLIED UPON REQUEST BY NAVAL AVIONICS FACILITY, INDIANAPOLIS, INDIANA 46218, AND SHALL BE USED TO PRODUCE THE PRINTED WIRING BOARD. THE REQUEST FOR THE PHOTOTOOLS SHALL INDICATE THE IDENTIFICATION AND APPLICABLE REVISION LETTER AS INDICATED ON SHEET

B PHOTOTOOL MEASUREMENTS FOR REFERENCE ONLY

MINIMUM CONDUCTOR WIDTH - - - - - - - - - - - - - 0

MINIMUM CONDUCTOR SPACING - - - - - - - - 0

NEXT ASSY	USED ON
APPLICATION	

INTERPRET DRAWING IN ACCORDANCE WITH MIL-STD 100

DO NOT SCALE THIS DRAWING. DIMENSIONS ARE IN INCHES

UNLESS OTHERWISE SPECIFIED TOLERANCES ARE
3 PLACE DECIMALS ±   ANGLES ±
2 PLACE DECIMALS ±

REMOVE BURRS BREAK SHARP EDGES MAX

MATERIAL: 7

MATL ENGR | CMPNT ENGR

NAVAL AVIONICS FACILITY
INDIANAPOLIS IND 46218

PROJ ENGR
ENGINEER
CHECKED
PREPARED B...

APPROVED FOR THE COMMAND
19

DEPARTMENT OF THE NAVY
NAVAL ELECTRONIC SYSTEMS COMMAND
WASHINGTON D C 20360

PRINTED WIRE BOARD

SIZE	CODE IDENT NO.	DRAWING NO
B	28687	BT1103
SCALE		SHEET 1 OF 2

NAFI 8808/151 (8-73)

Figure B-12 (Sheet 1 of 2)

BT1103

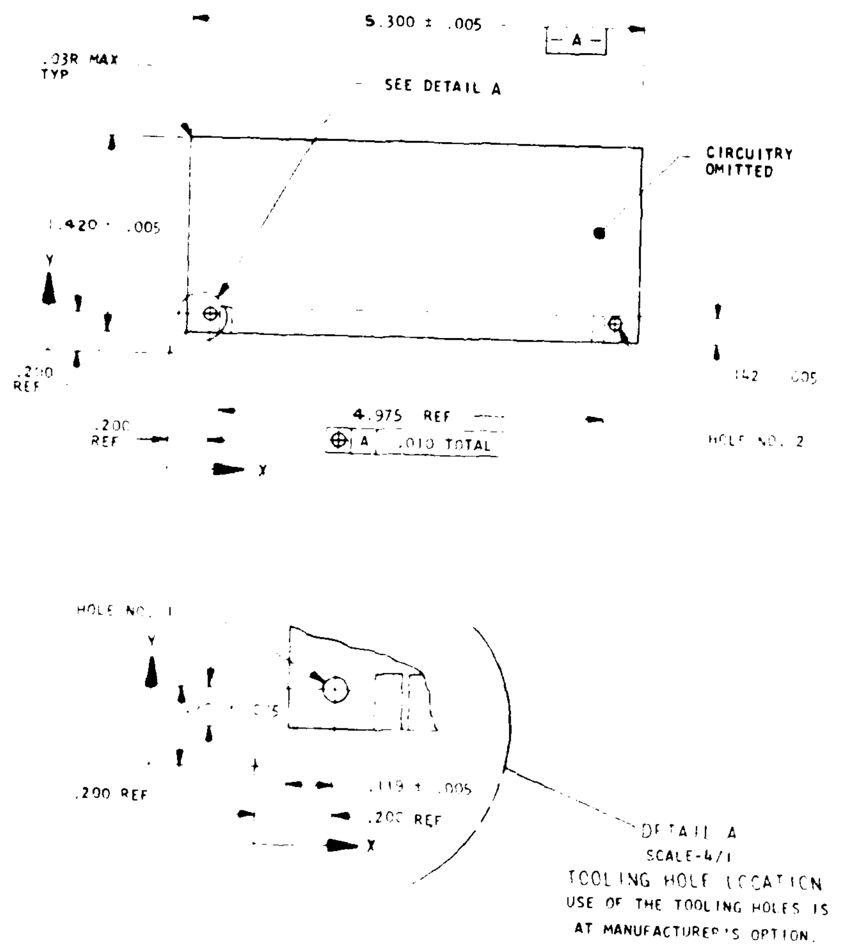

HOLE CHART

HOLE NO.	X → BSC	Y ↑ BSC	HOLE SIZE	LOCATION TOL.
1 SEE DETAIL A	.200	.200	.062 ± .001 DIA	⊕ .005 DIA
2 SEE DETAIL A	5.262	.200	.062 ± .001 DIA	⊕ .005 DIA

THIS PAGE IS BEST QUALITY PRACTICABLE
FROM COPY FURNISHED TO DDC

SIZE	CODE IDENT NO	
B	86887	BT1103
SCALE	REV	SHEET

NAC NAFI 4122/3 (9-73)

Figure B-12 (Sheet 2 of 2)

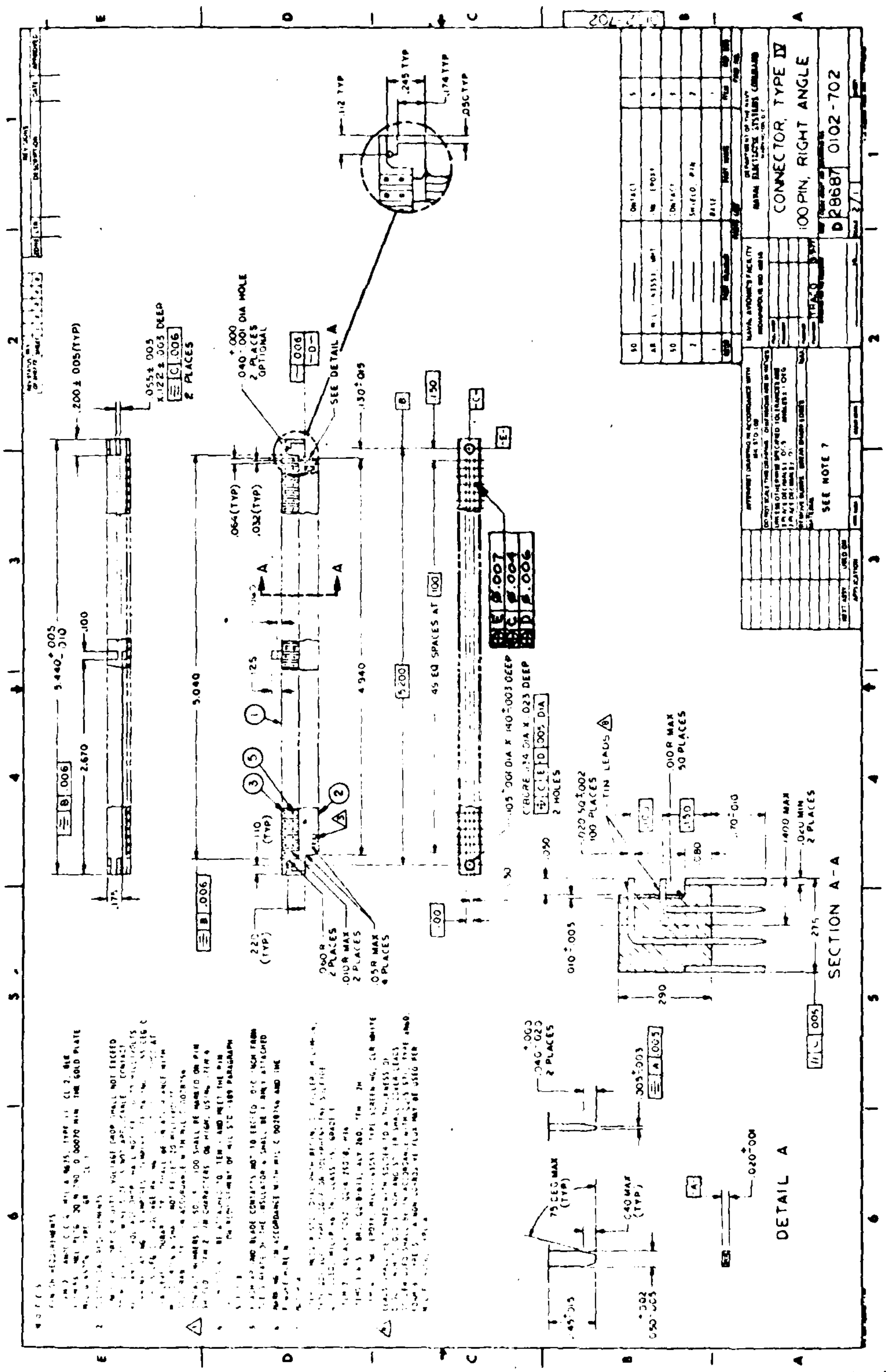
CONNECTOR, TYPE IV
100 PIN, RIGHT ANGLE
D 28687 0102-702
SECTION A-A
DETAIL A

Figure B-13

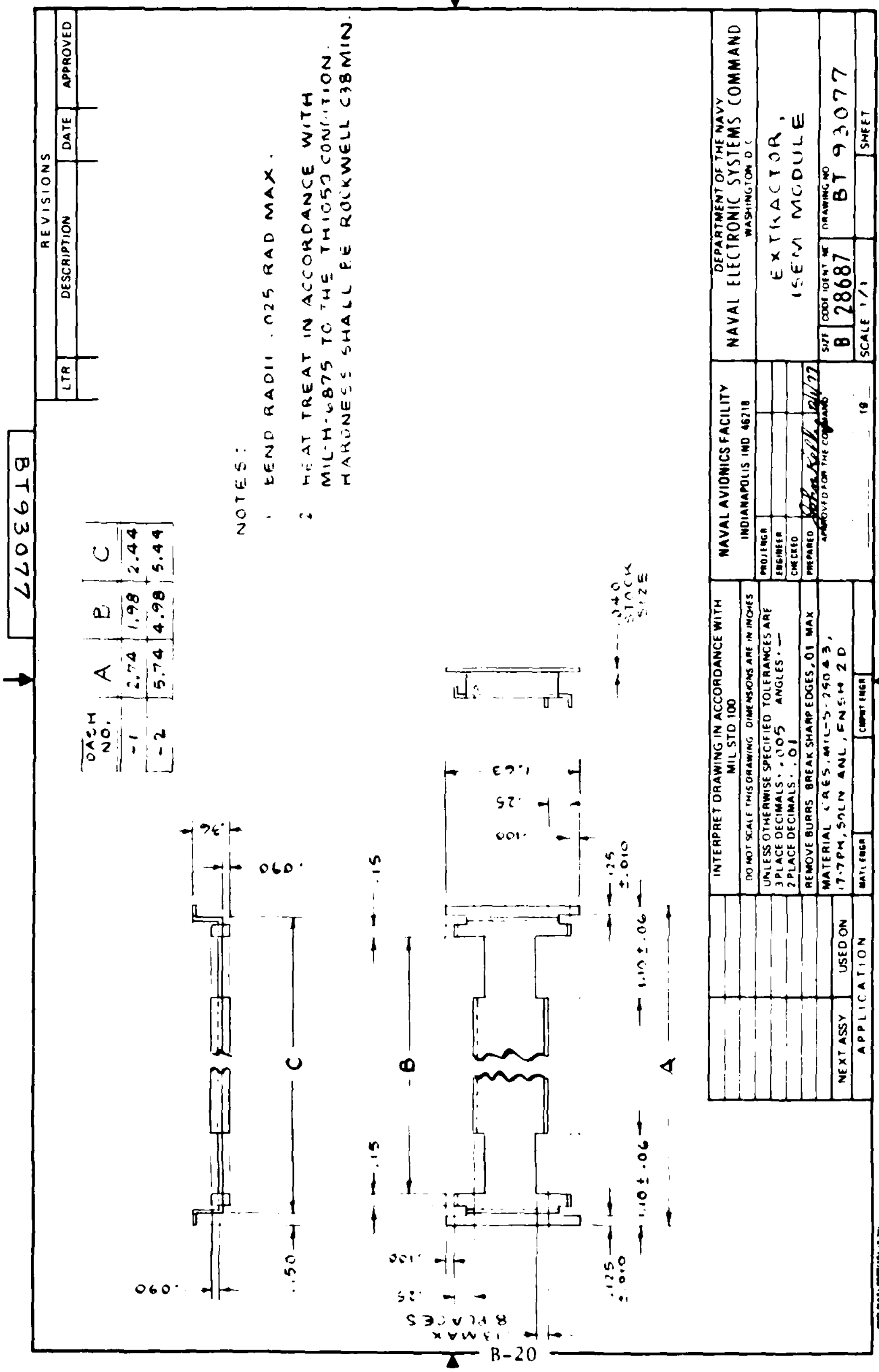
BT93077
REVISIONS
LTR
DESCRIPTION
DATE
APPROVED
NOTES:
1. BEND RADII .025 RAD MAX.
2. HEAT TREAT IN ACCORDANCE WITH MIL-H-6875 TO THE TH1050 CONDITION. HARDNESS SHALL BE ROCKWELL C38MIN.
DASH NO. | A | B | C
-1 | 2.74 | 1.98 | 2.44
-2 | 5.74 | 4.98 | 5.44
.040 STOCK SIZE
INTERPRET DRAWING IN ACCORDANCE WITH MIL STD 100
DO NOT SCALE THIS DRAWING. DIMENSIONS ARE IN INCHES
UNLESS OTHERWISE SPECIFIED TOLERANCES ARE
3 PLACE DECIMALS ± .005 ANGLES ± —
2 PLACE DECIMALS ± .01
REMOVE BURRS. BREAK SHARP EDGES .01 MAX
MATERIAL CRES, MIL-S-25043, 17-7PH, SOLN ANL, FNSH 2D
NAVAL AVIONICS FACILITY
INDIANAPOLIS IND 46218
DEPARTMENT OF THE NAVY
NAVAL ELECTRONIC SYSTEMS COMMAND
WASHINGTON D.C.
EXTRACTOR, ISEM MODULE
SIZE B
CODE IDENT NO 28687
DRAWING NO BT 93077
SCALE 1/1
SHEET
NEXT ASSY
USED ON
APPLICATION
APPROVED FOR THE COMMAND

Figure B-14

APPENDIX C

STRESS DEFLECTION ANALYSIS ON A 100-PIN WRAPOST PLATE

DEPARTMENT OF THE NAVY
NAVAL AVIONICS FACILITY
INDIANAPOLIS, INDIANA 46218

IN REPLY REFER TO:
712:DLH:11
5213/3
25 October 1977

MATERIALS TEST REPORT NO. 94-77

SUBJECT: Connector Wrapost Plate; stress and deflection analysis of

ENCLOSURES: (1) Appendix; Calculations
(2) References

INTRODUCTION:

1. D/933 requested a stress-deflection analysis on a 100 pin wrapost plate, 0102698, in a module support assembly. Information was needed on deflection caused by the insertion of the 100 pin connector. Where possible the calculated relationships were verified by experimentation. Calculations for the individual cases are presented in the Appendix.

EVALUATIONS AND RESULTS:

1. The first case considered is that of the subject wrapost plate in a 20" X 6" card cage of variable support spacing. The analysis assumes that a flat rectangular aluminum plate (0.075" thick X 5.75" span X variable width) is simply supported on all edges with a uniformly distributed load across the span equal to the maximum allowable pin insertion force for one connector. For a plate of infinite width, the calculation shows a maximum expected deflection of 0.055 inches. Imposing a plate deflection limit of 0.020 inches necessitates a card cage support spacing of 3.6 inches or less (Figure 2).

2. The second case is similar to the first except in plate configuration. The computation is made for a ribbed plate with a connector spacing to accommodate the ribs. The rib cross-sectional size is 0.10" X 0.10" spanning the plate with a spacing of 0.40" on center. For an infinite width, the plate deflects 0.019 inches and; therefore, does not require support spacers to achieve the 0.020 inches imposed limit.

3. The final calculation differs from the previous in that the maximum stress in a thin copper layer on the surface of a 1/8 inch thick "G-10" glass epoxy laminated wrapost plate was requested. This stress computes to be nearly 30,000 psi which is roughly the tensile strength of as plated copper foil. Designing to stresses of this magnitude is not advisable. A thicker, or supported, "G-10" board would be required to reduce the stress to an acceptable level.

CONCLUSIONS:

1. The subject unbraced wrapost plate of the 20" X 6" size will not support

712:DLH:11
5213/3 MTR 94-77
25 October 1977

the maximum pin insertion force without deflecting beyond the 0.020 inches imposed limit. A support spacing of 3.6 inches is required for this plate. An alternate solution is to switch to a ribbed plate as previously described. This plate will support the load for any width. A substituted 1/8 inch "G-10" wrapost plate will not support the load without over stressing plated copper foil on the surface of the board.

PREPARED BY: D. Hershberger
D. HERSHBERGER, Metallurgist

APPROVED: R. D. Hott
R. D. HOTT, Head
Metallurgical Materials Branch

B. C. Vaughn
B. C. VAUGHN, Director
Materials Laboratory and
Consultants Division

Copy to:
700
712
933 (Parmerlee)
File

CASE 1

Calculation of the deflection of a wrapost plate due to the pin insertion force

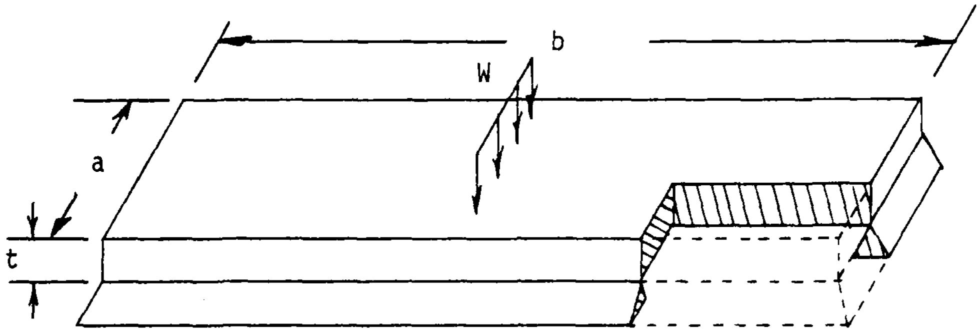

Figure 1

y = maximum deflection for the uniformly distributed load, W

$y = \frac{5/384}{1/48}\ y_{\text{concentrated load}}$ (Ref. 1 and verified experimentally)

$y = 5/8\ y_{\text{concentrated load}}$

therefore:

$$y = 5/8 \left[\kappa \frac{Wa^2}{Et^3} \right] \quad \text{(Ref. 2)}$$

Dimensions as above

E = modulus of elasticity

κ = constant dependent on the b/a ratio

For an infinitely wide plate:

$$b/a = \infty \longrightarrow \kappa = 0.185$$

$$y = 5/8 \left[0.185 \frac{Wa^2}{Et^3} \right]$$

W = (10 oz per pin) X (100 pins per connector) = 62.5 lbs

a = 5.75 inches

t = 0.075 inches

E = 10.3×10^6 psi for aluminum

$$y = 5/8 \left[0.185 \frac{62.5\ (5.75)^2}{10.3 \times 10^6\ (0.075)^3} \right]$$

y = 0.055 inches (verified experimentally)

For a maximum deflection of 0.020 inches, from trial and error assume a = 3.6 inches:

$$b/a = \frac{5.75}{3.6} = 1.6 \longrightarrow \kappa = 0.171$$

$$y = 5/8 \left[0.171 \frac{62.5\ (3.6)^2}{10.3 \times 10^6\ (0.075)^3} \right]$$

= 0.020 inches using a spacing of 3.6 inches (verified experimentally)

Figure 2

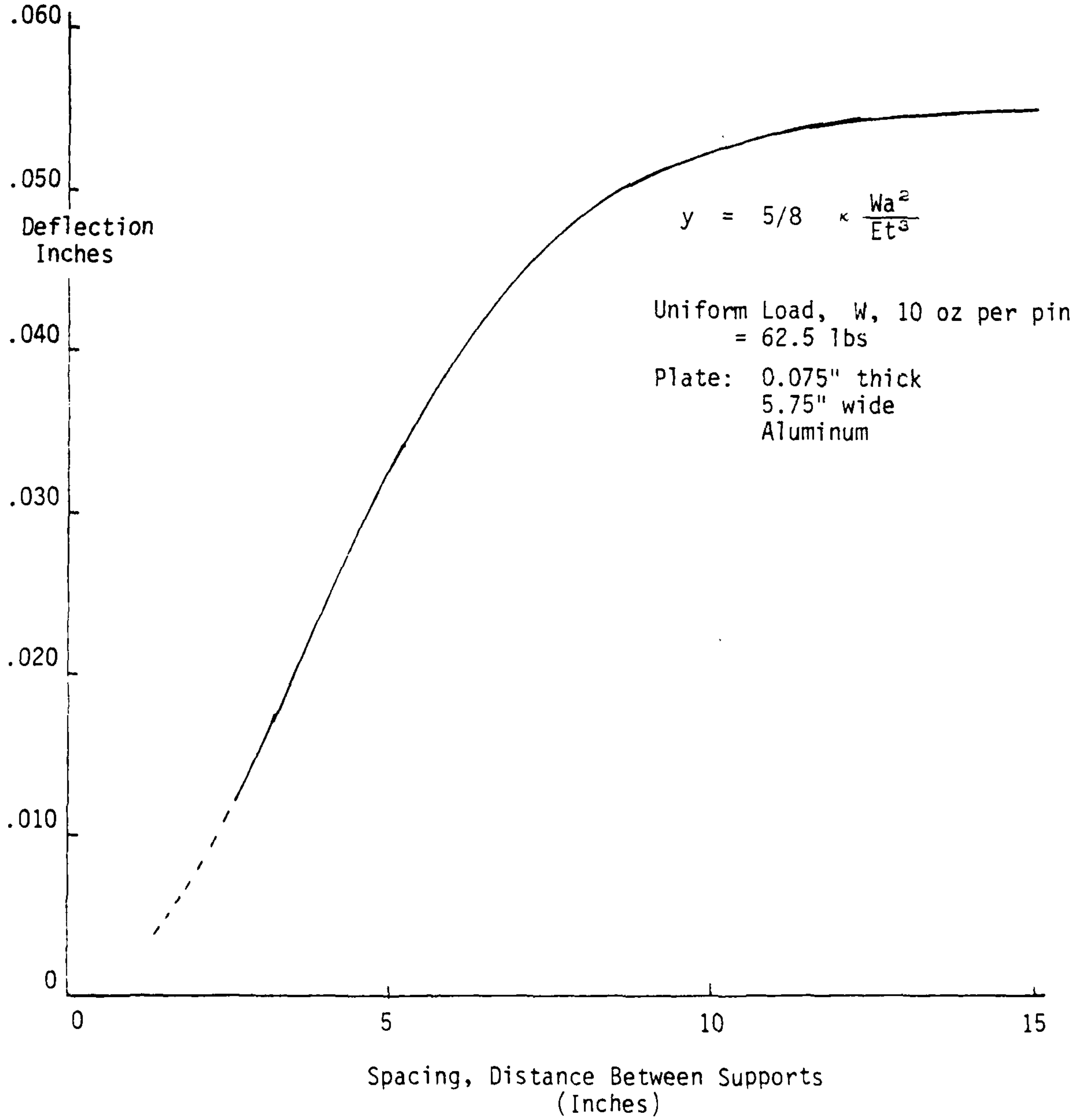
.060
.050
.040
.030
.020
.010
0
Deflection
Inches
y = 5/8 κ Wa²/Et³
Uniform Load, W, 10 oz per pin
= 62.5 lbs
Plate: 0.075" thick
5.75" wide
Aluminum
0
5
10
15
Spacing, Distance Between Supports
(Inches)

Calculation of Maximum Stress

Uniform load over small concentric circular area of radius r_o

$$\sigma_{max} = \frac{3W}{2\pi\, mt^2} \left[(m+1) \ln \frac{2b}{\pi r_o} + 1 - \beta m \right] \quad \text{(Ref. 3)}$$

$$W = 62.5 \text{ lbs}$$

$$m = \frac{1}{\gamma} = \frac{1}{.33} = 3$$

$$b = 3.6 \text{ in}$$

$$r_o = 0.20 \text{ in}$$

$$\beta = 0.125$$

$$t = 0.075 \text{ in}$$

$$\sigma_{max} = \frac{3\ (62.5)}{2\pi\ (3)\ (0.075)^2} \left[4 \ln \frac{2\ (3.6)}{\pi\ (.2)} + 1 - .375 \right]$$

$$= 18{,}400 \text{ psi}$$

$$\sigma_{uniform} = 1/2\ \sigma_{concentrated}$$

$$\max\ \sigma_{uniform} = 9{,}200 \text{ psi}$$

CASE 2

Calculation of the deflection of a ribbed plate

Momemt of Inertia Calculation

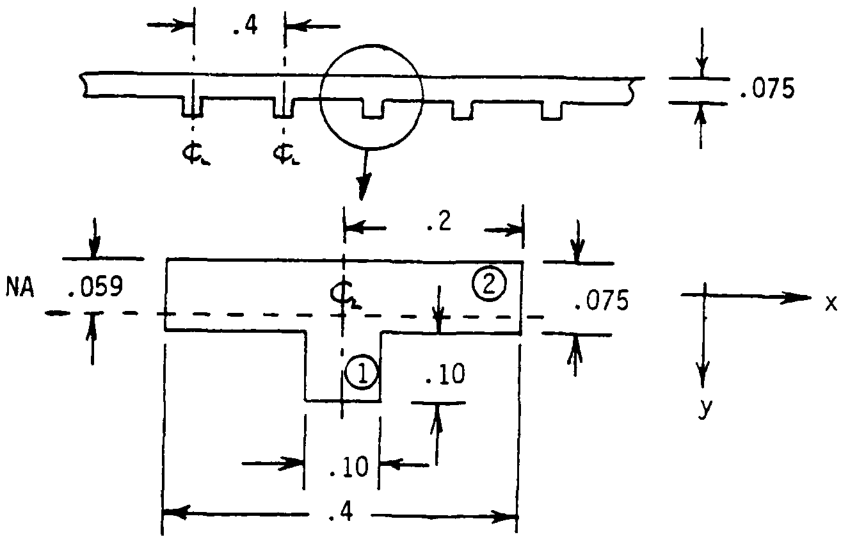

Figure 3

$$I = \frac{b_1 h_1^{3}}{12} + A_1 d_1^{2} + \frac{b_2 h_2^{3}}{12} + A_2 d_2^{2}$$

From the parallel axis theorem where d_1 and d_2 are the distances from the centroids of the areas A_1 and A_2 to the neutral axis.

Finding the centroids of the areas

$$A\bar{y} = A_1 y_1 + A_2 y_2$$

where $\bar{y}$ is the distance from the centroid of the area to the x axis and $A = A_1 + A_2$

$$A\bar{y} = .01\,(.075 + .050) + .03\,(.075/2)$$

$$\bar{y} = \frac{1}{.04}\left[.01\,(.125) + .03\,(.0375)\right]$$

$$\bar{y} = .059375 \text{ in}$$

$A_1 = .01 \text{ in}^2$

$A_2 = .03 \text{ in}^2$

$$d_1 = \frac{.01}{2} + (.075 - .059375)$$

$$= .020625 \text{ in}$$

$$d_2 = .059375 - \left(.075/2\right)$$

$$= .021875 \text{ in}$$

$$I = \frac{b_1 h_1^3}{12} + A_1 d_1^2 + \frac{b_2 h_2^3}{12} + A_2 d_2^2$$

$$= \frac{(.10)\ (.10)^3}{12} + (.01)\ (.020675)^2 + \frac{(.4)\ (.075)^3}{12}$$

$$+ .03\ (.021875)^2$$

$$= .8333 \text{ X } 10^{-5} + .4253 \text{ X } 10^{-5} + 1.4062 \text{ X } 10^{-5}$$

$$+ 1.4355 \text{ X } 10^{-5}$$

$$I = 4.1005 \text{ X } 10^{-5} \text{ in}^4$$

$$\frac{I_{ribbed}}{I_{flat\ plate}} = \frac{4.1005 \text{ X } 10^{-5}}{1.4062 \text{ X } 10^{-5}}$$

$$= 2.916$$

Deflection Calculation

$$y_{ribbed} = \frac{I_{flat\ plate}}{I_{ribbed}} \quad y_{flat\ plate}$$

for an unbraced plate ($b/a = \infty$)

$$y_{ribbed} = \frac{1}{2.916} \left[5/8\ (0.185) \frac{62.5\ (5.75)^2}{(10.3 \text{ X } 10^6)(.075)^3} \right]$$

$$= .019 \text{ in}$$

CASE 3

Calculation of stress in a thin copper layer on the surface of a G-10 plate

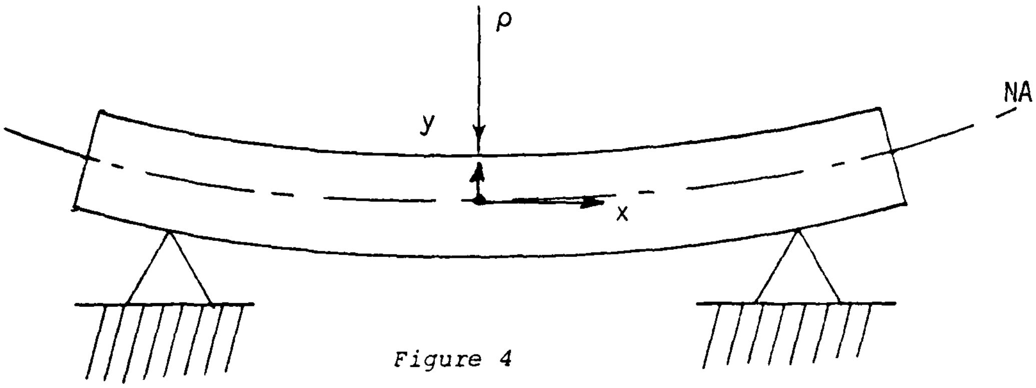

Figure 4

$$\epsilon = y'/\rho$$

where

ϵ = strain

y' = distance from the neutral axis (NA)

ρ = radius of curvature of the plate

$$\sigma = \epsilon E$$

where

σ = stress

E = modulus of elasticity

$$\sigma = y'/\rho \, E$$

$$\frac{\sigma}{y'E} = 1/\rho$$

For composite section

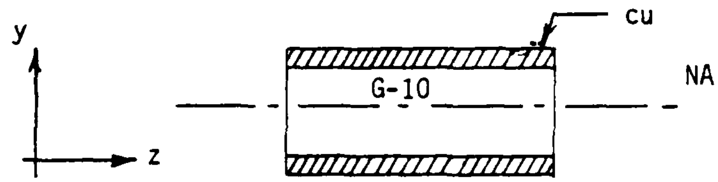

Figure 5

$$\frac{\sigma_{cu}}{y' E_{cu}} = 1/\rho = \frac{\sigma_{G-10}}{y' E_{G-10}}$$

when $y' = t/2$

$$\sigma_{cu} = \frac{E_{cu}}{E_{G-10}} \quad \sigma_{G-10}\Big]_{y' = t/2}$$

$$\sigma_{G-10}\Big]_{y' = t/2} = \sigma_{max} \ (1/2)$$

where

$$\sigma_{max} = \frac{3W}{2\pi m t^2} \left[(m+1) \ln \frac{2b}{\pi r_o} + 1 - \beta m \right]$$

$w = 62.6$ lbs

$m = 1/\gamma = 1/.3 = 3.33$

$b = 5.75$ in

$a = 19.55$ in

$\beta = 0.042$

$r_o = 0.20$ in

$t = 0.125$ in

$$\sigma_{G-10}\Big]_{y' = t/2} = (1/2) \frac{3\ (62.5)}{2\pi\ (3.3)(1.25)^2} \left[4.33\ \ln \frac{11.5}{\pi\ (.20)} + 1 = .14\right]$$

$$= 3855 \text{ psi}$$

$$\sigma_{cu} = \frac{E_{cu}}{E_{G-10}} \quad \sigma_{G-10}\Big]_{y' = t/2}$$

$$= \frac{17 \text{ X } 10^6}{2.2 \text{ X } 10^6} \quad (3855) \text{ psi}$$

$$= 29{,}800 \text{ psi}$$

REFERENCES

1. "Mechanical Engineering Design", Joseph Edward Shigley, McGraw-Hill Book Company, 1963, pages 595-6 , Cases 6 and 11.

2. "Advanced Strength of Materials", J. P. Den Hartog, McGraw-Hill Book Company, 1952, page 133.

3. "Formulas for Stress and Strain", Raymond J. Roark, McGraw-Hill Book Company, 1965, page 225

APPENDIX D

AIR AND LIQUID CARD CAGE ANALYSES

APPENDIX D

AIR AND LIQUID CARD CAGE ANALYSES

A. Introduction to Card Cage Analyses

1. While not included in the Statement of Work for Improved SEM Packaging Development, this appendix does present three feasible methods of cooling the card cage assembly, as shown in figure D-1. The first two methods (figure D-1A and D-1B) are cold plates, using air or liquid coolant flowing through the card guide rail, thereby preventing direct contact with the electrical components on the module. One of the goals was to preserve the 3" and 6" center-to-center distance of the guide rails, which limits the space available for fin height to about .18 inch. With this limitation, the fin must be oriented laterally, as shown in figure D-1A. To orient it in the longitudinal direction would result in preposterous pressure drop (over 140 inches of water pressure).

2. The third method (figure D-1C) is a liquid to air heat exchanger with the air being circulated through the air fin and directly impinging on the module components for efficient cooling.

B. Air Cold Plate

1. As mentioned earlier, calculations were made of an air cold plate, with the fin oriented in the longitudinal direction; however, the pressure drop turned out to be impractically high.

The following calculations show that air flowing in the transverse direction (see figure D-1A) can cool a card guide with 60 slots on .3 inch center spacing (18 inches long or about the size for a MIL-STD-189 cabinet), with a 14°C ΔT and 2" H_2O Δp between inlet and outlet air conditions and at a dissipation of 10 watts per card slot (600 total watts).

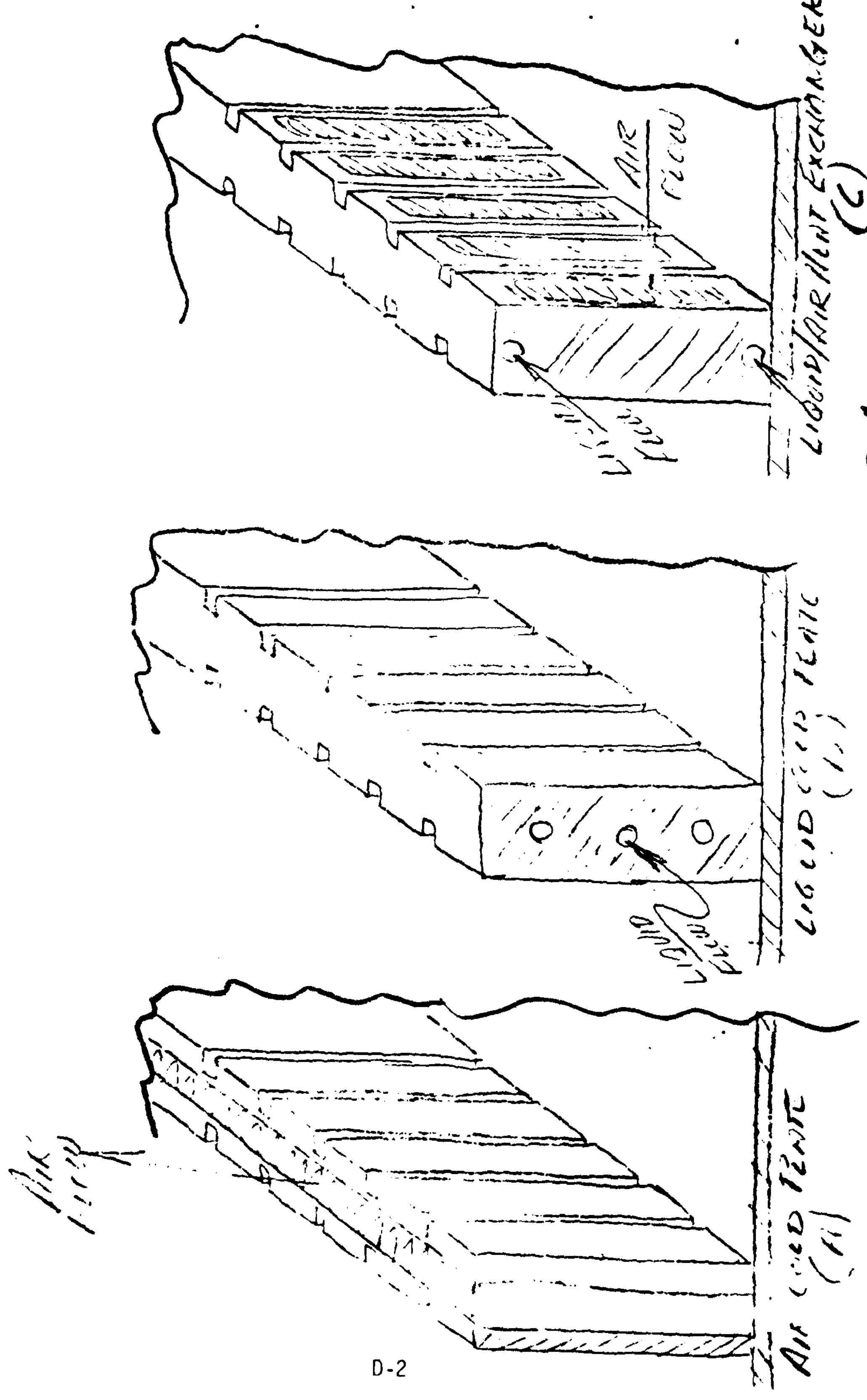
AIR FLOW
AIR COOLED PLATE (A)
LIQUID FLOW
LIQUID COOLED PLATE (B)
LIQUID FLOW
AIR FLOW
LIQUID/AIR HEAT EXCHANGER (C)

FIGURE D-1

2. From "Cooling of Electronic Equipment" by A. W. Scott, John Wiley & Sons, Inc., New York 1974, page 69, equation 4.2, the temperature rise of the coolant is as follows:

$$\frac{\Delta T(\text{air})}{Q} = \frac{1.73}{f}$$

Where:

ΔT (air)	is the temperature rise of the air in absorbing heat from the cooling fins (°C).
Q	is the total power that is being transferred (watts).
f	is the total air flow through the fins (CFM).

Solving for the air flow at 600 watts dissipation and 14°C air ΔT this equation becomes:

$$f = \frac{Q \times 1.73}{\Delta T(\text{air})} = \frac{600 \times 1.73}{14} = 74 \text{ cfm}$$

Note: The 14°C air ΔT is based on the requirement in MIL-E-16400, paragraph 3.8.1.1.

3. Using equation 4.3, the temperature rise of the fin in the card guide above that of the air flowing through it is as follows:

$$\frac{\Delta T(\text{fin-air})}{Q} = \frac{140\ w}{n^{.2} z^{.2} f^{.8} L}$$

Where:

ΔT (fin-air)	is the temperature rise of the fin surface above the air flowing through the cooling ducts between the fins (°C).
Q	is the total power that is being transferred (watts).

w	is the width of the ducts, i.e., the spacing between fins (inch).
z	is the height of the fins above the base (inch).
L	is the length of the fins along the direction of air flow (inch).
n	is the number of ducts through which the air flows.
f	is the total air flow through all the ducts (CFM).

The geometry of the cooling fins is shown in figure D-2, and this figure defines the critical fin dimensions w, z, and L.

$$\Delta T \text{ (fin-air)} = \frac{600 \times 140 \times .015}{\left(\frac{18}{.021}\right)^{.2} x .18^{.2} x 74^{.8} x 1.5}$$

$$= 9.8°C$$

y = .006
w = .015
z = .18
L = 1.5

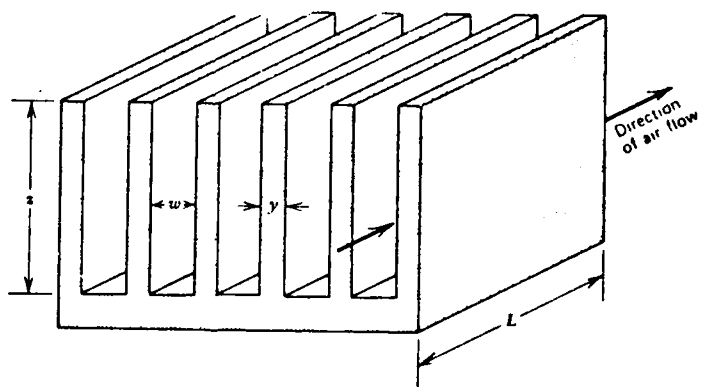

FIGURE D·2
Geometry of forced air cooled heat sink and important dimensions

From equation 4.4, the Δp across the guide rail is as follows:

$$\Delta p = \frac{\left(\frac{f}{n}\right)^2}{(wz)^2}\left[1 + .01\,\frac{L}{w}\right] \times 10^{-3}$$

Where:

Δp is the pressure drop through the fins (inches of water).

$$\Delta p = \frac{\left(\frac{74}{.857}\right)^2}{(.015x.18)^2}\left[1 + .01\,\frac{1.5}{.015}\right] \times 10^{-3}$$

$$= 2.04'' \text{ water}$$

4. It is to be noted that to produce the above performance in such a compact space, close fin spacing of .015" was necessary. While this can be produced at a reasonable cost, it does mean that close attention will need to be given to the design of the air filtration system to preclude fouling of these fins.

5. In addition, plenum ducts of the order of .3" height by 18" width would be necessary to provide the air inlet and exhaust channels for a card cage containing these air cold plate side rails, thereby complicating maintainability somewhat.

C. Liquid Cold Plate

1. Using the equations and techniques from chapter 5 of the previously mentioned test, figure D-3 (thermal resistance of duct to coolant versus flow rate of coolant) and D-4 (coolant pressure drop versus coolant flow rate) were generated for four coolants: water; glycol/water; FC-75; and coolanol 45. From the standpoint of thermal resistance and pressure drop alone, water is the best of the coolants considered. Applying the results of figures D-3 and D-4 to the configuration of guide rail, as

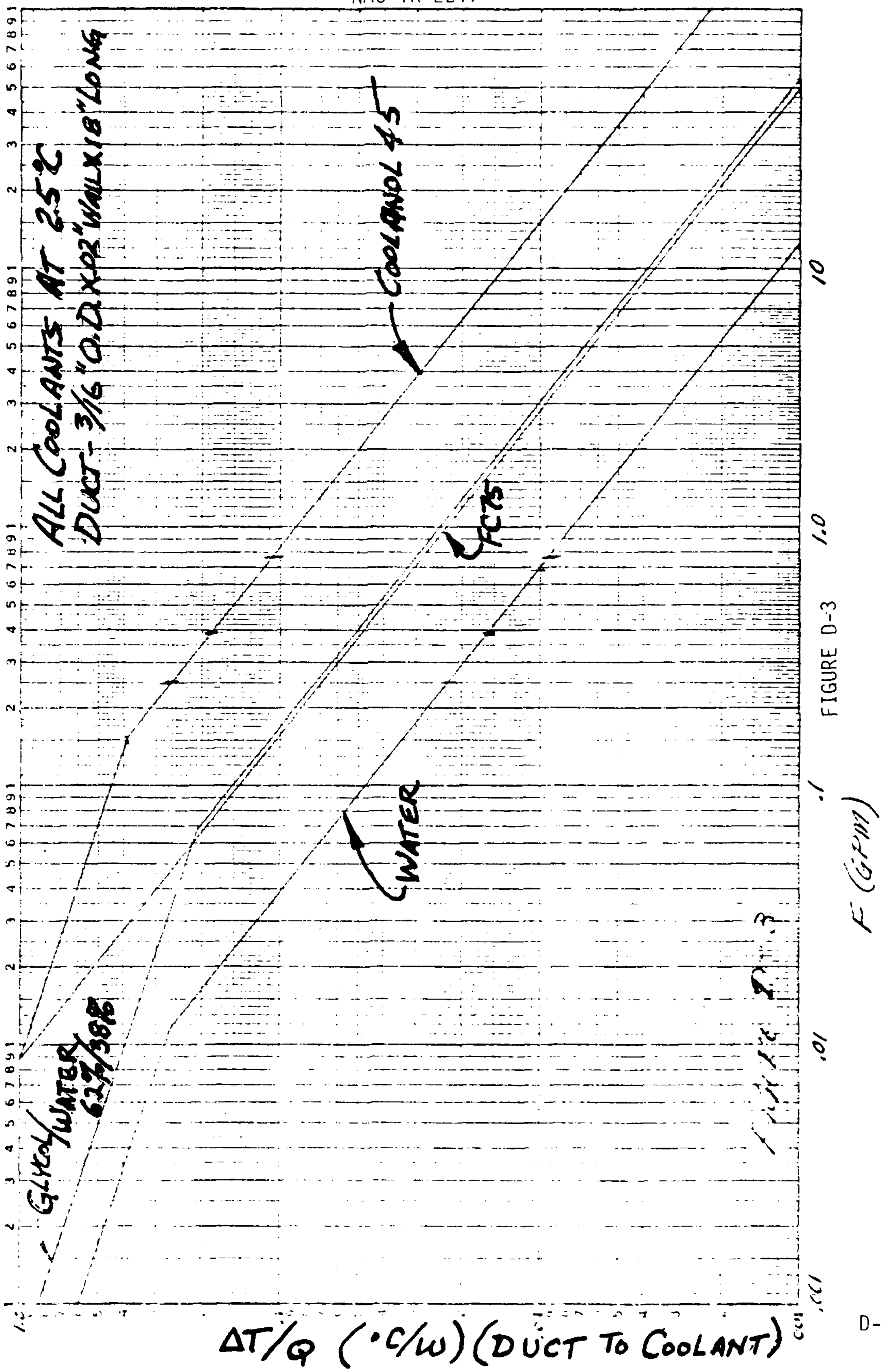
ALL COOLANTS AT 25°C
DUCT - 3/16" O.D X .02" WALL X 18" LONG
COOLANOL 45
FC75
WATER
GLYCOL/WATER 62%/38%
F (GPM)
ΔT/Q (°C/W) (DUCT TO COOLANT)
.001
.01
.1
1.0
10

FIGURE D-3

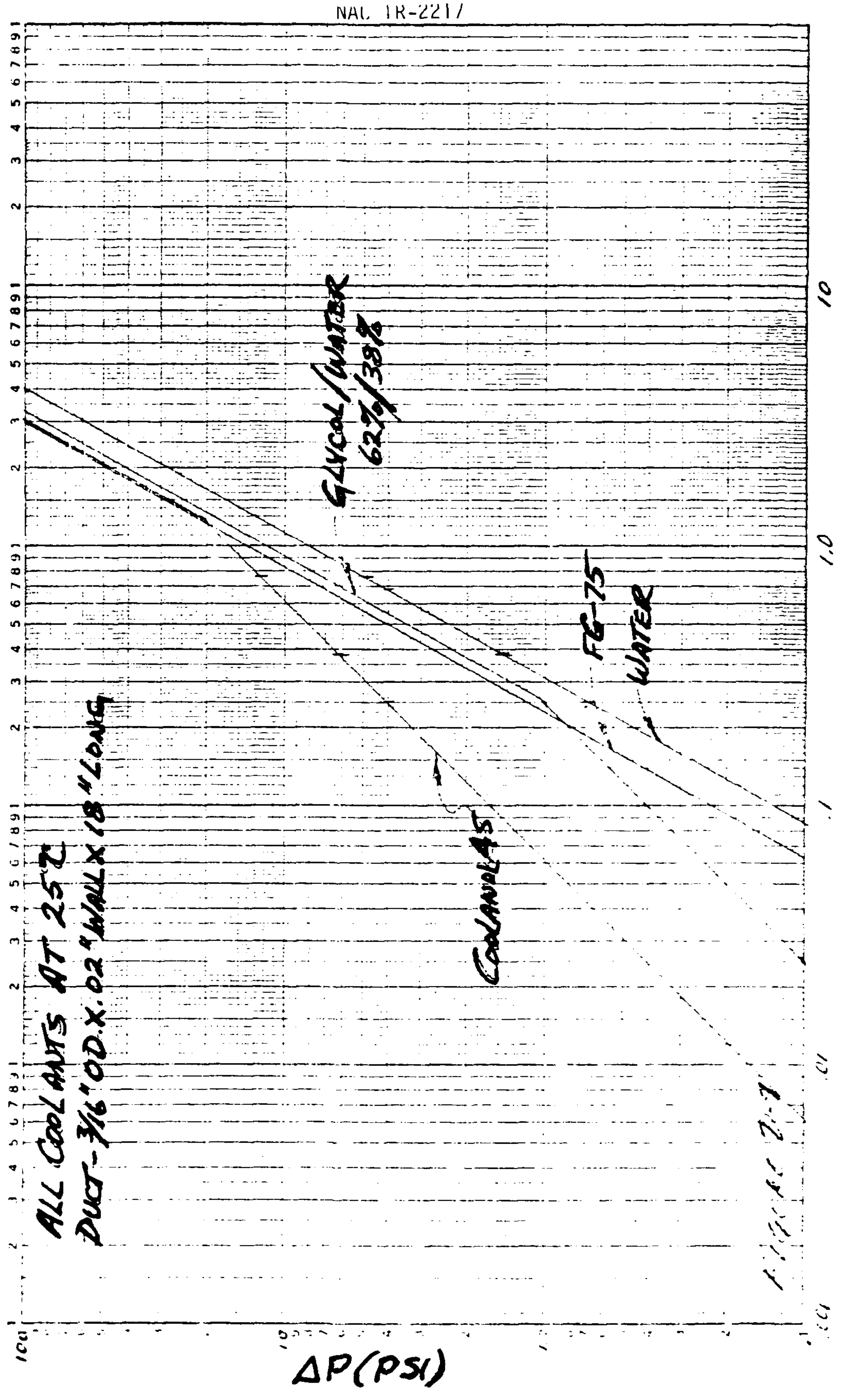
ALL COOLANTS AT 25°C
DUCT-3/16" OD. X .02" WALL X 18" LONG
GLYCOL/WATER 62%/38%
FC-75
WATER
COOLANOL 45
10
1.0
.1
.01
100
ΔP(PSI)
F (GPM)

FIGURE D-4

shown in figure D-1B, it is seen that shipboard requirements (MIL-W-21965) of 1.4 gpm maximum/KW at 3°C maximum and 10 PSI maximum pressure drop can be met at a dissipation of 600 watts per rail (10 watts per slot x 60 slots per 18 inch rail).

2. From equation 5.2, the temperature rise of the coolant is the following:

$$\frac{\Delta T\ (\text{coolant})}{Q} = \frac{3.8 \times 10^{-3}}{CgF}$$

Where:

ΔT (coolant)	is the temperature rise of the cooling liquid in absorbing heat (°C).
Q	is the total power being transferred (watts).
F	is the total coolant flow rate $\left(\frac{\text{gallon}}{\text{minute}}\right)$
C	is the specific heat of coolant $\left(\frac{\text{BTU}}{\text{pound-°F}}\right)$
g	is the specific gravity of coolant relative to water.

By rearranging and using 3°C ΔT (coolant), the required flow is as follows:

$$F = \frac{Qx3.8x10^{-3}}{Cg\Delta T} = \frac{600x3.8x10^{-3}}{1x1x3} = .76 \text{ gal/min.}$$

3. Figures D-3 and D-4 are based on a single 3/16" OD x .02" wall x 18" long, since it is of a size which could be practically employed in a card rail and maintain the 3" and 6" standard spacing. Entering figure D-3 at .76 gpm flow rate, the $\Delta T/Q$ (thermal resistance, duct to coolant) is about .0092°C/u so that at 600 watts input the ΔT between duct and coolant

would be 5.52°C, which is a suitable value. Likewise, from figure D-4, the pressure drop of water at .76 gpm is about 5 PSI. Another arrangement would be to use two tubes in series; in this case, the ΔT would be half or 2.76°C and the ΔP would be twice or 10 PSI that of one tube. This ΔP would be marginal, however, in a shipboard system, because of other fitting losses along the way.

A third alternative exists, as shown diagrammatically in figure D-5, to use 3 tubes (a pair of tubes in parallel with each other, and in series with a third tube). The values for ΔP, ΔT, flow, and power dissipation are shown along each branch.

4. These examples serve to show the flexibility of application by having more than one tube in a "standardized" guide rail; thereby, allowing latitude in matching the cabinet characteristics to those of the system.

← flow = .38 gpm, power = 150 watts, ΔP = 1.5 PSI, ΔT = 2.4°C

→ flow = .76 gpm, power = 300 watts, ΔP = 5 PSI, ΔT = 2.76°C

← flow = .38 gpm, power = 150 watts, ΔP = 1.5 PSI, ΔT = 2.4°C

Overall characteristics are flow = .76, power = 600 watts, ΔP = 6.5 PSI + elbow losses, ΔT = 2.4 to 2.76°C.

FIGURE D-5

D. Liquid to Air Heat Exchanger

1. Figure D-1C shows an arrangement where heat, which has been picked up by direct air impingement over a module, proceeds on through finned windows between module slots, where it is conducted through the metal into the water side circuit. The calculations for this design are as follows:

$$\text{air flow/slot} = f = \frac{Q \times 1.73}{\Delta T\ (\text{air})}$$

$$= \frac{10\ \text{watts/card} \times 1.73}{7°\text{C (assumed)}}$$

$$= 2.47\ \text{cfm/slot or } 148°\ \text{cfm for a 60 slot rail}$$

$$\Delta T\ (\text{fin-air}) = \frac{140\ Q\ W}{n^{.2} z^{.2} f^{.8} L}$$

$$= \frac{140 \times 10 \times .01}{94^{.2} \times .18^{.2} \times 2.47^{.8} \times .5} = 7.7°\text{C}$$

Where:

$Q = 10$ watts/slot

$w = .01$ inch

$n \approx \frac{1.5}{.01+.006} = 94$ fins

$z = .18$ inch

$f = 2.47$ cfm

$L = .5$ inch

(See figure D-2 for application.)

$$\text{fin pressure drop} = \Delta p = \frac{\left(\frac{f}{n}\right)^2}{(wz)^2}\left[1 \div .01\,\frac{L}{w}\right] \times 10^{-3}$$

$$= \frac{\left(\frac{2.47}{94}\right)^2}{(.01x.18)^2}\left[1 + .01\,\frac{.5}{.01}\right] \times 10^{-3}$$

= .320" water

Assuming an effective free flow area between modules of .20 square inches, the average air velocity would be as follows:

$$V = \frac{f\ 144}{A\ 60}$$

Where:

V = velocity (fps)
f = flow (cfm)
A = area (in^2)

$$V = \frac{f\ 144}{A\ \ 60}$$

$$= \frac{2.47x144}{.20x60}$$

= 29.64 fps

From figure A-9, the pressure drop for 3 modules in series on .3 center spacing at 30 fps is about 1.5" water, therefore, the pressure drop per module is about 1.5/3 or .5" water.

The maximum component junction temperature is the summation of the initial water temperature and all the temperature gradients along the path to the junction as follows:

Inlet water temperature	=	45 °C	(MIL-W-21965)
ΔT (coolant)	=	3 °C	(MIL-W-21965)
ΔT (duct to coolant)	=	2.76°C	(see previous section)
ΔT (fin to duct by conduction)	=	5.5 °C	(estimated)
ΔT (air to fin)	=	7.7 °C	
ΔT (air)	=	7 °C	
ΔT (component junction to air)	=	35 °C	(See below)
Worst-case junction temperature	=	105.96°C	

The component junction to air temperature drop is composed of the junction to case drop, plus the case to air drop as follows:

$$\Delta T \text{ (junction to case)} = 25°\text{C/w (assumed)} \times \frac{10 \text{ watts/2A module}}{16 \text{ DIPS/2A module}} = 15.6°\text{C}$$

$$\Delta T \text{ (case to air)} = 31°\text{C} \times \frac{10 \text{ watts}}{16 \text{ DIPS}} = 19.4°\text{C}$$

$$\text{Total} = 35.0°\text{C}$$

(See table A-3 for 25 fps.)

In summary, then, a liquid to air heat exchanger assembled integral with the module guide rail, as shown in figure D-1C, would have the following characteristics:

Number of module positions	= 60
Module pitch	= .3 inch
Module dissipation	= 10 watts/module
Total air flow	= 148 cfm
Total air pressure drop across the air fins and a row of SEM 2A modules	= .82" water
Average air velocity	≈ 30 fps
Worst-case junction temperature	= 106°C

As in the case with the air cold plate design, the close fin spacing requires close attention in the design of the air filtration system to preclude fouling.